Volume II.I

Midwestern Regional Carbon Sequestration Partnership (MRCSP) Phase III (Development Phase)

Geochemical Changes in Response to CO_2 Injection in a CO_2-EOR Complex in Northern Michigan

Prepared by:

Battelle
505 King Avenue
Columbus, Ohio 43201

Principal Investigator: Dr. Neeraj Gupta

Authors: Matthew Place, Jared Hawkins, Ben Grove, Laura Keister, Julie Sheets, Sue Welch, David Cole, and Neeraj Gupta

Submitted to:

The U.S. Department of Energy, National Energy Technology Laboratory
Program Manager: Andrea McNemar

DOE MRCSP Project #DE-FC26-05NT42589

September 2020

BATTELLE

Notice

This report was prepared by Battelle as an account of work sponsored by an agency of the United States Government and other project sponsors, including Core Energy, LLC and The Ohio Development Services Agency. Neither the United States Government, nor any agency thereof, nor any of their employees, nor Battelle and other cosponsors, makes any warranty, express or implied, or assumes any liability or responsibility for the accuracy, completeness, or usefulness of any information, apparatus, product, or process disclosed, or represents that its use would not infringe privately owned rights. Reference herein to any specific commercial product, process, or service by trade name, trademark, manufacturer, or otherwise does not necessarily constitute or imply its endorsement, recommendations, or favoring by the United States Government or any agency thereof. The views and the opinions of authors expressed herein do not necessarily state or reflect those of the United States Government or any agency thereof.

Battelle does not engage in research for advertising, sales promotion, or endorsement of our clients' interests including raising investment capital or recommending investments decisions, or other publicity purposes, or for any use in litigation.

Battelle endeavors at all times to produce work of the highest quality, consistent with our contract commitments. However, because of the research and/or experimental nature of this work the client undertakes the sole responsibility for the consequence of any use or misuse of, or inability to use, any information, apparatus, process or result obtained from Battelle, and Battelle, its employees, officers, or Trustees have no legal liability for the accuracy, adequacy, or efficacy thereof.

Acknowledgements

Sponsorships - This report is part of a series of reports prepared under the Midwestern Regional Carbon Sequestration Partnership (MRCSP) Phase III (Development Phase). These reports summarize and detail the findings of the work conducted under the Phase III project. The primary funding for the MRCSP program is from the US Department of Energy's National Energy Technology Laboratory (NETL) under DOE project number DE-FC26-05NT42589 with Ms. Andrea McNemar as the DOE project manager. The past DOE project managers for MRCSP include Dawn Deel, Lynn Brickett, and Traci Rodosta. Many others in the DOE leadership supported, encouraged, and enabled the MRCSP work including but not limited to Kanwal Mahajan, John Litynski, Darin Damiani, and Sean Plasynski.

The Michigan Basin large-scale test received significant in-kind cost share from Core Energy, LLC, who also provided essential access to the field test site and related data. This contribution by Core Energy CEO Robert Mannes, VP Operations Rick Pardini, and Allan Modroo, VP Exploration, and the entire Core Energy staff is gratefully acknowledged. MRCSP work in Ohio has been supported by the Ohio Coal Development Office in the Ohio Development Services Agency under various grants (CDO D-10-7, CDO-D-13-22, CDO-D-D-13-24, and CDO-D-15-08) with Mr. Greg Payne as the OCDO project manager. Finally, several industry sponsors and numerous technical team members from State Geological Surveys, universities, and field service providers have supported MRCSP through cash and in-kind contributions over the years as listed in the individual reports.

Program Leadership – During the MRCSP Phase III project period, several Battelle staff and external collaborators contributed to the successful completion of the program through their efforts in field work, geological data analysis and interpretation, and/or reporting. The primary project managers over the MRCSP performance period have included Rebecca Wessinger, Neeraj Gupta, Jared Walker, Rod Osborne, Darrell Paul, David Ball. Additional project management support has been provided by Andrew Burchwell, Christa Duffy, Caitlin McNeil, and Jacqueline Gerst over the years.

Principal Investigator: Neeraj Gupta (614-424-3820/ gupta@battelle.org)

Report Authors and Principal Technical Contributors – Matthew Place, Jared Hawkins, Ben Grove, Laura Keister, Neeraj Gupta (Battelle), Julie Sheets, Sue Welch, and David Cole (Ohio State University)

Other Technical Contributors – Mark Kelley, Mackenzie Scharenberg (Battelle), Kelly Lang (Ohio State University)

Table of Contents

Page

Acknowledgements iii
Acronyms and Abbreviations ix
1.0 Introduction and Background 1
1.1 Purpose and Objectives 3
1.2 Geochemistry Study Sites 3
1.2.1 Dover 33 4
1.2.2 Charlton 19 7
1.2.3 Bagley Field 8
2.0 Brine, Gas, and Core Sampling Methods 11
2.1 Brine Samples Collected and Methods 11
2.1.1 Dover 33 11
2.1.2 Charlton 19 13
2.1.3 Bagley Field 14
2.2 Gas Sampling Methods 14
2.3 Core Sampling Methods 17
3.0 Analytical Methods 19
3.1 Brine Analytical Methods 19
3.2 Gas Analytical Methods 20
3.3 Core Analytical Methods 21
3.3.1 Light Microscopy (LM) 22
3.3.2 Scanning Electron Microscopy (SEM) 22
3.3.3 X-Ray Diffraction Analysis (XRD) 22
3.3.4 X-Ray Computed Tomography Analysis (XCT) 22
3.3.5 Solid-Phase Isotopic Analyses 23
4.0 Analytical Results, Equilibrium Modeling, and Discussion 25
4.1 General Geochemistry of Formation Brines 25
4.1.1 Discussion (Significance of Brine Geochemistry Analytical Results) 29
4.2 Geochemical Equilibrium Modeling 29
4.2.1 Model Limitations 33
4.2.2 Results 33
4.2.3 Carbonate Minerals 37
4.2.4 Hydroxide and Silicate Minerals 37
4.3 Formation/Injection Gas Analyses 38
4.3.1 Results 38
4.4 Carbonate Isotopic Analyses 45
4.4.1 Discussion (Significance of Carbon Isotope Results) 50
4.5 Core Analyses 50
4.5.1 Comparative X-Ray Diffraction (XRD) Analysis 51
4.5.2 Petrographic Light Microscopy (LM) and Scanning Electron Microscopy (SEM) Analysis of Mineralogy, Fractures, and Pores 53
4.5.3 X-ray Computed Tomography (XCT) 60
4.5.4 Carbon Isotope Analyses of the Core Matrix and Vug Precipitates 61

5.0 Conclusions 63
5.1 Brine 63
5.2 Gas 63
5.3 Rock Core 64
6.0 References 67

List of Tables

Page

Table 2-1. Sample locations for the brine, gas, and core samples 11
Table 2-2. Brine Samples Collected from the Three Reefs as Part of the Geochemistry Study 12
Table 2-3. Details of the gas sample collection. 15
Table 2-4. Conventional core acquisition parameters for Lawnichak 9-33 18
Table 3-1. Analytical Methods, Preservation, and Holding Times for the Individual Brine Analyses 19
Table 3-2. Overview of core subsamples used for geochemical analyses. 21
Table 4-1. General Geochemical Analytical Results from the Brine Samples Collected as Part of the Geochemistry Study. 27
Table 4-2. Summary of brine geochemistry (moles per kg water). 31
Table 4-3. General hydrologic conditions for the Michigan Basin. 33
Table 4-4. Concentrations of selected ions and saturation indices of minerals. 35
Table 4-5. Precipitation of phases in each of the samples (•) and changes in pH and concentrations of constituents of interest. 37
Table 4-6. Composition of the Gas Collected from the Dover 33, Charlton 19, Bagley Field Reefs and the Dover 36 GPF. 39
Table 4-7. Isotopic Composition of the Carbon Dioxide and Methane in the Gas Samples Collected from the Dover 33, Charlton 19, Bagley Field Reefs and the Dover 36 GPF 41
Table 4-8. Carbon isotope values ($\delta^{13}C$) of DIC in the brine samples collected from the three Niagaran reefs. 46
Table 4-9. Carbon isotope values for the core samples collected from depths of 5,960, 5,700, and 5,606 ft. 62

List of Figures

Page

Figure 1-1. Potential Chemical and Physical Reactions involving CO_2 injected into Brine Solutions. 2
Figure 1-2. Location of the Reefs Studied for the MRCSP Geochemistry Study within the Northern Niagaran Reef Trend. 4
Figure 1-3. Map of the Dover 33 reef Showing Wells included in the Geochemistry Study. L-M 1-33 (29565), L-M 2-33 (55942), L-M 5-33 (51603), Lawnichak 9-33 (35584), and Fieldstone 2-33 (60296). 6
Figure 1-4. Map of the Charlton 19 Reef Showing Wells Included in the Geochemistry Study. EMH 1-18/EMH 1-18A (41801), EMH 2-18 (42766), and EMH 1-19D (57261). 8
Figure 1-5. Map of the Bagley Field Reef Complex Showing Wells included in the Geochemistry Study. J-M 1-11 (37794) and J-S 3-11 (38286). 9
Figure 2-1. Preparation (Filtering) of the Brine Samples. 13
Figure 2-2. Collection of a Gas Sample from the Well Tubing. 16

Figure 2-3. Collection of a Gas Sample from the Dover 36 Pure CO_2 Pipeline. 17
Figure 4-1. Piper diagram of the major cation/anion concentrations in the brine samples collected from the three reefs. 29
Figure 4-2. $\delta^{13}C$ and $\delta^{18}O$ of CO_2 for the injected gas (either L-M 1-33 or Dover 36 comingled sample, red) and 5-33 monitoring well (blue). 43
Figure 4-3. Presentation of the $\delta^{13}C$ of DIC in brine samples collected from the Dover 33, Charlton 19, and Bagley Field reefs, with wells without CO_2 interaction on the left and wells with CO_2 interaction on the right. 47
Figure 4-4. Fractionation of ^{13}C during the dissolution of CO_2 and the dissociation of carbonic acid. 48
Figure 4-5. Powder X-Ray Diffraction spectra for core samples collected from depth of 5,588, 5,630, and 5,655 ft. The sample collected from a depth of 5,630 ft near the oil/water interface displays a complex mineralogy, perhaps from geochemical reactions. 51
Figure 4-6. XRD analysis shows bulk mineralogy of the matrix material from the 5690.25' sample. Arrows point to key diffraction maxima that correspond to minerals identified in the core. 52
Figure 4-7. XRD analysis shows that, in addition to matrix material (dolomite, quartz, albite), the vug contains anhydrite and fluorite that may have precipitated recently. 52
Figure 4-8. (left**)** Digital light micrograph of thin section prepared from sidewall core trim sample 5,655 ft, in the oil-water transition zone. Blue dye epoxy highlights the pores, (right) zoomed image of vug with secondary mineralization lining the pore space, sample 5,655 ft. Large rectangular white crystal (arrowed, lower left) is anhydrite. Transparent rhombohedral crystals (carbonates) also line the vug (arrowed, center). 53
Figure 4-9. Digital light micrograph of recrystallized fossil-rich region, (white coarser-grained material) depth 5,588 ft. Blue epoxy is concentrated in areas with greater porosity, demonstrating uneven distribution of pores in the sample. 54
Figure 4-10. Cross-polarized light micrograph of sidewall trim sample shows dolomite matrix (high birefringence appearing milky gray) with anhydrite precipitation (first order red, blue birefringence) in a vug in the CO_2-EOR interval (5,630 ft). 55
Figure 4-11. SEM BSE image of high-Mg carbonate mineral precipitate in a pore in the CO_2-EOR interval (from 5,655 ft). 56
Figure 4-12. EDXS spectra of the high-Mg carbonate mineral precipitate in the sample from 5,655 ft. 56
Figure 4-13. Image of low-Mg calcite detected on the aggregate sample collected from a depth of 5,690 ft. 57
Figure 4-14. Backscattered SEM image of potassium feldspar adjacent to a vuggy pore containing dolomite. The potassium feldspar grain cleaves in a different geometry than the dolomite and displays a brighter BSE signal intensity. Some potassium feldspar grains contained euhedral dolomite inclusions. 58
Figure 4-15. Backscattered SEM image of a fluorite infilling in a vuggy matrix region. The brighter mineral is fluorite and the darker gray mineral is dolomite. The fluorite contains inclusions of dolomite. 59
Figure 4-16. SEM imagery shows salts (sylvite) precipitated in a vug in the CO_2-EOR (5,630 ft) interval. 60
Figure 4-17. XCT scans of the core (5690.25'), a 3D image of the core and its inclusion was constructed for two different orientations. Aviso software was used to render a 3D image from XCT scans of sample 5690.25', including the partly infilled vug. 61

List of Equations

Page

Equation 3-1 20
Equation 3-2 20
Equation 3-3 21
Equation 4-1 49

Acronyms and Abbreviations

ALS	Australian Laboratory Services
BSE	Backscattered Electron
CCUS	Carbon capture utilization and storage
CO_2	Carbon dioxide
CP	Cross-Polarized
CPF	Central Processing Facility
DIC	Dissolved Inorganic Carbon
DOT	Department of Transportation
EDS	Energy-dispersive Detector
EDXS	Energy-dispersive X-ray Spectroscopy
EMH	El Mac Hills
EOR	Enhanced Oil Recovery
GC	Gas Chromatography
GPF	Gas Processing Facility
IC	Ion Chromatography
ICP-OES	Inductively Coupled Plasma Optical Emission Spectrometry
LM	Light Microscopy
MD	Measured Depth
MRCSP	Midwest Regional Carbon Sequestration Partnership
NETL	National Energy Technology Laboratory
NNRT	Northern Niagaran Reef Trend
OM	Organic Matter
OSU	Ohio State University
PLM	Polarized Light Microscope
SEM	Scanning Electron Microscopy
SEMCAL	Subsurface Energy Materials Characterization and Analysis Laboratory
SI	Saturation Index
TDS	Total Dissolved Solids
VSMOW	Vienna Standard Mean Ocean Water
WAG	Water Alternating Gas
XCT	X-Ray Computed Tomography
XRD	X-Ray Diffraction

1.0 Introduction and Background

Carbon capture utilization and storage (CCUS) has been used to capture CO_2 released from the combustion of fossil fuels and store it in underground repositories. This is part of an effort to reduce rising atmospheric CO_2 concentrations and mitigate global warming or increase oil production from reservoirs. The most significant underground storage sites are deep saline aquifers and depleted hydrocarbon (oil and gas) fields (e.g., Benson and Cole 2008; Boreham et al., 2011; DePaolo and Cole, 2013; Jenkins et al., 2012; Kharaka et al., 2006; 2013; Lu et al., 2012; Mayer et al., 2013) that have the added advantage of utilizing the injected CO_2 in enhanced oil recovery (EOR). General geochemical conditions and natural isotopic tracers are widely used in CCUS studies (Johnson et al., 2011a,b; Kharaka et al., 2013; Li and Pang, 2015; Mayer et al., 2013) in order to determine geochemical processes occurring in the deep subsurface, the rates of CO_2 interaction with subsurface brine, oil, and rocks, and the fate of the injected gas/liquid.

Multiple processes can affect the fate and transport of CO_2 in the subsurface. These include hydrodynamic processes, such as advection, dispersion, and mixing/dilution, as well as chemical processes such as diffusion into low permeability materials, partitioning into non-aqueous phases (e.g., oil), dissolution/precipitation of carbonate minerals, and water/rock interactions (See Figure 1-1) (Hitchon, 1996). Geochemical monitoring that identifies and quantifies the processes affecting CO_2 transport for a given subsurface environment is essential for determining the fate and transport of the injected CO_2 and for estimating the storage characteristics and capacity of that reservoir. Whereas reservoir models can be designed to simulate those processes, the accuracy of these models depends upon input parameters that adequately represent *in situ* conditions, that the models are sufficiently equipped to handle the geochemical conditions of the environment (i.e., ionic strength, etc.), and on careful validation through field testing.

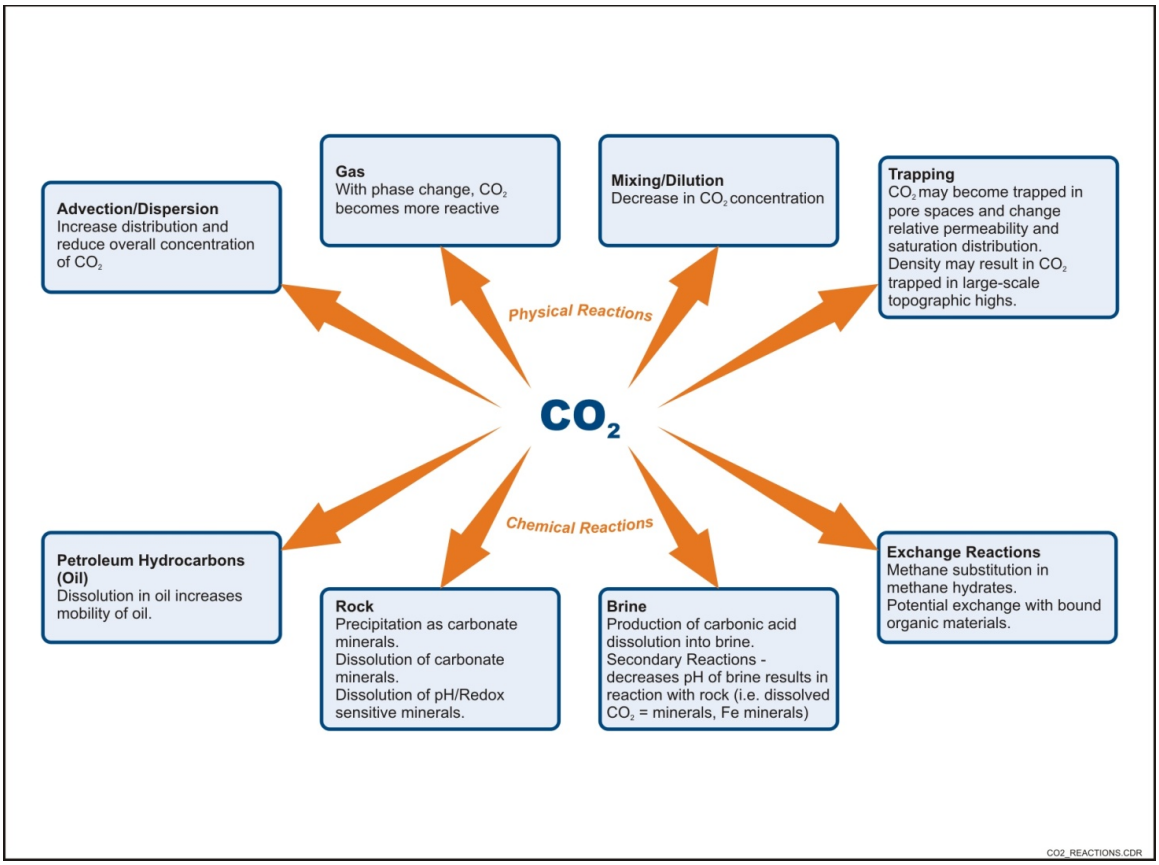

Figure 1-1. Potential Chemical and Physical Reactions involving CO_2 injected into Brine Solutions.

Geochemical tracers utilizing gas, brine, and isotope compositions are an important tool for in situ subsurface characterization, allowing detailed examination of complex systems with moving, mixing, and reacting components. For example, naturally occurring stable isotopes of the light elements (O, H, C, S, N) have been used extensively to determine the sources of fluid and gas species and their mechanisms of migration to assess the extent of fluid/rock interactions and to quantify the residence times of fluids in the subsurface (e.g., Boreham et al., 2011; Emberley et al., 2004; Mayer et al., 2013, 2015). Naturally occurring constituents and their isotopic compositions have a number of benefits for geochemical applications: (a) they commonly occur in a variety of earth materials, such as gas, brine, and rock; (b) sensitive mass spectrometric methods exist for quantifying their abundance and/or isotopic ratio; and (c) many of the necessary kinetic and equilibrium partitioning data are available to interpret these processes.

The proposed injection of large-volumes of CO_2 into different types of geological formations (e.g., aqueous, coal-bed, oil and gas fields) provides an opportunity for the use of isotope monitoring techniques with monitoring of general geochemical parameters to determine the fate of the CO_2. This is because the injected CO_2 can be treated as an applied tracer derived from anthropogenic or other sources, which should have a very distinct isotopic signature compared to that of background atmospheric CO_2, soil/groundwater CO_2, or the in situ CO_2. Stable isotopes have been used extensively and successfully as indicators in the hydrogeology, oil/natural gas exploration, and geothermal resource assessment (e.g., Cantucci et al., 2009; Kharaka et al., 2013; Kharaka and Cole, 2011; Kendall and McDonald, 1998; Tissot and Welte, 1984). By accounting for how stable isotopes of carbon and oxygen in CO_2 ($\delta^{13}C$ and $\delta^{18}O$) vary during the injection process, the complex geochemical processes are better

understood. Additionally, both short- and long-term consequences of subsurface CO_2 injection and sequestration, and possible leakage from the system, then can be quantitatively assessed and monitored. A complex set of physical and chemical reactions occurring among the gaseous, solution, and solid phases in the subsurface should be anticipated which, in turn, will lead to a variety of isotopic fractionation trends.

A number of processes can influence the chemical and isotopic signals in gas, fluids and solids, including mixing between fluid or gas in the reservoir, dissolution or exsolution of gases between brines and hydrocarbons, sorption onto mineral surfaces, microbially mediated reactions, fluid-rock interactions and mineralization. Changes may occur in the overall geochemistry and the isotopic signatures of the fluids or gas in the reservoir because of these geochemical mechanisms. Also, evidence of chemical changes may be observed through the analysis of rock core samples that could display evidence of precipitation or dissolution.

1.1 Purpose and Objectives

The overall purpose of the geochemical monitoring program under Midwestern Regional Carbon Sequestration Partnership (MRCSP) is to use stable and radiogenic isotope geochemistry in concert with analysis of general geochemical parameters of fluids and gases and analysis of core samples to determine geochemical processes occurring in the reef structure because of CO_2 injection. Specifically, brine and gas samples were collected and analyzed to determine changes occurring between reefs prior to and following CO_2 injection. The analytical results for general geochemical parameters were modeled with chemical equilibrium models to determine if the injection of CO_2 resulted in the mineral dissolution or precipitation. Finally, core samples were collected and analyzed to determine if there was evidence of dissolution features or mineral precipitation. Due to the unique isotopic signature of the injected CO_2, isotopic analyses of the CO_2 in the gas and the dissolved inorganic carbon in the brine were used as tracers to monitor changes in the geochemistry and as an indicator of mineral precipitation resulting from the injection of CO_2.

1.2 Geochemistry Study Sites

The MRCSP geochemical study focused on three Silurian pinnacle reefs in the Northern Niagaran Reef Trend (NNRT) near Gaylord, Michigan—Dover 33, Charlton 19, and the Bagley Field (Figure 1-2). These reefs are typical of Silurian Niagaran pinnacle reefs that form a northern and a southern trend— both are curvilinear and situated along the perimeter of the Michigan Basin. The reefs that were studied are three of more than 700 pinnacle reef structures in the NNRT that follow a SW-NE trending band approximately 150 miles long. These carbonate reef structures are typically 300 to 600 feet tall and vary in areal extent from 50 to 400 acres. These reefs are generally buried at depths of approximately 3,000 to 7,000 ft below surface.

A recent geological model for Silurian pinnacle reef structures suggests that they are asymmetrical in shape, with a sedimentary rock apron situated along the flanks of a carbonate reef core whose slope and lateral extent depend on paleowind direction (Rine et al., 2016). Much of the reef carbonate facies have been dolomitized, more extensively in the southern trend. Within the NNRT, there is less dolomitization, with more calcite comprising reefs located closer to the center of the basin (Rine et al., 2016). Approximately 400 million barrels of oil (an estimated 25 percent of oil in place in the northern reef trend) were produced from these structures over four decades of production, indicating significant potential oil reserves that could be extracted by EOR.

The reefs studied as part of the geochemistry effort have been operated through the primary production phase and are currently in a tertiary recovery phase where CO_2 is used to enhance the recovery of the remaining oil. The CO_2 used for the EOR activity is sourced from the stratigraphically shallower Antrim Shale (Toelle et al., 2008). This gas had not been analyzed for its isotopic composition prior to the start of the MRCSP Phase III injection tests, though there have been several studies that have focused on the composition of gas from the Antrim Shale (e.g., Martini et al., 2008). The CO_2 that was injected for the EOR was typically recycled through several nearby reef structures to a gas processing facility (Dover 36 GPF) to recover the oil and reuse the gas.

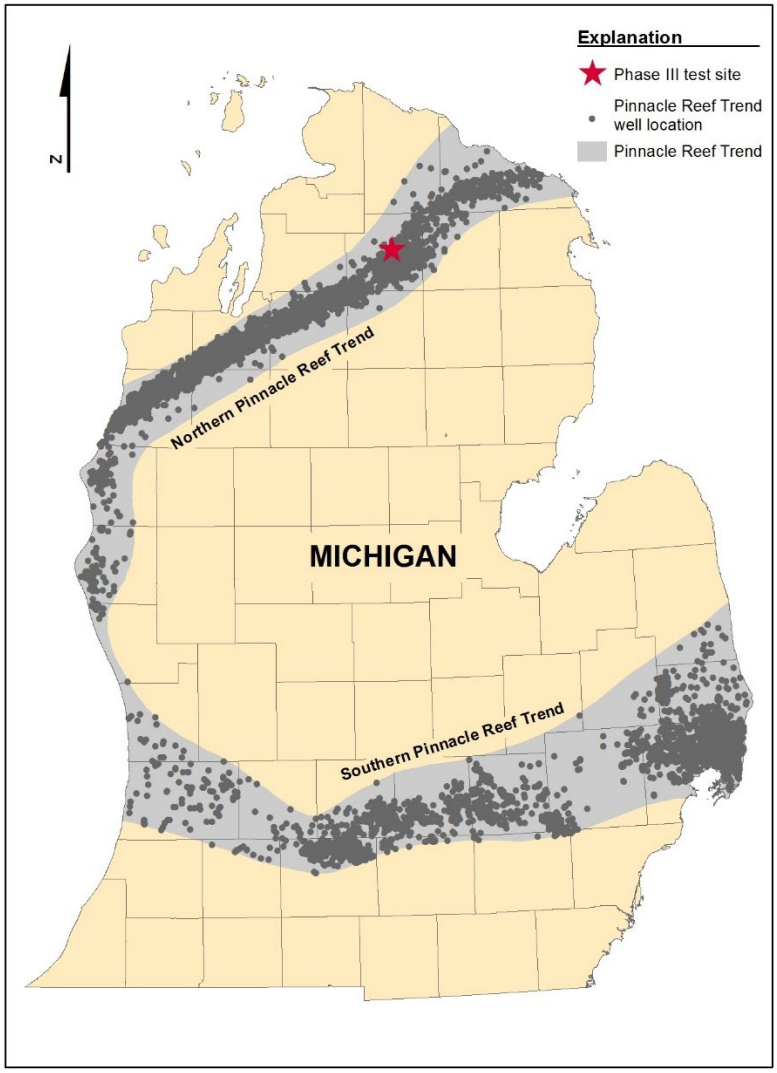

Figure 1-2. Location of the Reefs Studied for the MRCSP Geochemistry Study within the Northern Niagaran Reef Trend.

1.2.1 Dover 33

The Dover 33 reef serves as a late-stage reef (i.e., it has received significant CO_2 injection for nearly two decades prior to the start of the geochemical monitoring) for the geochemical study. From January 1996 through December 2008, approximately 1.29 million tonnes of CO_2 were injected into the reef, and prior to the MRCSP Phase III injection study, approximately 200,000 tonnes of this CO_2 were retained in the reef.

From January 2008 through December 2012, there was much lower activity in this reef as compared to the previous 12-year interval (Kelley et al., 2014).

The Dover 33 reef structure covers approximately 100 acres and has a height of approximately 260 feet. The depth to the top of the reef is approximately 5,400 feet. There currently are four wells within the reef and one in adjacent area that were used to collect fluid and gas samples throughout the course of this study (Figure 1-3). Due to the different casing and directional configurations and changing physical conditions (fluid/gas levels and pressures) in these wells, the sampling techniques and the ability to collect samples were different throughout the study (discussed in Section 2.1). Brine samples also were collected from the Fieldstone 2-33 well, which is in a lobe of the Dover 33 reef that is semi-isolated (hydraulically) from the main reef. This structure and well experienced increased pressure during the injection tests conducted during the MRCSP Phase III experiments. However, since it was isolated by the geologic structure, it was not believed to be in contact with the injected gas.

Over the course of the MRCSP geochemistry study, approximately 244,000 tonnes of CO_2 were injected into the L-M 1-33 well between February 2013 and August 2014 at rates of approximately 100 to 1,000 tonnes/day to investigate CCUS and reef integrity. The injection of CO_2 was not consistent, but instead performed during several periods (often lasting months) followed by down periods that allowed for other CO_2 monitoring activities (microseismic, wireline logging, gravity surveys, etc.) to occur, as well as reservoir pressure monitoring to determine how the reef would respond to CO_2 injection. The “baseline” geochemical sampling was done in the weeks prior to restarting CO_2 injection in the reef, and then further sampling of gas and fluids for geochemical monitoring was done over the next four years. Although CO_2 was injected as a supercritical fluid, pressure and temperature measurements in the reef structure (made using downhole pressure/temperature gauges) suggest that phase changes occurred over time, from vapor to liquid and then back to a supercritical fluid, as pressure increased. These past and current engineered activities all make monitoring and interpreting the fate of CO_2 and its interaction with the brine very challenging.

The injection well (L-M 1-33) is a vertical well located near the center of the reef. The total depth of this well is 5,662 feet, which extends into the Gray Niagaran Formation. Prior to the start of the MRCSP Phase III injection study, fluid filled the well, allowing brine and oil samples to be collected. However, after CO_2 injection started (February 2013), the fluid was displaced by the CO_2, and only gas (primarily CO_2) samples could be collected from this well.

The L-M 2-33 monitoring well has a total length of 7,134 feet measured depth (MD). The surface completion of this well is along the eastern edge of the reef, but a horizontal uncased (lateral) extends to the north and west of the well and continues across the northern portion of the reef (Figure 1-3). There is an uncased lateral section of the well (extending from 5,768 to 7,134 feet MD) that acts as a perforated zone over the entire length and is used to monitor the reef at a depth of approximately 5,500 feet true vertical depth. Based on field observations and analysis of samples collected from the L-M 2-33 well, it appears that the lateral portion of the well, or at least the end of the tubing, is contained within the water saturated zone of the reef. Gas samples could be collected from the wellhead, but the pressure of the samples was near atmospheric and the gas composition was significantly different than the gas collected from the L-M 1-33 injection well or the L-M 5-33 monitoring well. During the baseline sampling, fluid samples could only be collected by swabbing the well, and therefore, were collected under minimal pressure. Toward the end of the geochemical study, the tubing was filled with formation brine all the way to the surface (suggesting the end of tubing was below the water level in the reservoir).

The L-M 5-33 monitoring well is a deviated well that has a total depth of 6,450 feet MD and is oriented at an angle of approximately 80 degrees in the lower 1,300 ft of the well. The wellhead location for this well is also along the eastern side of the reef, but the well deviates to the southwest. This well is perforated

within the Brown Niagaran section of the well. Initially, the L-M 5-33 well was equipped with a pump jack that could be used to produce gas and brine samples under pressures similar to reservoir conditions. However, within six months of CO_2 injection, the reservoir pressures had increased to a level such that only gas (primarily CO_2) was being pushed to the wellhead. Subsequently, only gas samples could be collected from the well.

The Lawnichak 9-33 well was installed during 2016 as part of the MRCSP research with the surface completion along the western flank of the reef. This well was completed to a total depth of 6,085 ft (MD), and deviates toward the northeast in the lower portion of the well. Even with the deviation, the well is completed along the western flank of the reef and is only perforated in the Brown Niagaran Formation. This well was used to collect post-injection gas and brine samples. Both samples were collected shortly after the well was completed (December 2016).

The Fieldstone 2-33 well is in a small lobe of the Dover 33 reef that is partially hydraulically isolated from the main reef. Based on pressure responses in the well, there appears to be some hydraulic connectivity between this lobe and the main lobe of the reef; however, there is no indication of the migration of CO_2 from the main lobe to the southern lobe. In addition, the Fieldstone 2-33 well is not owned by Core Energy, so only limited monitoring and testing occurred in this well.

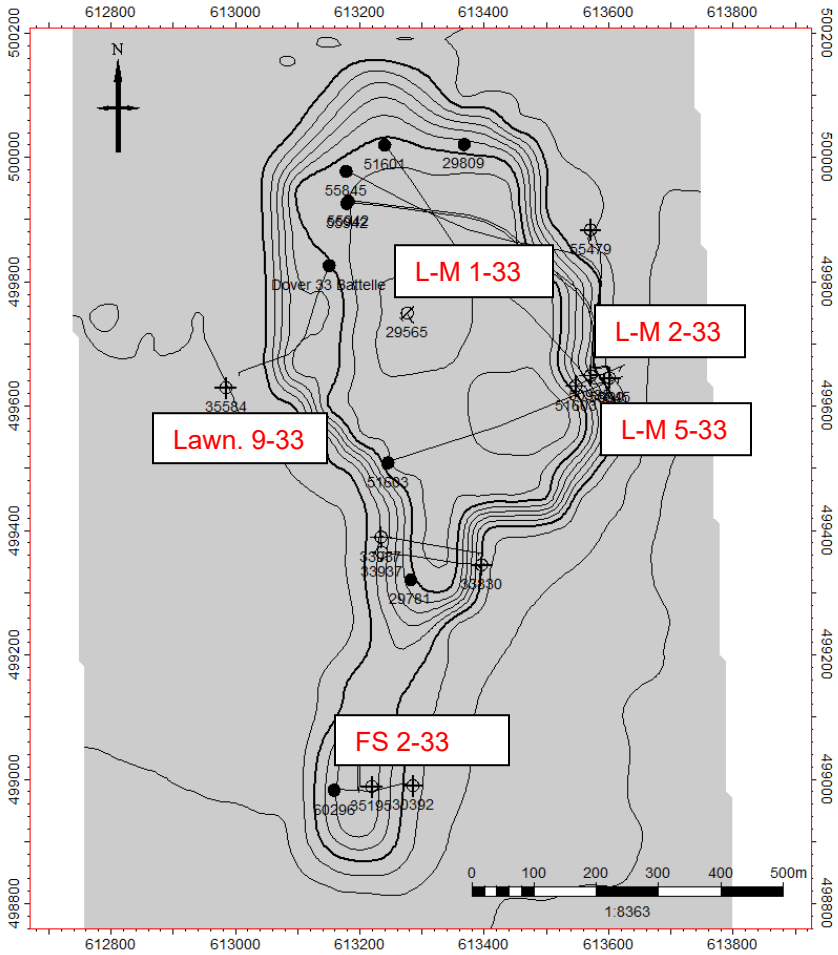

Figure 1-3. Map of the Dover 33 reef Showing Wells included in the Geochemistry Study. L-M 1-33 (29565), L-M 2-33 (55942), L-M 5-33 (51603), Lawnichak 9-33 (35584), and Fieldstone 2-33 (60296).

1.2.2 Charlton 19

The Charlton 19 reef had produced oil through primary production and served as a true baseline condition (sampled prior to any CO_2 injection) for the geochemical study (Figure 1-4). The baseline samples were collected from the Charlton 19 (El Mac Hills) well in January 2015, approximately two months prior to starting CO_2 injection into the reef. The wells also were sampled following approximately 42 months of CO_2 injection and the production of oil from the reef, allowing geochemical conditions resulting from CO_2 injection to be determined in June 2018. During this injection period, a total of approximately 285,000 tonnes of CO_2 were injected into the reef. Due to the relatively low pressures in the reef (approximately 100 psi) at the time the baseline samples were collected, the injected CO_2 would have initially been in gaseous phase and converted to a supercritical fluid over time as pressures increased to 1,700 psi. Over the 42-month injection phase, CO_2 was typically injected at rates between 50 and 650 tonnes/day.

The Charlton 19 reef structure consists of two pods: a larger reef to the north and a smaller lobe to the south, which when combined cover approximately 300 acres with a height of approximately 330 feet. The depth to the top of the reef is approximately 5,400 feet from ground surface. There are currently three wells within the reef that were used to collect fluid and gas samples throughout the course of this study—El Mac Hills (EMH) 1-18, EMH 2-18, and EMH 1-19D (Figure 1-4). Note that one of the wells (EMH 1-18) was found to be damaged and was replaced between the baseline and repeat sampling events (EMH 1-18A), but the new well was located at the same place as the original and would likely produce similar data. Due to the differences in the well configurations between the three wells and the changing physical conditions (fluid/gas levels and pressures) in these wells, the sampling techniques and the ability to collect samples were different throughout the study (discussed in Section 2.1).

The injection well for the Charlton 19 reef is the EMH 2-18 and it is in the northern pod of the reef. This well is deviated and has a surface location near the western edge of the reef, but deviation allows the bottom of the well to be near the core of the reef. The total measured depth of this well is 5,555 feet, which extends into the Gray Niagaran Formation. However, the well is perforated across the Brown Niagaran and A1 Carbonate Formations. Prior to the start of the geochemical study, there was only a small volume of fluid present near the bottom of the well, and the pumping system was inoperable, so only gas samples were obtained from this well.

The EMH 1-18 is a vertical well that is also located in the northern pod of the reef and is positioned along the eastern side of the reef. This well is currently being used as a production well and served as a monitoring well for the geochemical study. Following the collection of the baseline brine and gas samples (in January 2015), a defect was found in the well, and the well needed to be abandoned. This well was then replaced with a sidetracked well in mid-2017 (EMH 1-18A). The new well has a total depth of 5,463 ft, which extends into the Gray Niagaran Formation; however, the well is only perforated in the Brown Niagaran section.

The EMH 1-19D is a deviated well, installed near the core of the southern lobe of the reef has a total depth of 5,496 feet MD. Pressure monitoring results suggest that the southern lobe of the Charlton 19 reef has a limited hydraulic connection with the northern lobe, which indicates that movement of the injected CO_2 from the northern lobe to the southern lobe is unlikely. Therefore, analytical results from the baseline and repeat samples were not expected to display significant differences despite the 285,000 tonnes of CO_2 injected into the reef complex.

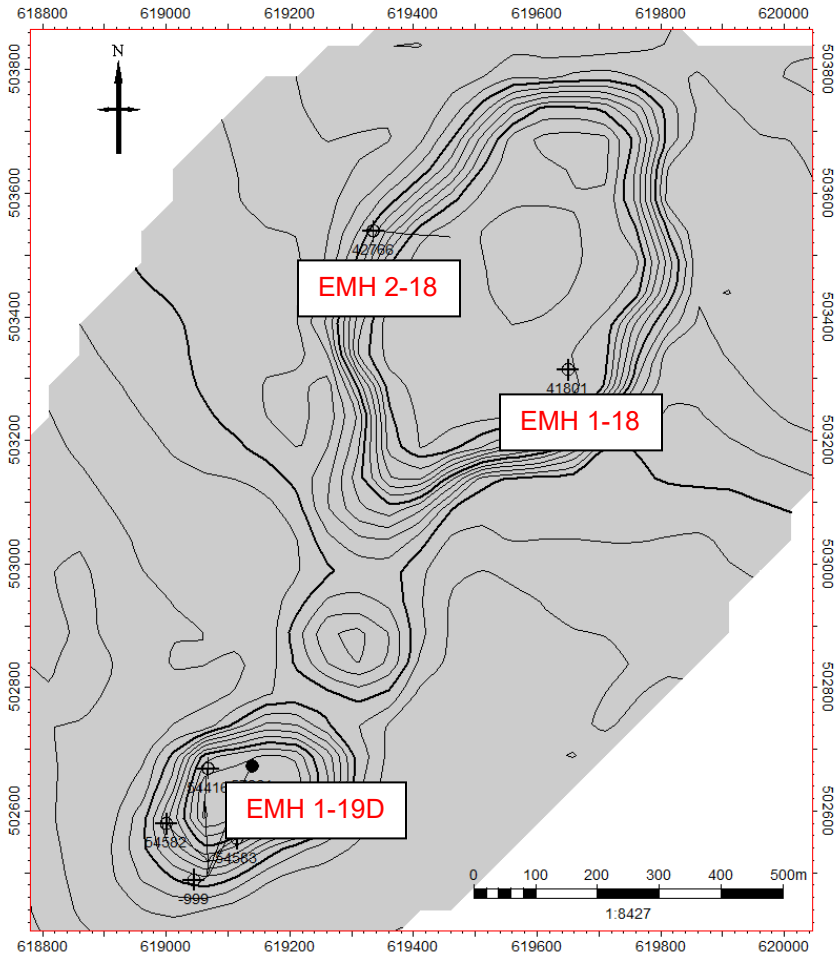

Figure 1-4. Map of the Charlton 19 Reef Showing Wells Included in the Geochemistry Study. EMH 1-18/EMH 1-18A (41801), EMH 2-18 (42766), and EMH 1-19D (57261).

1.2.3 Bagley Field

The Bagley Field reef complex also was used to collect true baseline geochemical samples in October 2015, but post-CO_2-injection samples were not able to be collected from this reef due to the well conditions/configurations. Therefore, the samples collected from the Bagley Field only provide baseline conditions prior to CO_2 injection. Following the collection of the brine samples, approximately 485,000 tonnes of CO_2 were injected into the reef complex between January 2016 and March 2018 (when resampling was attempted), typically at a rate between 300 and 800 tonnes/day. As with the other two reefs used in the geochemical study, the Bagley Field complex started out with low pressures following primary production (<100 psi at the time the baseline samples were collected) and increased to approximately 900 psi by March 2018.

The Bagley Field complex consists of three pods extending in a southwest to northeast direction and covers an area of approximately 1,200 acres. The heights of the pods in this complex are nearly 350 feet, and the depth to the top of the reef is approximately 5,900 feet from ground surface. There are seven wells within the reef complex, but only two were sampled for the geochemistry study (Figure 1-5). These two wells are in the northern pod of the complex, along with the injection well for this pod (Daughters of

Friel 2-11). The samples that were collected from the two wells were collected via the downhole pump/pump jack that was used during primary production.

The Janik-Mackowiac (J-M) 1-11 provided a well to collect baseline samples from the Bagley Field and is in the northern pod of the complex. This well is a deviated well that was used as a monitoring well throughout the geochemical study. The surface location for the J-M 1-11 well is along the eastern flank of the reef, but the trajectory of the deviation places the bottom of the well within the southern portion of the reef core. The total depth of the J-M 1-11 is 6,326 feet MD (within the Gray Niagaran), but the well is perforated across the A1 Carbonate and Brown Niagaran Formations. The formation of salt plugs in the tubing of this well prevented the collection of repeat geochemical samples.

The Janik-Stevens (J-S) 3-11 well also is located within the northern pod of the reef complex and was used to collect baseline geochemical samples. The surface location of the J-S 3-11 well is along the eastern flank of the reef, but the well is deviated to the southwest, so the bottom of the well is located near the eastern core of the reef. The total depth of the well extends to the Brown Niagaran Formation at a depth of 6,045 feet below ground surface, and the well is perforated only in the Brown Niagaran Formation.

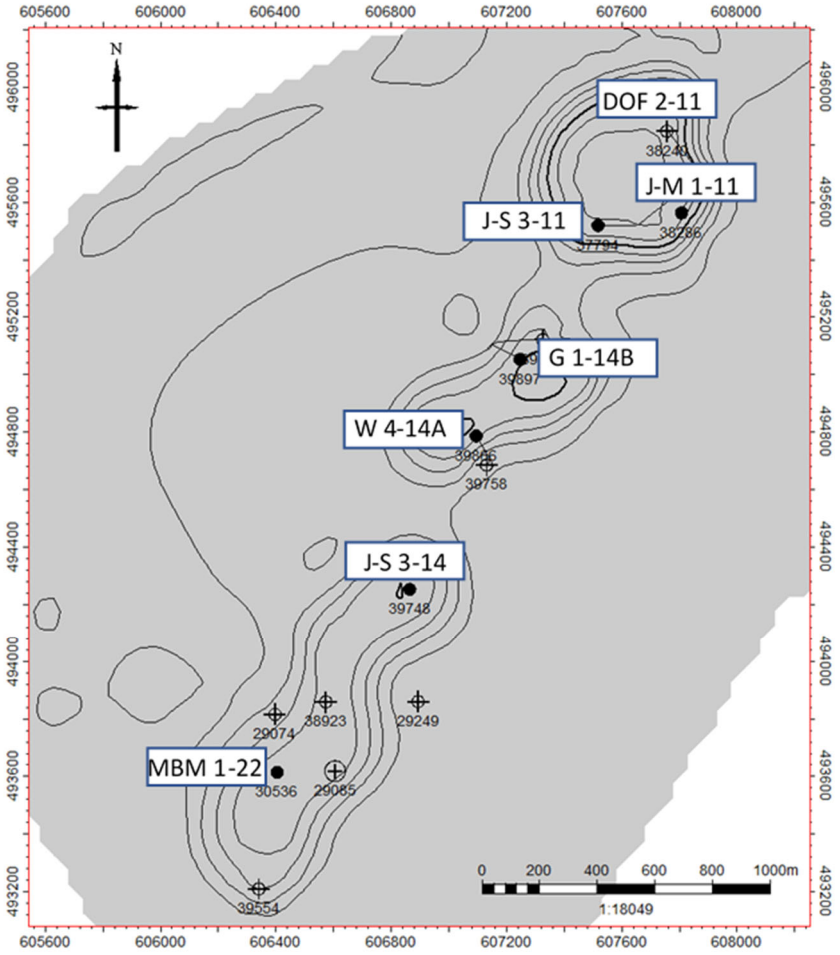

Figure 1-5. Map of the Bagley Field Reef Complex Showing Wells included in the Geochemistry Study. J-M 1-11 (37794) and J-S 3-11 (38286).

2.0 Brine, Gas, and Core Sampling Methods

2.1 Brine Samples Collected and Methods

Brine, gas, and core samples were collected from the three reefs included in the geochemical study: Dover 33, Charlton 19, and Bagley Field. Table 2-1 shows the samples that were collected from each reef. Brine and gas samples were collected from each of the wells in the Dover 33 and Charlton 19 reefs, and two wells in the Bagley Field were used to collect brine and gas samples. A single core sample was collected from the Lawnichak 9-33 well in the Dover 33 reef.

Table 2-1. Sample locations for the brine, gas, and core samples

Reef/ Well ID	Brine Sample	Gas Sample	Core Sample
Dover 33			
• L-M 1-33	X	X	
• L-M 2-33	X	X	
• L-M 5-33	X	X	
• Lawnichak 9-33	X	X	X
• Fieldstone 2-33	X		
Charlton 19			
• EMH 1-18	X	X	
• EMH 2-18	X	X	
• EMH 1-19D	X	X	
Bagley Field			
• J-M 1-11	X	X	
• J-S 3-11	X	X	
• Glasser 1-14B		X	
• Wrubel 4-14A		X	

2.1.1 Dover 33

A total of nine brine samples were collected from the five wells within the Dover 33 reef. Sampling was performed prior to restarting CO_2 injection and then repeat samples were collected throughout the remainder of the study. Table 2-2 shows the dates that brine samples were collected from the Dover 33 reef and the analyses that were performed on those samples. See Figure 1-3 for the locations of the wells in the Dover 33 that were sampled.

Baseline samples of brine were collected in October/November 2012 and were analyzed for a complete suite of analyses (general geochemistry, water isotopes, CO_2 isotopes, and water isotopes). The samples from the L-M 1-33 and L-M 2-33 wells were collected via a swab method, and two to three casing volumes were swabbed from the well prior to sample collection to sufficiently purge stagnant water from the well. The initial sample from the L-M 5-33 was collected using the downhole pump/pump jack present at the well. This system permitted the collection of brine samples at near-reservoir pressures; however, following the collection of the sample at 400 psi, the brine was transferred to unpressurized bottles for processing. Here there was notable degassing of the sample, which may have resulted in changes to the overall geochemistry in the sample. In addition, degassing likely occurred in the samples from the L-M 1-33 and L-M 2-33 because these samples sat for approximately two hours to permit breakdown of the oil-brine emulsions. Following the collection of the baseline samples in 2012, the remainder of the brine samples to be analyzed for ^{13}C isotopes were preserved with a $NH_4OH/SrCl_2$ solution to stabilize the CO_2 in the samples and prevent fractionation of the carbon isotopes through volatilization.

Table 2-2. Brine Samples Collected from the Three Reefs as Part of the Geochemistry Study

Well ID	Sample Date	Analyses			$SrCl_2$
		Major Ions	Trace Metals	^{13}C	
L-M 1-33	10/11/12	X	X	X	-
L-M 1-33	10/23/12	X	X	X	-
L-M 2-33	11/7/12	X	X	X	-
L-M 2-33	8/21/13	X	X	X	X
L-M 2-33	12/16/13	X	X	X	X
L-M 5-33	11/14/12	X	X	X	-
L-M 5-33	8/23/13	X	X	X	X
Fieldstone 2-33	5/2/16	X	X	X	X
Lawnichak 9-33	12/7/16	-	-	X	X
EMH 1-18	1/28/15	X	X	X	X
EMH 1-18A	6/21/18	X	-	X	X
EMH 1-19D	2/6/15	X	X	X	X
EMH 1-19D	6/21/18	X	-	X	X
J-M 1-11	10/14/15	X	X	X	X
J-S 3-11	10/12/15	X	X	X	X

The bulk brine sample was filtered under positive pressure using a 0.45-µm capsule filter and distributed into several bottles for specific analyses (Figure 2-1). The samples to be analyzed for cations and trace metals were acidified with trace metal grade nitric acid. The samples for anions, pH, alkalinity, total dissolved solids, dissolved inorganic carbon (DIC), and specific gravity analyses were not preserved in the field. Following the processing of the individual samples, the samples were placed on ice and shipped to the analytical laboratories (OSU, ALS, or Intertek, depending on the timing of sample collection and the specific analysis to be performed).

Repeat sampling at select wells within the Dover 33 reef was conducted in August 2013, December 2013, May 2016, and December 2016. The L-M 2-33 and L-M 5-33 wells were sampled in August 2013, and only the L-M 2-33 well was sampled in December 2016. Samples could not be collected from the L-M 1-33 after the baseline sampling was performed because the injected CO_2 pushed the brine away from the well. Later in the project, brine samples were collected from the Fieldstone 2-33 and Lawnichak 9-33 wells in May and December of 2016, respectively. All the repeat samples were collected using a swabbing method to bring the samples to surface; therefore, the samples were all collected at atmospheric pressures. The samples to be analyzed for ^{13}C isotopes were preserved with $NH_4OH/SrCl_2$ to prevent degassing and fractionation of the CO_2. The remainder of the samples were filtered with a 0.45 µm canister filter and the metals and trace element samples were acidified with nitric acid before distributing the samples to individual containers for specific analyses.

Figure 2-1. Preparation (Filtering) of the Brine Samples.

2.1.2 Charlton 19

Baseline and repeat brine samples were collected in January 2015 and June 2018, respectively, from the EMH 1-18 and EMH 1-19D wells in the Charlton 19 reef (see Table 2-2). Attempts were made to collect baseline samples from the EMH 2-18, but the pump in the well was not working, making sample collection unfeasible. The baseline samples from these two wells were collected using the downhole pump/pump jack systems that were present at the wells; therefore, the samples were collected under atmospheric pressures. Note that the reservoir was also under low pressure (<100 psi) at the time the baseline samples were collected. The pumping systems were operated for a enough time to allow two to three casing volumes of brine to be purged from the well prior to collection of the samples. Although baseline brine samples could not be collected from the EMH 2-18 well in January 2015, brine samples were collected from the well using a bailer in July 2015, following approximately five months of CO_2 injection. The repeat brine samples from the EMH 1-18A and EMH 1-19D also were collected from the wells using a slickline operated bailer. All repeat brine samples would have equilibrated to atmospheric pressures by the time the sampler reached the wellhead.

All samples collected from the Charlton 19 reef were filtered (except those for ^{13}C analyses) and preserved according to the sampling protocols. All samples were filtered under positive pressure through a 0.45 µM cartridge filter, and the samples for cations and trace metals were preserved before filling separate bottles for individual analyses. The individual sample bottles were placed on ice and shipped to the laboratory via express delivery for analysis. Although the reservoir was at low pressure prior CO_2 injection during the baseline sampling event, the samples for ^{13}C analyses were preserved with $NH_4OH/SrCl_2$ to precipitate and stabilize the DIC present.

2.1.3 Bagley Field

Due to the well conditions when repeat sampling was attempted, (see Table 2-2) only baseline samples could be collected from the Bagley Field complex. The baseline samples were collected from the J-M 1-11 and J-S 3-11 wells in October 2015. The downhole pump/pump jack systems present at the wells were used to recover brine for geochemical analyses, and these samples were collected at atmospheric pressures. As was performed with the other samples, two to three casing volumes of brine were purged from the well prior to collection to remove stagnant water from the well and obtain brine from the formation. Additionally, the freshwater injection system that was used with these wells to prevent salt plugging of the tubing was shut off three days prior to sample collection to prevent contamination of the samples with fresh water.

Samples from the Bagley Field to be analyzed for cations, anions, trace metals and chemical/physical properties were filtered through a 0.45 µM cartridge filter under positive pressure and prior to preparing the individual samples. The samples to be analyzed for ^{13}C analyses were not filtered but were preserved with $SrCl_2$ to stabilize the carbonate/DIC present in the sample even though the samples were collected under low pressure conditions prior to CO_2 injection. The individual sample bottles were placed on ice and shipped to the laboratory via express delivery for analysis.

2.2 Gas Sampling Methods

A total of 32 gas samples were collected from 11 wells and from the Dover 36 GPF during the geochemical study—three samples from the L-M 1-33, six samples from the L-M 2-33 ,six samples (not including duplicates) from the L-M 5-33, three samples from the EMH 1-18(A), two samples from the EMH 1-19D, and one sample each from the Lawnichak 9-33, EMH 2-18, Wrubel 1-14A, J-S 3-11, J-M 1-11, and Glasser 1-14 wells. In addition, five gas samples were collected from the Dover 36 GPF from the pure, recycled, and comingled (mixture of pure and recycled gas) gas streams. Details about the collection of the gas samples are provided in Table 2-3 and the locations of the wells are presented in Figure 1-3 through Figure 1-5. These represent ‘pure’ CO_2 recovered from the Antrim Shale, gas that has passed through the reefs and subsequently been produced, and gas to be injected into the reefs, respectively.

Table 2-3. Details of the gas sample collection.

Sample Location	Sample Point	Sample Method
Dover 33		
• L-M 1-33	Wellhead Tubing	Flow-through cylinder
• L-M 2-33	Wellhead Tubing	Evacuated cylinder
• L-M 5-33	Wellhead Tubing	Flow-through cylinder
• Lawn. 9-33	Wellhead Tubing	Flow-through cylinder
Charlton 19		
• EMH 1-18	Wellhead Tubing	Flow-through cylinder
• EHM 2-18	Wellhead Tubing	Evacuated cylinder
• EMH 1-19D	Wellhead Tubing	Evacuated cylinder
Bagley Field		
• J-M 1-11	Wellhead Tubing	Flow-through cylinder
• J-S 3-11	Wellhead Tubing	Flow-through cylinder
• Glass. 1-14	Wellhead Tubing	Flow-through cylinder
• Wrub. 1-14A	Wellhead Tubing	Flow-through cylinder
Dover 36 GPF		
• Pure	Flow Line Tap	Flow-through cylinder
• Recycled	Flow Line Tap	Flow-through cylinder
• Comingled	Flow Line Tap	Flow-through cylinder

Prior to the start of the geochemistry study, gas was injected and then recycled through the Dover 33 and several nearby reef structures as part of the ongoing EOR process in these fields. After the injection began in the Dover 33 reef, there was no gas produced from this reef during the remainder of the geochemical study. Additional gas samples were collected from the three wells in the Charlton 19 reef prior to and following CO_2 injection to obtain baseline values for the gas composition and to investigate changes in the gas composition and ^{13}C values caused by the injection of CO_2. The repeat gas samples were collected following the injection of 285,000 tonnes of CO_2 into the reef and production of oil and gas from the reef. Gas samples collected from the Bagley Field were all collected following at least one year of CO_2 injection into the reef complex. The gas samples collected from the Dover 36 GPF provide information on the composition of the gas and ^{13}C values of the CO_2 prior to contact with the reef gases during the EOR efforts.

Gas samples from the reefs and the GPF were collected in Swagelok 300 ml stainless steel cylinders (Department of Transportation [DOT] rated 1800 psi) with valves on both ends. All gas sample cylinders had been evacuated in the laboratory prior to sampling. The samples collected at the wells were obtained from the injection/production tubing string at the wellhead (Figure 2-2), and the samples collected at the GPF were captured by connecting the sample bottles to sample taps in the main pipelines (Figure 2-3). Most of the cylinders were purged for several minutes with the sample gas in the field; however, several of the samples from the L-M 2-33 well were at low (atmospheric pressure) and were collected by allowing the gas to flow into the evacuated cylinder at the well head.

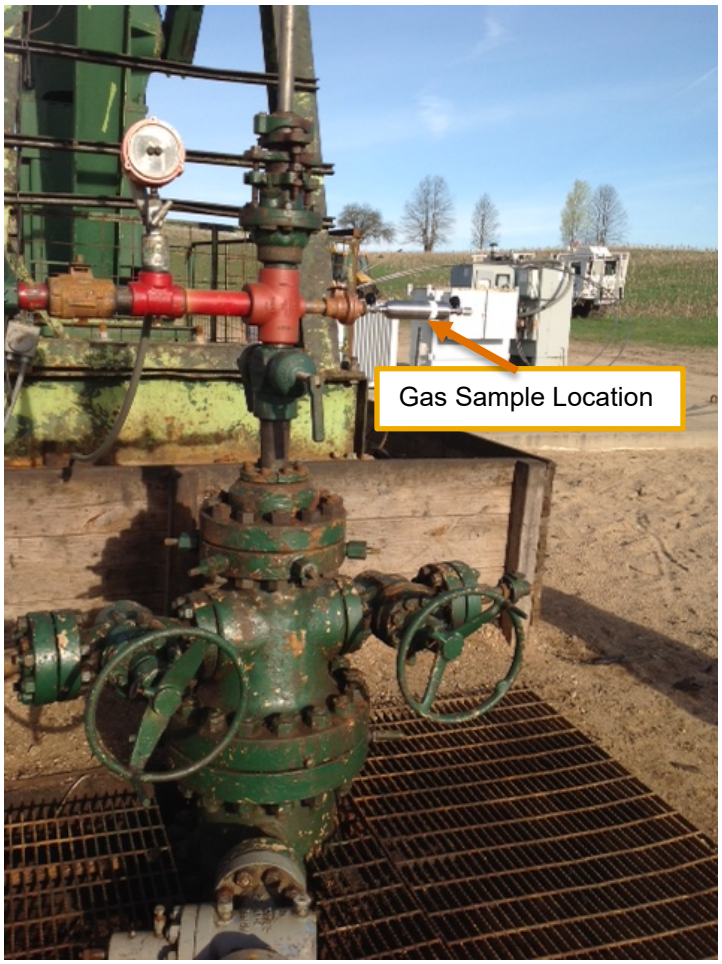

Figure 2-2. Collection of a Gas Sample from the Well Tubing.

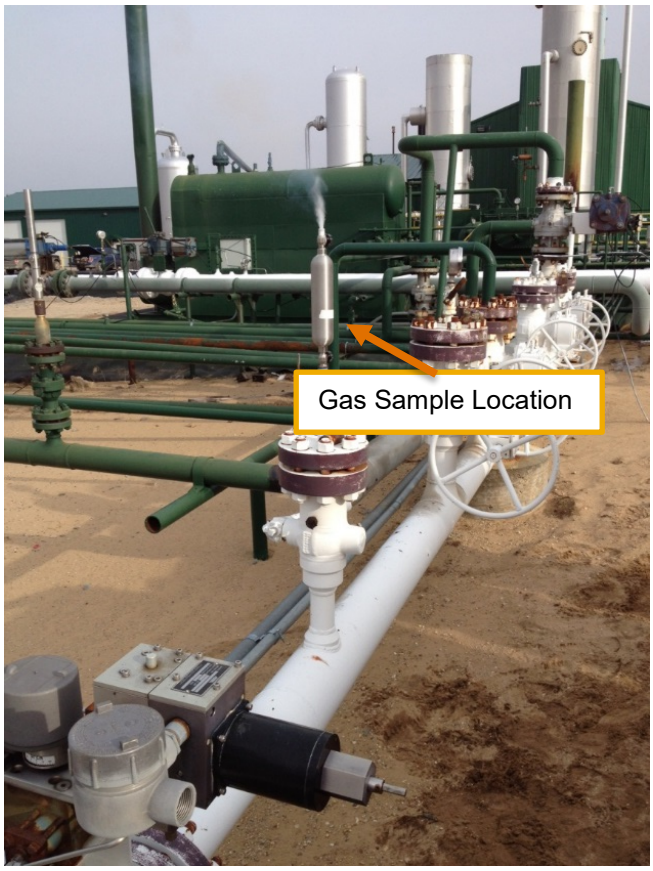

Figure 2-3. Collection of a Gas Sample from the Dover 36 Pure CO_2 Pipeline.

2.3 Core Sampling Methods

A total of 118.15 feet of whole core, divided into seven coring runs, was recovered from the Lawnichak 9-33 well. The cored interval spans a discontinuous section of the Brown Niagaran Formation between 5,525 and 5,763 feet MD (Table 2-4). Approximately 30 feet and 80 feet of drilling occurred between Core Runs #2 and #3 and between Core Runs #4 and #5, respectively. The core samples were acquired with a conventional 4-inch coring system fitted with aluminum liners. Upon retrieval of the core at ground surface, the core was cut into 3-foot lengths (still inside the aluminum liners) and were sealed to prevent desiccation of the samples. Plugs were selected from the whole core by inspecting the core of for fracture features or vugs that may contain evidence of precipitation or dissolution. Plugs were collected from the whole core at the core laboratory with a plugging bit and nitrogen coolant, and three plugs were selected for further analysis as part of the geochemistry study. The plugs were collected from the following depths: 5,606.1, 5,690.25, and 5,700.25 feet, and represent portions of the reservoir above, at, and below the oil/water contact surface.

Table 2-4. Conventional core acquisition parameters for Lawnichak 9-33

Core Run #	Coring Vendor	Start Depth (ft MD)	End Depth (ft MD)	Core Cut (ft MD)	Core Recovered (ft MD)	Core Recovery (%)	ROP (ft/hr)
1	ALS	5525	5559	34	33	97%	5.7
2	ALS	5559	5568	9	5.9	66%	1.5
3	ALS	5598	5608	10	8.4	84%	1.5
4	ALS	5608	5610	2	1.6	80%	0.4
5	Premier	5690	5718	28	27	96%	3.5
6	Premier	5718	5749	31	31.4	101%	3.9
7	Premier	5749	5763	14	10.85	78%	2.2

Whole core collection was difficult with several the coring runs and core recovery in Core Runs #2, #3, #4, and #7 did not generate full recovery. Therefore, sidewall cores were collected in the gaps between whole core samples in order to characterize the reservoir in these zones. Sidewall coring was performed with a wireline-operated coring tool that can position the core within ±0.5 feet of the target and collect cores of 3 inches in length by 1.5 inches in diameter. A total of 69 sidewall core samples were collected and three of those samples were selected for geochemical analysis (5,588 ft, 5,630, and 5,655 feet).

3.0 Analytical Methods

3.1 Brine Analytical Methods

Brine samples were analyzed for major and trace element composition of the brine, chemical/physical properties (e.g., pH, density), isotopic composition of water, $^{87}Sr/^{86}Sr$ ratios of dissolved Sr, isotopic composition of DIC, and chemical and isotopic composition of gas.

ALS-Kelso or Intertek Laboratories performed the general geochemical analyses on the brine samples using standard analytical methods. The analytical methods performed on the samples and the reporting limit for each analysis are presented in Table 3-1. Major ions in the brines were analyzed using inductively coupled plasma optical emission spectrometry (ICP-OES) or inductively coupled plasma mass spectrometry (ICP-MS) for cations, ion chromatography (IC) for anions, DIC using a carbon analyzer, and alkalinity by titration. Samples were diluted by 100 to 5000-fold in 2 % trace metal grade HNO_3 for analysis. Anion samples were diluted by 100 to 2000-fold with Milli Q™ water and then analyzed using a Dionex ICS-2100 Ion Chromatograph. Typical reproducibility for replicate samples for major element analysis was within 10%.

Table 3-1. Analytical Methods, Preservation, and Holding Times for the Individual Brine Analyses

Parameters	Method*	Preservation/Preparation	Container	Holding Time
Total Metals by ICP Na, K, Ca, Mg, Fe, Mn, Li, Al	200.7LL	HNO_3 to pH<2, Filter 4-µm	1.5 L Poly[a]	6 months
Total Metals by ICPMS Sb, As, Ba, Be, B, Cd, Cr, Cu, Pb, Ni, Se, Ag, Sr, Ti, Zn	200.8	HNO_3 to pH<2, Filter 4-µm	1.5 L Poly[a]	6 months
Anions Cl, SO_4, Br, F, NO_2, NO_3	300.0	Cool, 4±2°C, no chemical preservation	1 L Poly[b]	28 days
pH	M4500-H+ B	Cool, 4±2°C, no chemical preservation	1 L Poly[b]	None
Alkalinity	SM2320 B	Cool, 4±2°C, no chemical preservation	1 L Poly[b]	28 days
Total Dissolved Solids	M2540C	Cool, 4±2°C, no chemical preservation	1 L Poly[b]	7 days
Specific Gravity	SM2710F	None	1 L Poly[b]	None
Dissolved Silica	M4500 Si-D	Cool, 4±2°C, no chemical preservation	1 L Poly[b]	28 day
DIC	SM5310C	Cool, 4±2°C, Filter 4-µm,	100 mL Poly	7 days

*- EPA Methods provided and performed by ALS-Kelso.

Water isotope compositions were measured at Isotech Laboratory or at Ohio State University (OSU) using Picarro water isotope analyzers. The instrument at OSU uses a salt mesh to retain salts in the injection port of the vaporizer and an increased injection volume to account for the lower water content in these saline brines. The isotopic compositions of H and O for water are reported relative to Vienna Standard Mean Ocean Water (VSMOW). Typical precision for isotopic analysis for $\delta^{18}O$ and δD on water using the Picarro instrument at OSU are 0.5‰ and 2‰, respectively.

The isotopic composition of dissolved inorganic carbon was measured at the Subsurface Energy Materials Characterization and Analysis Laboratory (SEMCAL) at OSU using either an OI Analytical carbon analyzer or an Automate Autoprep sampler interfaced to a Picarro carbon isotope analyzer. Typical reproducibility for replicate analysis of $\delta^{13}C$ of DIC using the Picarro carbon isotope analyzer was approximately 1‰. Analyses were also done using a Thermo Scientific Gas Bench II interfaced to a Delta V mass spectrometer at SEMCAL for comparison to the results obtained from the Picarro. DIC analyses were initially done on fluid samples. However, because the isotopic composition of the DIC can change as the sample degasses, brines collected following the baseline event (Oct/Nov 2012) were preserved by coprecipitation with ammonia/$SrCl_2$ (Singleton et al., 2012). Stable carbon and oxygen isotope compositions are always reported as the difference between the ratios of the two isotopes of interest in the sample and the ratio in a primary reference standard. That is,

$$\delta X_{(sample)} = [(R_{sample} - R_{standard})/R_{standard}] \times 1000$$

Equation 3-1

where X represents the isotope of interest, ^{13}C or ^{18}O, and R represents the ratio of $^{13}C/^{12}C$, or $^{18}O/^{16}O$. The δ value is expressed in terms of per mil ($^{0}/_{00}$), or parts per thousand.

3.2 Gas Analytical Methods

Gas samples were analyzed for isotopic composition ($\delta^{13}C_{CO2}$, $\delta^{13}C_{CH4}$, δD_{CH4}, and $\delta^{18}O_{CO2}$) and major gas constituents (He, H_2, Ar, O_2, CO_2, N_2, CO, CH_4, C_2, C_2H_4, C_3, C_3H_6, iC_4, nC_4, iC_5, nC_5, and C_6+). Isotech Laboratory conducted analysis of concentrations and isotopic composition of major constituents in gas samples.

Concentrations of major constituents (hydrocarbons and fixed gases) were measured by gas chromatography (GC). Major gas concentrations were measured using either a Shimadzu 2010 Gas chromatograph or a Shimadzu 2014 Gas Chromatograph. For hydrocarbon analysis, helium is used as the carrier gas. The resulting component peak areas are quantified by the instrument control software, yielding raw percent values, by comparing them to previously run standards. The raw total can vary from day to day depending on atmospheric pressure, with acceptable raw total ranging from 96% to 104%. Once the baseline for each run is QA/QCd, the raw percentage values for each sample are normalized to 100%.

The $\delta^{13}C$ of CO_2 and CH_4, $\delta^{18}O$ of CO_2, and δD of CH_4 were measured by isotope ratio mass spectrometry. For $\delta^{13}C$ and δD of hydrocarbon gases, offline sample preparation is required prior to analysis. Natural gas samples must be separated into individual hydrocarbons of interest and then quantitatively converted to CO_2 and water for mass spectrometric analysis. Because $\delta^{13}C$ and $\delta^{18}O$ analyses are performed simultaneously using a Finnigan MAT Delta S IRMS. Isotope ratio determination involves multiple direct comparisons of the sample to a reference standard (generally at least six comparisons). Stable carbon and oxygen isotope compositions are always reported as the difference between the ratios of the two isotopes of interest in the sample and the ratio in a primary reference standard. That is,

$$\delta X_{(sample)} = [(R_{sample} - R_{standard})/R_{standard}] \times 1000$$

Equation 3-2

where X represents the isotope of interest, ^{13}C or ^{18}O, and R represents the ratio of $^{13}C/^{12}C$, or $^{18}O/^{16}O$. The δ value is expressed in terms of per mil (‰), or parts per thousand. Measurements of δD are performed similarly to carbon and oxygen, using a Finnigan Delta Plus XL IRMS where

$$\delta D_{(sample)} = [(^{2}H/^{1}H_{sample} - {}^{2}H/^{1}H_{standard})/^{2}H/^{1}H_{standard}] \times 1000.$$

Equation 3-3

The isotopic compositions of C and O for gas species are reported with respect to VPDB; H is reported relative to VSMOW. Typical precision for isotopic analysis is approximately 0.06‰ for $\delta^{13}C$ of CO_2 and CH_4, and 0.08‰ for $\delta^{18}O$ of CO_2. Analysis of the three higher pressure gas samples collected within several minutes of each other from the L-M 5-33 well had precision of 0.06‰ for $\delta^{13}C$ of CO_2, 0.06‰ for $\delta^{18}O$ of CO_2, 0.03‰ for $\delta^{13}C$ of CH_4 and 1.0‰ for δD of CH_4.

3.3 Core Analytical Methods

Core samples from the Lawnichak 9-33 well (Dover 33 reef) collected during the installation of the well were analyzed to investigate the presence of minerals that may have precipitated as the result of CO_2 injection in the reef, as suggested by the equilibrium model results. The SEMCAL at OSU was interested in studying cores above, near, and below the oil-water contact, estimated from resistivity log data to be between approximately 5,627 and 5,639 feet with a transitional region from oil to water between 5,643 and 5,685 feet (Table 3-2). In addition, $\delta^{13}C$ analyses were performed on select subsamples of the core to determine the isotopic values of the matrix carbonates and secondary mineral precipitates found in the rock. The core samples were analyzed using a Scanning Electron Microscope (SEM) to examine the fine details of the core samples and to determine the chemical composition of the bulk rock and precipitates that filled pores, veins and vugs that had been identified. Also, samples were viewed under a polarizing light microscope to determine mineral phases and textures of the rock. X-Ray Diffraction (XRD) analyses were performed on the rock samples to determine the mineralogy/crystallography of the samples. Both micro- and macro- X-Ray Computed Tomography (XCT) analyses were performed on the core samples to identify zones of the rock that may exhibit indications of dissolution or precipitation. All core analyses (except for the micro-XCT analyses) were performed by the SEMCAL at OSU. The micro-XCT analyses were performed by Lawrence Livermore National Laboratory. Finally, samples of the rock matrix and vug-filling precipitates were analyzed with mass spectrometry to determine the isotopic compositions of these materials.

Table 3-2. Overview of core subsamples used for geochemical analyses.

Core Depth (ft.)	Core Type	Core Position Relative to OWC	Formation	SEM	Light Microscope	XRD	XCT	$\delta^{13}C$
5,606.10	Plug	Above	B Niagaran	✓	✓	✓	✓	✓
5,690.25	Plug	Near	B Niagaran	✓	✓	✓	✓	✓
5,700.00	Plug	Below	B Niagaran	✓	✓	✓	✓	✓
5,588.00	Trim Cut	Above	B Niagaran	✓	✓	✓	✓	✓
5,630.00	Trim Cut	At OWC	B Niagaran	✓	✓	✓	✓	✓
5,655.00	Trim Cut	Transition	B Niagaran	✓	✓	v	✓	✓

3.3.1 Light Microscopy (LM)

Thin section samples of the Lawnichak 9-33 core were prepared and imaged using a Leica DMS 1000 digital light microscope and an Olympus SX50 polarizing light microscope. Difference in birefringence, pore distribution, and the presence of fractures were examined on the millimeter to centimeter scale. The blue-dyed epoxy that was used to impregnate the samples and stabilize them for grinding and polishing showed through pores, thereby enhancing areas with more pore space in the matrix. Low-magnification whole-slide analysis was conducted for all three trim samples. Using the photomicrographs, target areas of interest were later correlated with the slides' positions in the SEM for more detailed analysis.

3.3.2 Scanning Electron Microscopy (SEM)

A FEI Quanta 250 Field Emission Gun SEM was used to study the composition of the matrix carbonate, identify accessory minerals, examine textures of the rock matrix and the pore spaces, and view fractures on the micrometer scale. Pore spaces and fractures were observable due to the contrast between the dark epoxy base and the brighter matrix. Thin sections of all three depths were coated with electrically conductive carbon and adhered with copper tape to minimize charging in the SEM. Energy dispersive X-ray spectra acquired from spot analyses aided mineral identification, especially when combined with XRD analyses of the bulk specimens.

3.3.3 X-Ray Diffraction Analysis (XRD)

A PANalytical X'Pert Pro X-ray diffractometer available at SEMCAL was used for XRD analyses to determine bulk mineralogy of the three trim samples and composition of vug material for the 5,690 feet core plug sample (below oil-water interface). Corners were taken off the trim samples and ground by hand with an agate mortar and pestle to prepare the samples of the rock matrix. Vug-filling minerals from the plug sample were picked out by hand after the intact core was broken with a rock hammer. The mineral precipitates extracted from the vug were medium silt- to coarse sand-sized (0.02 mm to 0.4 mm) grains (determined by SEM images). For each sample, approximately one gram of material was loaded directly into standard sample holders for the SEM. Samples were scanned with CuKα radiation from 4.0 to 70.0º 2-theta, 0.02º 2θ per step (count time 20 seconds per step) at 45 kV, 40 mA. PANalytical HighScore Plus, Data Viewer, and PDF 4+ database were used for qualitative mineralogical analysis and determination of bulk composition.

In addition, XRD analysis was conducted on precipitates that were filtered from select brine fluid samples, and some select samples (matrix, vug, and fracture regions in core slabs) that were extracted for carbon isotope analysis.

3.3.4 X-Ray Computed Tomography Analysis (XCT)

Micro-XCT scans (resolution averaging tens of micrometers per voxel) of all three core plugs were produced, and 0.625 mm/voxel XCT scans of both core plug and trim samples (all six depths) were acquired. Fiji and Avizo were used for rendering 3D views by cropping, adjusting contrast, and then stacking the 2D image data. The purpose of studying the image contrast in 3D was to help identify mineralogical differences, vugs and high porosity areas potentially connected by fractures. Regions of interest were later correlated with position along the core using the slice number and resolution (625 microns along a voxel edge).

3.3.5 Solid-Phase Isotopic Analyses

Small subsamples of the core sample were analyzed for $\delta^{13}C$ of carbonate phases using a Picarro G1111-i Isotopic CO_2 analyzer. Small samples (approximately 50-500 of mg) were selected from bulk matrix of the core, phases that appeared to be secondary, veins, and surfaces of some of the larger vugs that had been identified in XCT scans.

4.0 Analytical Results, Equilibrium Modeling, and Discussion

4.1 General Geochemistry of Formation Brines

Table 4-1 summarizes the general brine chemistry for the wells sampled in the Dover 33 reef, Charlton 19 Reef, and the Bagley Field reef complex. The analytical results for general geochemistry from the samples reflect that they were collected from carbonate reservoirs with anhydrite/salt caprock layers (i.e., elevated concentrations of Ca, Mg, K, and Na, high alkalinity values, elevated concentrations of sulfate).

These conditions show the range of in situ chemistry in the reservoir during CO_2 injection. The brine samples collected prior to CO_2 injection display very high salinity and a low to neutral pH. Post-CO_2 injection samples show similar overall chemistry but with lower pH, suggesting that the injected CO_2 reacted with the brines to produce carbonic acid. The results of the general geochemical analyses are similar in composition to other reefs sampled throughout the Northern and Southern Niagaran Trends (Haagsma et al, 2020).

Figure 4-1 is a Piper diagram that indicates the chemical similarity of the major cation/anion concentrations between all samples collected throughout the geochemical study. All the samples (both pre- and post-CO_2 injection) plot in a similar location of the diagram showing that the injection of CO_2 does not significantly affect the overall chemistry of the brines. Although the reefs included in this geochemistry study are in relative proximity to one another, the Piper diagram also suggests that the general geochemistry of the reefs is not significantly affected by the geographic location of the reef and degree of dolomitization.

Table 4-1. General Geochemical Analytical Results from the Brine Samples Collected as Part of the Geochemistry Study.

Analyte	Analytical Result														
	L-M 1-33 10/11/12	L-M 1-33 10/23/12	L-M 2-33 11/7/12	L-M 2-33 8/21/2013	L-M 2-33 12/16/13	L-M 5-33 11/14/12	L-M 5-33 8/23/13	Fieldstone #1 5/2/16	Fieldstone #2 5/2/16	EMH 1-18 1/28/15	EMH 1-18A 6/21/18	EMH 1-19D 2/6/15	EMH 1-19D 6/21/18	J-M 1-11 10/14/15	J-S 3-11 10/12/15
Aluminum (µg/L)	<500	<500	<1,000	1,000	<1,000	<200	1,000	NA	NA	<250	NA	<250	NA	<500	<500
Arsenic (µg/L)	<5.0	<5.0	8.6	12.6	<5.0	<5.0	27.6	NA	NA	<5.0	NA	<5.0	NA	<5.0	<5.0
Antimony (µg/L)	37.1	18.2	6.06	5.4	31.3	13.1	11.7	NA	NA	33.5	NA	32.8	NA	<10.0	<10.0
Barium (µg/L)	606	800	382	402	776	332	1,370	NA	NA	788	600	2,240	800	733	664
Beryllium (µg/L)	1.15	1.23	1.01	0.2	<0.20	0.51	0.4	NA	NA	<0.20	NA	<0.20	NA	<0.20	<0.20
Boron (µg/L)	298,000	265,000	273,000	293,000	303,000	275,000	91,900	NA	NA	162,000	NA	216,000	NA	199,000	209,000
Calcium (µg/L)	95,200,000	86,400,000	84,900,000	88,800,000	87,500,000	99,400,000	47,100,000	72,550,000	71,850,000	67,500,000	54,052,300	87,200,000	61,028,700	107,000,000	110,000,000
Cadmium (µg/L)	<0.20	1.53	2.44	0.25	1.91	<0.20	4.69	NA	NA	<0.20	NA	1.3	NA	<0.20	<0.20
Chromium (µg/L)	23.9	11.5	111	37	2	41.2	33	NA	NA	9.4	NA	23.09	NA	4.6	<2.0
Cobalt (µg/L)	NA	NA	NA	35.3	7.29	NA	121	NA	NA	1.8	NA	7.4	NA	1.3	<0.20
Copper (µg/L)	41.7	21.6	50.4	286	95.5	4	12.8	NA	NA	<1.0	NA	7.1	NA	6.14	7.01
Iron (µg/L)	243,000	55,000	156,000	654,000	52,400	117,000	1,500,000	13,000	17,500	129,000	71,800	86,900	42,900	12,900	10,000
Lead (µg/L)	314	1,690	561	229	685	126	501	NA	NA	2.65	NA	71.8	NA	2.55	4.14
Lithium (µg/L)	NA	NA	NA	80,400	77,300	NA	57,000	10,000	10,000	70,500	NA	88,800	NA	78,000	82,000
Magnesium (µg/L)	11,200,000	9,980,000	10,900,000	10,700,000	11,000,000	8,060,000	8,550,000	7,985,000	7,990,000	8,850,00	7,078,400	11,500,000	7,742,200	11,400,000	12,100,000
Manganese (µg/L)	4,430	1,720	2,880	9,150	3,950	2,200	2,150	NA	NA	2,390	NA	2,680	NA	1,330	1,360
Nickel (µg/L)	55.1	18.9	88.2	326	76.1	28.7	343	NA	NA	103	NA	63	NA	23.1	22
Potassium (µg/L)	18,400,000	16,200,000	17,700,000	17,000,000	18,000,000	18,100,000	6,350,000	12,660,000	12,700,000	11,000,000	10,134,300	14,800,000	10,925,900	15,500,000	16,600,000
Silica (µg/L)	23.5	18.6	5.9	1.94	2.04	13.6	5	NA	NA	5.3	NA	14.6	NA	0.69	0.967
Silver (µg/L)	0.23	<0.20	<0.20	0.2	0.26	<0.20	33	NA	NA	<0.20	NA	<0.20	NA	<0.20	<0.20
Sodium (µg/L)	19,000,000	16,200,000	19,100,000	14,400,000	21,300,000	15,900,000	3,450,000	21,897,500	22,472,500	17,300,000	19,396,500	24,400,000	14,692,000	16,900,000	15,300,000
Selenium (µg/L)	<5.0	1.2	<5.0	5	<5.0	<5.0	<5.0	NA	NA	<5.0		<5.0	NA	10.7	13
Strontium (µg/L)	3,470,000	308,000	3,210,000	3,310,000	3,270,000	3,700,000	1,470,000	266,250	273,500	2,450,000	2,185,300	3,150,000	2,325,300	3,990,000	4,250,000
Zinc (µg/L)	1,100	1,720	1,510	4,100	21,800	1,880	2,760	NA	NA	103	NA	1,110	NA	452	695
pH	4.1	4.62	4.62	4.33	4.87	4.38	6.09	NA	NA	5.88	5.25	5.19	6.02	4.9	4.83
Salinity (g/Kg)	380	411	395	398	450	402	183	NA	NA	610	371	662	336	348	368
Conductivity (µmhos/cm)	164,000	162,000	535,000	186,000	168,000	589,000	179,000	NA	NA	192,000	193,000	191,000	190,000	52,700	51,900
Chloride (mg/L)	267,000	251,000	253,000	255,000	261,000	274,000	115,000	246,309	249,155	188,000	156,654	249,000	159,542	265,000	270,000
Bromide (mg/L)	ND	2,720	2,950	2,800	2,800	3,250	<0.10	2,638	2,648	2,280	NA	3,030	NA	2,810	2,940
Sulfate (mg/L)	134	150	126	44	45	143	424	96.7	97.1	81	57.3	157	39	152	83
Fluoride (mg/L)	0.3	0.34	0.34	0.22	0.24	0.32	0.77	0.39	0.34	<0.20	NA	<0.20	NA	0.26	0.2
Nitrite (mg/L)	<0.050	<0.050	<0.050	<0.050	<0.050	<0.050	<0.050	NA	NA	<0.050	NA	<0.050	NA	<0.50	<0.50
Nitrate (mg/L)	<0.050	<0.050	0.065	0.06	0.183	0.053	<0.050	NA	NA	<0.20	NA	<0.20	NA	<0.50	<0.050
TDS (mg/L)	423,000	422,000	453,000	447,000	405,000	446,000	205,000	NA	NA	312,000	NA	406,000	335,469	409,000	424,000
TOC (mg/L)	199	343	67	66	27	79	258	NA	NA	<50	NA	79	NA	<250	<25
TIC (mg/L)	40	82	83	<40	54	113	<200	NA	NA	<200	NA	<200	NA	<40	<20
DOC (mg/L)	183	295	42	73	16	79	227	NA	NA	<50	NA	66	NA	<250	<50
DIC (mg/L)	47	83	75	<200	47	110	ND	NA	NA	<200	NA	<200	NA	<40	<20
Alkalinity – CO3 (mg/L)	<9.0	<90	<9.0	<15	<15	<9.0	<9.0	NA	NA	322	0	384	NA	296	297
Alkalinity – HCO3 (mg/L)	357	631	515	<9.0	259	785	951	NA	NA	322	468.5	384	644	296	297
Specific Gravity	1.29	1.28	1.28	1.29	1.29	1.27	1.12	NA	NA	1.2	1.22	1.25	1.23	1.24	1.29
Charge Balance (%)	-3.8	-6.67	-5.5	-6.04	-5.2	-11.81	2.48	-11.61	-12.48	-1.83	1.003	-5.07	1.033	-0.55	-0.60

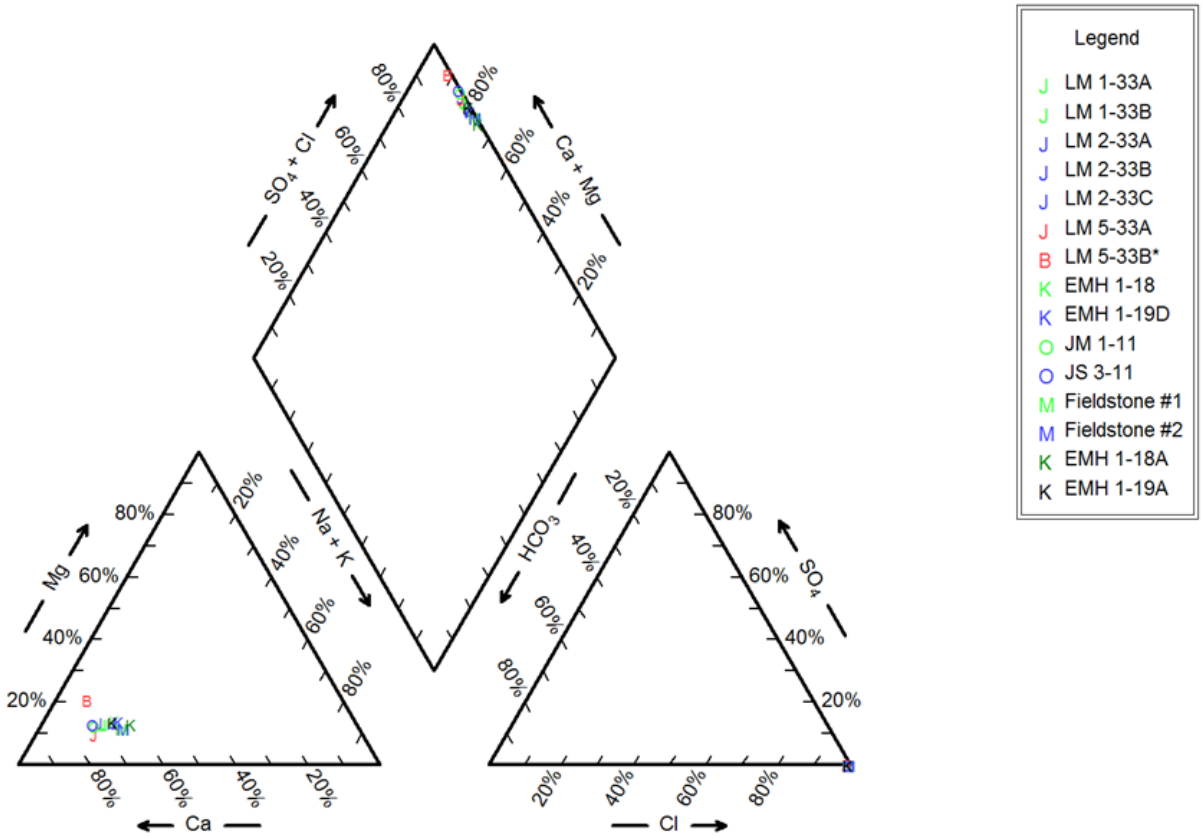

Figure 4-1. Piper diagram of the major cation/anion concentrations in the brine samples collected from the three reefs.

4.1.1 Discussion (Significance of Brine Geochemistry Analytical Results)

The water samples measured are Ca-Na-Cl brines with a total dissolved salt content of approximately 400 g/L. Apart from one sample collected on August 23, 2013 from a holding tank downstream from well L-M 5-33, the major element concentrations vary by less than 20 percent (Welch et al., 2019). Although the reefs included in this geochemistry study are in relatively close proximity, Figure 4-1 shows that the general composition of the reef brines is not significantly affected by geographic location. Because the results of the general geochemical analyses are similar to those of other reefs sampled throughout the Northern and Southern Niagaran Reef Trends (McNutt et al., 1987; Wison and Long, 1993 a.b.; Kharaka and Hanor, 2007; Haagsma et al., 2020), reef location and degree of dolomitization do not appear to influence brine chemistry.

4.2 Geochemical Equilibrium Modeling

PHREEQC Interactive, v. 3.4.0.12927 with the Pitzer database was used for geochemical speciation modeling, and the general geochemical results were converted to a mol per kg of water to be used in the geochemical equilibrium modeling (Table 4-2). The pH was determined at equilibrium using the alkalinity values and charge was balanced using sodium. Two model simulations were constructed to answer the following questions:

- What saturation state of minerals is expected to be present in the environment (Referred to in this text as the Equilibrium Model)?
- What minerals are precipitating from initial brine solution (Referred to in this text as the Equilibrium Phases Model)?

The *equilibrium model*, the simplest scenario, involves determining the minerals that are saturated, undersaturated, and supersaturated. This information can be used to determine the tendency for a mineral phase to precipitate, dissolve, or undergo no net change (i.e., at equilibrium). The equilibrium model is used to determine the stability of mineral phases of interest in cements, caprock, and reservoir rock when CO_2 is present.

The *equilibrium phases model* is designed to determine the amount of a mineral that will precipitate under given conditions. In addition to brine chemistry, the model requires defining mineral phases as "equilibrium phases." The model will then achieve equilibrium by precipitating or dissolving the defined mineral phases to achieve a log saturation index (SI) of 0 (equilibrium). These models can be configured in two ways—by defining no initial phases and allowing minerals to precipitate from the brine, and by defining initial phases equivalent to specific solids and allowing mineral phases to dissolve or precipitate to achieve equilibrium.

Table 4-2. Summary of brine geochemistry (moles per kg water).

Constituent	L-M 1-33	L-M 1-33	L-M 2-33	L-M 2-33	L-M 2-33	L-M 5-33	Fieldstone #1	Fieldstone #2	EMH 1-18	EMH 1-18A	EMH 1-19D	EMH 1-19D	J-M 1-11	J-S 3-11
	10/11/2012	10/23/2012	11/7/2012	8/21/2013	12/16/2013	11/14/2012	5/2/2016	5/2/16	1/28/15	6/21/18	2/6/18	6/21/15	10/14/15	10/12/15
Ca^{2+}	1.84	1.69	1.66	1.72	1.7	1.96	1.42	1.4	1.4	1.74	2.15	2.13	1.11	1.24
Mg^{2+}	0.36	0.32	0.35	0.34	0.35	0.26	0.26	0.26	0.3	0.38	0.38	0.39	0.239	0.259
Na^{+}	0.64	0.55	0.65	0.49	0.72	0.55	0.75	0.76	0.63	0.85	0.59	0.52	0.692	0.52
K^{+}	0.37	0.32	0.35	0.34	0.36	0.37	0.25	0.25	0.23	0.3	0.32	0.33	0.212	0.227
Sr^{2+}	0.031	0.003	0.029	0.029	0.029	0.033	0.002	0.002	0.023	0.029	0.037	0.038	0.02	0.022
Cl^{-}	5.85	5.54	5.58	5.58	5.72	6.1	5.44	5.5	4.42	5.63	6.03	5.91	3.62	3.66
SO_4^{2-}	0.0011	0.0012	0.001	0.0004	0.0004	0.0012	0.000788	0.000791	0.0007	0.0013	0.0013	0.0007	0.000489	0.00033
HCO_3^{-}	0.00352	0.00634	0.00517	0.0000388	0.00256	0.008	0.0061	0.0061	0.00368	0.00405	0.00316	0.00292	0.0063	0.00862
Br^{-}	--	0.027	0.029	0.027	0.027	0.032	0.026	0.026	0.024	0.03	0.028	0.029	--	--
$Fe^{2+/3+}$	0.0034	0.0008	0.0022	0.0091	0.0007	0.0017	0.000182	0.000245	0.0019	0.0012	0.0002	0.0001	0.001054	0.000625
SiO_2	6.50E-07	5.18E-07	1.64E-07	5.36E-08	5.64E-08	3.82E-07	2.00E-07	2.00E-07	1.57E-07	4.17E-07	1.98E-08	2.67E-08	1.59E-07	1.57E-07
pH	4.1	4.62	4.62	4.33	4.87	4.38	5.88	5.25	5.88	5.19	4.9	4.83	5.25	6.02
Alk[(a)]	357	631	515	4.5	259	785	455	455	322	468.5	384	644	296	297
Salinity[(b)]	380	411	395	398	450	402	--	--	610	371	662	336	348	368

Notes: Baseline (pre-injection) data obtained from samples from five wells in fields (or lobes) that have not seen CO_2: EMH 1-18 and EMH 1-19D in El Mac Hills (Charlton 19), Janik-Mackowiack 1-11, Janik-Stevens 3-11 in the Bagley Field, and the Fieldstone well (two samples) in the southern lobe of Dover 33. Post-injection data are from three wells drilled in the Dover 33 reef, which has had CO_2 injected since 1996: L-M 1-33 (two samples), L-M 2-33 (three samples), and L-M 5-33 (one sample).

a. Alkalinity is mg/L as HCO_3^{-}.

b. Salinity as g/kg.

General hydrologic conditions used as input into the geochemical models are presented in Table 4-3.

Table 4-3. General hydrologic conditions for the Michigan Basin.

Parameter	Reservoir
Depth (ft bgs)	6,000
Reef/Reservoir Thickness (ft)	18-280
Temperature (°F)	102
Pressure (psi)	3,000
Water Saturation (%)	20-30
Fluid Density (Specific Grav.)	1.12-1.29
Porosity (%)	3-11

a. Thermal gradient (depth [ft] x 0.01°F/ft + 40°F)
b. Pressure gradient (depth [ft] x 0.43 psi/ft + 14.7 psi)

4.2.1 Model Limitations

For all models, the Pitzer geochemical database and equations were used. Pitzer calculations are used for slightly higher activity brines than other geochemical calculations like extended Debye-Huckel; however, the activities of the brines of interest in this study are beyond the conditions normally used for Pitzer calculations. The Pitzer database also has fewer mineral phases than other available databases. Geochemical data for carbonate minerals that are likely present in the Michigan reefs are in the database; however, there are currently no iron bearing mineral phases or redox reactions included in this database.

4.2.2 Results

Based on their saturation indices at equilibrium and their likelihood of occurrence in the Niagaran reefs undergoing carbon dioxide enhanced oil recovery (CO_2-EOR), minerals were separated into carbonates and silicates for the presentation of data. Mineral saturation indices are shown in Table 4-4.

Table 4-4. Concentrations of selected ions and saturation indices of minerals.

Sample No.	Sample ID	Concentration (mol/kgw)				Carbonate Saturation Indices (SIs)					Silicate SIs	
		Ca^{2+}	Mg^{2+}	Si	HCO_3^-	Calcite	Aragonite	Dolomite	Huntite	Magnesite	Brucite	Talc
1	L-M 1-33 10/11/2012	1.84	0.36	6.5E-7	0.004	3.2	2.9	6.0	9.1	1.9	-1.3	3.1
2	L-M 1-33 10/23/2012	1.69	0.32	5.2E-7	0.006	3.5	3.2	6.6	10.2	2.2	-1.0	3.2
3	L-M 2-33 11/07/2012	1.66	0.35	1.6E-7	0.005	3.4	3.1	6.4	9.8	2.1	-1.1	1.1
4	L-M 2-33 8/21/2013	1.72	0.34	5.4E-8	3.9E-5	0.9	0.6	1.4	-0.3	-0.4	-3.3	-6.9
5	L-M 2-33 12/16/2013	1.70	0.35	5.6E-8	0.003	3.1	2.8	5.8	8.6	1.8	-1.4	-1.4
6	L-M 5-33 11/14/2012	1.96	0.26	1.6E-7	0.008	3.7	3.4	6.8	10.5	2.2	-1.3	2.2
7	EMH 1-18 01/28/2015	1.40	0.30	4.2E-7	0.004	3.0	2.7	5.6	8.2	1.7	-2.0	-1.8
8	EMH 1-19D 02/06/2015	1.74	0.38	2.0E-8	0.004	3.3	3.0	6.2	9.4	2.0	-0.3	4.8
9	J-M 1-11 10/14/2015	2.15	0.38	2.7E-8	0.003	3.2	2.9	5.9	8.8	1.8	-0.5	-0.8
10	J-S 3-11 10/12/2015	2.13	0.39	1.6E-7	0.003	3.1	2.8	5.8	8.7	1.8	0.9	2.1
11	EMH 1-18A 06/21/2018	1.11	0.24	1.6E-7	0.006	2.5	2.2	4.5	6.0	1.2	-3.9	-7.9
12	EMH 1-19D 06/21/2018	1.24	0.26	2.0E-7	0.009	2.3	2.0	4.2	5.3	1.0	-4.5	-9.7
13	Fieldstone #1 05/02/2016	1.42	0.26	2.0E-7	0.006	3.3	3.0	6.2	9.3	2.0	-2.5	-2.6
14	Fieldstone #2 05/02/2016	1.40	0.26	6.5E-7	0.006	3.3	3.0	6.2	9.3	2.0	-2.5	-2.5

4.2.3 Carbonate Minerals

All carbonate minerals are supersaturated in nearly every sample, controlled mainly by pH and, to a lesser extent, the concentration of bicarbonate (Table 4-5). The exceptions are huntite ($Mg_3Ca(CO_3)_4$) and magnesite ($MgCO_3$) in Sample #4 (L-M 2-33 / 21 Aug 2013). Solution #4 has the lowest concentration of bicarbonate and the second lowest pH value at equilibrium. Calcite is the only carbonate mineral that precipitates from any of the solutions; it precipitates from each of the solutions at a rate controlled by the concentration of bicarbonate(Table 4-5).

4.2.4 Hydroxide and Silicate Minerals

At least one silicate or hydroxide mineral is supersaturated in most samples, Exceptions include Sample #4 (L-M 2-33 / 21 Aug 2013), Sample #11 (EMH 1-18A / 21 Jun 2018), and Sample #12 (EMH 1-19D / 21 Jun 2018). These three samples have the lowest pH at equilibrium of all samples (less than 6.6).

Other silicate and hydroxide minerals were supersaturated in a more select group of samples. Brucite ($Mg(OH)_2$) was undersaturated in all solutions except Sample #10 (J-S 3-11 / 12 Oct 2015). Brucite also precipitated from this solution (Table 4-5). This solution has the highest calculated pH at equilibrium (8.5), suggesting that this mineral is stable in alkaline solutions.

Table 4-5. Precipitation of phases in each of the samples (•) and changes in pH and concentrations of constituents of interest.

No.	Sample	Brucite	Calcite	Changes from Initial Solution[1]			
				pH	HCO_3^-	Ca^{2+}	Mg^{2+}
1	L-M 1-33		•	▼	▼	▼	--
2	L-M 1-33		•	▼	▼	▼	--
3	L-M 2-33		•	▼	▼	▼	--
4	L-M 2-33		•	▼	▼	▼	--
5	L-M 2-33		•	▼	▼	▼	--
6	L-M 5-33		•	▼	▼	▼	--
7	EMH 1-18		•	▼	▼	▼	--
8	EMH 1-19D		•	--	▼	▼	--
9	J-M 1-11		•	--	▼	▼	--
10	J-S 3-11	•	•	▼	▼	▼	▼
11	EMH 1-18A		•	▼	▼	▼	--
12	EMH 1-19D		•	▼	▼	▼	--
13	Fieldstone #1		•	▼	▼	▼	--
14	Fieldstone #2		•	▼	▼	▼	--

Changes in pH of ±0.1 or more. ▼ indicates a decrease of pH **or decrease in** concentration with respect to initial solution. Changes in concentration attributable to numerical errors (i.e., changes in concentration without corresponding precipitation of minerals) not reported.

4.3 Formation/Injection Gas Analyses

As mentioned previously, the samples were collected from the wells and Dover 36 GPF prior to starting CO_2 injection and during injection. Sampling originally was planned to be undertaken as a time series to investigate the changes in the general and isotopic composition of the gas and fluids in the reef complex associated with CO_2 injection. However, after the initial samples were analyzed, gas samples were only obtained opportunistically in conjunction with other activities at the field sites. The initial samples collected from the Charlton 19 reef represent baseline conditions (prior to the injection of CO_2) to determine the original gas composition in the reefs, while the "pure" samples collected from the Dover 36 GPF provide the composition of the gas prior to injection into the reefs.

The gas samples that were collected during the geochemistry study from 2012 to 2018 were obtained under different reservoir pressures and EOR operating conditions. For example,

- the initial/baseline samples collected from the Dover 33 reef were collected under low pressures (atmospheric to 100 psi). However, following significant EOR operations with the long-term injection of CO_2, the subsequent sampling events occurred under increasing reservoir pressures.
- baseline gas samples collected from the Charlton 19 reef were collected under low reservoir pressures (near atmospheric), and prior to any CO_2 injection into the reef. The repeat sampling at the EMH 1-18A well was performed following approximately two to three years of CO_2 injection and the wellhead pressures at the time of collection (270 and 390 psi) were greater than those during the baseline sampling event.
- all gas samples collected from the Bagley Field reef were collected after approximately 220,000 tons of CO_2 were injected into the reef; therefore, the samples were collected under moderate pressures (350 to 660 psi) when the reef was partially full of CO_2.
- the Dover 36 GPF operates independent of the processes at the individual reefs and CO_2 pressure conditions and composition of the gas samples collected from the Dover 36 GPF is relatively constant over time.

4.3.1 Results

The results of the general gas compositional analyses are presented in Table 4-6 and the gas isotopic analytical data are presented in Table 4-7. Results are summarized below.

Table 4-6. Composition of the Gas Collected from the Dover 33, Charlton 19, Bagley Field Reefs and the Dover 36 GPF.

Well ID	Sample Date	Pressure (psi)	He (%)	H_2 (%)	Ar (%)	O2 (%)	CO_2 (%)	N_2 (%)	CO (%)	CH_4 (%)	C2 (%)	C2H4 (%)	C3 (%)	C3H6 (%)	iC4 (%)	nC4 (%)	iC5 (%)	nC5 (%)	C6+ (%)
1-33	5/6/2013	700	ND	ND	ND	ND	96.75	0.071	ND	2.30	0.458	ND	0.257	ND	0.0484	0.0660	0.0228	0.0138	0.0101
1-33	7/30/2013	700	ND	0.0439	ND	ND	95.72	0.055	ND	2.78	0.569	ND	0.300	ND	0.0895	0.145	0.0951	0.0660	0.141
1-33	10/3/2013	794	ND	ND	ND	ND	96.20	0.052	ND	2.43	0.622	ND	0.392	ND	0.0836	0.119	0.0463	0.0286	0.0228
2-33	5/6/2013	~atm	ND	5.42	0.0981	2.20	79.51	8.45	ND	1.86	0.709	0.0007	0.669	0.0003	0.179	0.292	0.148	0.103	0.361
2-33	7/30/2013	~atm	ND	25.59	0.237	5.36	47.55	20.31	ND	0.191	0.0803	0.0010	0.106	0.0004	0.0435	0.0870	0.0775	0.0636	0.304
2-33	8/21/2013	~atm	ND	ND	0.901	20.34	0.64	78.09	ND	0.0010	0.0006	ND	0.0019	ND	0.0012	0.0028	0.0031	0.0025	0.0112
2-33	10/3/2013	~atm	ND	1.26	ND	ND	98.52	0.049	ND	0.0816	0.0119	0.0001	0.0034	ND	0.0005	0.0012	0.0013	0.0013	0.0697
2-33	12/13/2013		ND	ND	0.937	21.05	0.067	77.94	ND	0.0004	ND	ND	ND	ND	ND	ND	ND	ND	0.0011
5-33	11/14/2012	100	ND	0.0027	ND	0.011	93.94	0.061	ND	2.76	1.44	ND	1.02	ND	0.211	0.282	0.115	0.0706	0.0915
5-33 (Dup)	11/14/2012	100	ND	0.0023	ND	0.007	94.07	0.061	ND	2.78	1.42	ND	0.960	ND	0.192	0.254	0.102	0.0630	0.0856
5-33 (Dup 2)	11/14/2012	100	ND	0.0025	ND	0.010	94.11	0.068	ND	2.81	1.40	ND	0.927	ND	0.184	0.244	0.0989	0.0611	0.0814
5-33	5/6/2013	~atm	ND	0.502	1.14	2.47	0.036	95.21	ND	0.168	0.0949	0.0002	0.0934	0.0003	0.0373	0.0586	0.0457	0.0309	0.116
5-33 (Dup)	5/6/2013	~atm	ND	0.477	1.14	2.70	0.045	95.01	ND	0.149	0.0843	0.0002	0.0825	0.0003	0.0359	0.0531	0.0477	0.0318	0.145
5-33	7/30/2013	~atm	ND	2.59	1.04	5.32	0.17	89.58	ND	0.437	0.153	0.0005	0.165	0.0007	0.0665	0.107	0.0836	0.0595	0.225
5-33	8/20/2013	500	ND	ND	ND	ND	95.58	0.028	ND	1.10	0.663	ND	0.948	ND	0.349	0.567	0.313	0.203	0.249
5-33	10/3/2013	600	ND	0.437	ND	ND	96.08	0.030	ND	1.33	0.623	ND	0.685	ND	0.205	0.312	0.138	0.0814	0.0833
5-33	12/18/2013	650	ND	0.010	ND	ND	96.29	0.041	ND	2.34	0.703	ND	0.412	ND	0.065	0.087	0.023	0.0135	0.0129
9-33	12/7/2017	700	ND	0.0102	ND	0.02	90.47	6.200	ND	1.30	0.6	ND	0.4	ND	0.3	0.3	0.2	0.2	0.0
EMH 1-18	1/27/2015	~20	ND	0.0154	ND	0.017	0.025	0.14	ND	9.50	40.12	ND	34.45	0.0003	5.82	7.00	1.61	0.822	0.484
EMH 1-18A	8/4/2017	270	NA	NA	NA	NA	93.770	0.03	NA	1.49	1.02	NA	1.43	NA	0.48	0.77	0.38	0.250	0.390
EMH 1-18A	6/18/2018	390	ND	ND	0.0125	0.250	94.580	1.00	ND	1.37	0.82	ND	0.997	ND	0.262	0.370	0.143	0.087	0.112
EMH 2-18	12/31/2015	~20	0.0077	1.48	ND	ND	ND	0.72	ND	67.61	17.63	0.0003	7.95	0.0001	1.37	1.84	0.613	0.369	0.412
EMH 1-19D	2/20/2015	~20	NA	0.02	0.0243	1	0.07	2.54	NA	35.82	26.36	NA	20.72	NA	5.17	5.59	1.770	0.841	0.471
EMH 1-19D	6/18/2018	10	ND	3.1500	1.110	0.05	0.008	95.03	ND	0.0096	0.0092	0.0015	0.321	0.120	0.0328	0.370	0.143	0.081	0.112
Wrubel 1-14A	8/4/2017	350	NA	NA	NA	NA	66.70	0.24	NA	18.19	8.45	ND	3.98	NA	0.86	0.90	0.34	0.180	0.170
J-S 3-11	6/19/2018	560	ND	4.35	0.0184	0.40	78.38	1.77	ND	5.50	3.01	0.0002	6.17	0.0001	0.26	0.13	0.00	0.001	0.001
J-M 1-11	6/19/2018	560	ND	0.721	ND	ND	95.48	0.026	ND	0.766	0.241	ND	1.27	ND	0.916	0.575	0.0026	0.0014	0.0012
Glasser 1-14	6/19/2018	660	ND	1.46	ND	ND	88.61	0.07	ND	5.58	2.39	ND	1.66	ND	0.116	0.0906	0.0106	0.0042	0.0119
Pure	11/14/2012	1,250	ND	ND	ND	ND	99.73	0.016	ND	0.205	0.0166	ND	0.0128	ND	0.0035	0.0057	0.0035	0.0025	0.0044
Pure	5/6/2013	1,250	ND	ND	ND	0.017	99.74	0.050	ND	0.150	0.0130	ND	0.0107	ND	0.0032	0.0052	0.0034	0.0023	0.0053
Comingled	11/14/2012	1,300	ND	ND	ND	ND	96.12	0.061	ND	2.43	0.621	ND	0.418	ND	0.0917	0.133	0.0532	0.0340	0.0363
Comingled	5/6/2012	1,300	ND	0.0017	ND	0.009	96.27	0.12	ND	2.31	0.563	ND	0.378	ND	0.0856	0.128	0.0564	0.0365	0.0428
Recycled	5/6/2012	1,300	ND	ND	ND	ND	94.23	0.10	ND	3.74	0.940	ND	0.580	ND	0.119	0.170	0.0608	0.0366	0.0285

Table 4-7. Isotopic Composition of the Carbon Dioxide and Methane in the Gas Samples Collected from the Dover 33, Charlton 19, Bagley Field Reefs and the Dover 36 GPF

Well ID	Sample Date	Pressure (psi)	d13C CO_2 (‰)	d13C CH_4 (‰)	dDC CH_4(‰)	d18O CO_2 (‰)
1-33	5/6/2013	700	20.55	-52.08	-273.1	2.16
1-33	7/30/2013	700	20.34	-52.10	-276.3	1.56
1-33	10/3/2013	794	20.48	-51.67	-277.5	NA
2-33	5/6/2013	~atm	18.73	-48.21	-266.2	8.87
2-33	7/30/2013	~atm	18.61	NA	NA	14.02
2-33	8/21/2013	~atm	18.12	NA	NA	7.61
2-33	10/3/2013	~atm	18.75	NA	NA	NA
2-33	12/13/2013	~20	NA	NA	NA	NA
5-33	11/14/2012	100	20.83	-50.71	-266.1	4.95
5-33 (Dup)	11/14/2012	100	20.88	-50.71	-268.1	4.93
5-33 (Dup 2)	11/14/2012	100	20.76	-50.65	-266.4	5.04
5-33	5/6/2013	~atm	NA	NA	NA	NA
5-33 (Dup)	5/6/2013	~atm	NA	NA	NA	NA
5-33	7/30/2013	~atm	NA	NA	NA	NA
5-33	8/20/2013	500	20.20	-50.03	-270.6	4.20
5-33	10/3/2013	600	20.38	-51.53	-277.2	10.0
5-33	12/18/2013	650	20.59	-51.84	-260.8	NA
EMH 1-18	1/27/2015	~20	NA	-50.57	-286.0	NA
EMH 1-18A	6/18/2018	270	20.46	-51.56	-260.9	NA
EMH 2-18	12/31/2015	~20	NA	-50.19	-273.9	NA
EMH 1-19D	2/20/2015	~20	NA	-50.13	-268.8	NA
EMH 1-19D	6/18/2018	10	NA	NA	NA	NA
J-M1-11	6/19/2018	560	18.54	-54.44	-276.6	NA
J-S 3-11	6/19/2018	560	19.49	-53.64	-267.6	NA
Glasser 1-14	6/19/2018	660	20.32	-54.14	-291.8	NA
Pure	11/14/2012	1,250	20.25	NA	NA	2.16
Pure	5/6/2013	1,250	20.48	NA	NA	1.96
Comingled	11/14/2012	1,300	20.51	-51.92	-274.3	2.51
Comingled	5/6/2012	1,300	20.56	-51.62	-268.9	2.02
Recycled	5/6/2012	1,300	20.49	-52.01	-275.8	2.40

4.3.1.1 Dover 36 Gas Processing Facility (GPF)

The gas samples collected at the Dover 36 GPF had similar concentrations and isotopic compositions during the entire 13-month sampling period. Differences that are observed reflect the source of the gas and mixing of gas within the facility. The compositions of the two **high-purity CO_2 gas samples** collected in November 2012 and May 2013 are nearly identical (Table 4-7). The high-purity gas is comprised almost entirely of CO_2 (> 99.7%) with mean $\delta^{13}C_{CO2}$ of 20.37‰ and $\delta^{18}O$ of 2.06‰ (Table 4-7). This $\delta^{13}C$ value is consistent with previously published data for $\delta^{13}C_{CO2}$ of Antrim Shale gas (Martini et al., 1996, 2003, 2008), which is the source of the gas used in this long-term injection study (Gupta et al., 2013a,b; Toelle et al., 2008) and should be distinctively heavier than the $\delta^{13}C$ for carbonate minerals in the reef structure or for DIC in equilibrium with these minerals. The high-purity CO_2 gas contains trace amounts of other gases, predominately N_2 and methane, although quantities of these gases were insufficient to determine their isotopic composition.

The **recycled stream** represents gas produced (along with oil) from several the reef structures before it is combined with other gas streams prior to reinjection into the reefs. The one sample collected from this stream was predominately CO_2— approximately 94% (Table 4-6), with an isotopic composition that is similar to the comingled or high-purity gas stream, $\delta^{13}C_{CO2}$ of 20.49‰ and $\delta^{18}O$ of 2.40‰ (Table 4-7). The recycled stream also contains higher concentrations of hydrocarbons (C_1-C_5), though predominately methane (approximately 3.74%), reflecting the source of this gas.

The **comingled stream** represents a mixture of gas from the recycled stream and the pure CO_2 stream. The two comingled samples collected are composed of approximately 96% CO_2 (Table 4-6) with a mean $\delta^{13}C_{CO2}$ of 20.54‰ and $\delta^{18}O$ of 2.27‰ (Table 4-7). The gas from the comingled stream travels between approximately three and eight miles through pipelines from the Dover 36 GPF to the injection wells at the different reefs included in the geochemistry study. During injection, the pressure at the L-M 1-33 injection well (the only injection well sampled) was typically between approximately 650 and 750 psi when samples were collected, or about half the pressure of the Dover 36 GPF. The concentrations and isotopic compositions of CO_2 samples collected at the L-M 1-33 injection well are similar to those measured at the gas processing facility, approximately 96% CO_2 with mean $\delta^{13}C_{CO2}$ of 20.46‰ and $\delta^{18}O$ of 2.06‰ for the three samples collected.

Methane was the predominate hydrocarbon gas measured in samples collected at the Dover 36 GPF, with concentrations ranging from approximately 0.2% in the pure CO_2 stream to between 2 and 4% in the recycled and comingled streams. There was insufficient methane in the pure CO_2 stream for an isotopic analysis; however, there was little variation observed in the isotopic composition ($\delta^{13}C_{CH4}$ and δD) of methane for the comingled, recycled and injected streams with means of $\delta^{13}C_{CH4}$ and δD of -51.8‰ and -273‰, -52.0‰ and -276‰, and -51.95‰ and -276‰, respectively.

4.3.1.2 Dover 33

The L-M 1-33 samples collected from a tap in the wellhead display relatively consistent gas compositions throughout the sampling events performed (all in in 2013) (Table 4-6). These samples represent the injected CO_2 pumped from the Dover 36 GPF and were expected to show similar results over time with significant CO_2 concentrations and minimal concentrations of other gases. The average concentration of CO_2 in the samples from the L-M 1-33 samples is 96.2%, and the next most abundant gas is methane with an average concentration of 2.5%. All other gases account for the remaining 1.3% of the gas volume. The $\delta^{13}C$ isotopic values of the CO_2 and methane are also similar between the three samples collected over time from the L-M 1-33 with an average $\delta 13CO_2$ of 20.45‰ and an average δ13CH4 of -51.95‰ (Table 4-7).

There was considerable variability in the compositions and concentrations of gas samples collected from the L-M 5-33 and L-M 2-33 monitoring wells (Table 4-6). However, these differences are likely attributed to difficulties sampling at the well head or atmospheric contamination, either when the samples were collected or when the well head configuration was changed. The low pressure (atmospheric) samples taken from the L-M 5-33 monitoring well in May and July of 2013 are composed primarily of N_2, with lesser amounts of O_2, Ar, H_2, CO_2, and traces of other hydrocarbons (C1-C5), and thus are not representative of the gas stored within the reef structure. Although the N_2 concentrations in the sample are greater than N_2 concentrations in the atmosphere, Ar/N_2 ratios are similar to atmospheric composition, approximately 0.012, suggesting atmospheric contamination. In addition, these gas samples contained coexisting H_2 and O_2, reflecting a mixing of gas that reacted with the corroded steel pipe within the well and atmospheric gas introduced during sampling.

However, when gas samples were collected from the L-M 5-33 and L-M 2-33 at elevated pressures (between 50 and 600 psi), the concentrations and isotopic compositions of the major constituents are

similar to those measured in the "comingled" stream from the Dover 36 GPF or from the injection well, indicating that there is little evidence of isotopic exchange between the injected CO_2 and the carbonate minerals in the reef over the duration of the sampling period. Nonetheless, there are small but systematic differences in the gas compositions over time that are probably due to mixing of the injected gas with the CO_2 gas that was in the reef at the beginning of the geochemical survey (Figure 4-2). Changes over time reflect mixing/dilution of gas in Dover 33 reef at the beginning of the study with gas injected during the geochemical survey.

Results of the analyses for replicate samples from the L-M 5-33 (#1, #2, and #3) collected in November 2012 are similar; the samples consist primarily of CO_2 at approximately 94%, with the remainder consisting of low molecular weight (C1-C5) hydrocarbons. The mean of the $\delta 13C_{CO2}$ from well 5-33 was slightly higher than the CO_2 gas from either the high-purity stream or the comingled stream; approximately 20.8‰ compared to 20.48‰ and 20.56‰. Gas samples collected in August, October, and December 2013 from the L-M 5-33 well were collected at higher pressures at approximately 300 to 600 psi. These samples contained slightly higher CO_2 concentrations— approximately 96% with a mean $\delta 13C_{CO2}$ of 20.39‰ which more closely matches the isotopic composition of the injected gas. The slight increase in CO_2 concentration and decrease in the $\delta^{13}C$ of CO_2 could reflect mixing and dilution with the injected gas or reactions with the carbonate minerals in the reef. The $\delta^{18}O$ of CO_2 is notably different than that measured for the injected gas, and with the exception of an anomalously high value of 10‰ for the gas sample collected in October 2013, shows a small but systematic decrease from a mean of 4.97‰ (November 2012), to 3.82‰ (December 2013). The shift in $\delta^{18}O$ of CO_2 could reflect mixing and dilution of the baseline gas sample with the lower $\delta^{18}O$ of CO_2 in the injection gas, dissolution and partitioning of CO_2 into the oil, or oxygen isotopic exchange with the brine samples over time.

The methane concentrations and compositions of the higher-pressure gas samples from the L-M 5-33 well are similar, although slightly more variable, than those measured in the injection well. Methane concentration ranges from approximately 1 to 3%, with $\delta 13C_{C1}$ ranging from -50.0‰ to -51.8‰ and δD ranging from -261‰ to -277‰. These values fall within the range previously reported for methane derived from the Antrim Shale (Martini et al., 1996), which is the source of CO_2 for the Dover EOR (Welch et al., 2019).

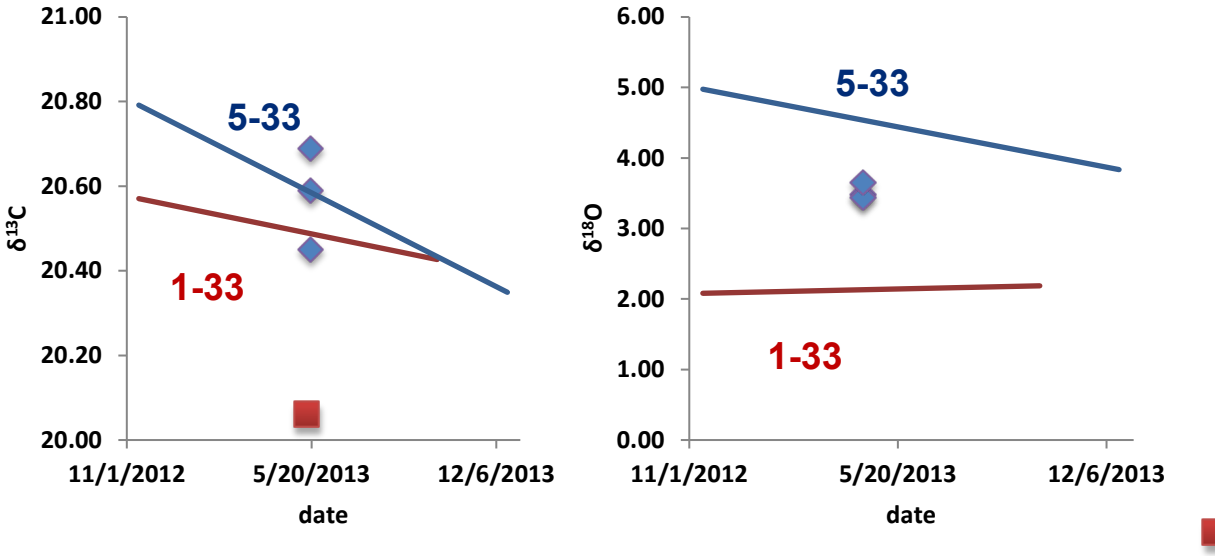

Figure 4-2. $\delta^{13}C$ and $\delta^{18}O$ of CO_2 for the injected gas (either L-M 1-33 or Dover 36 comingled sample, red) and 5-33 monitoring well (blue).

The compositions and concentrations of gas collected from the L-M 2-33 monitoring well are extremely variable, likely due to difficulties in collecting representative gas samples and atmospheric contamination from this low pressure well. Two of the samples, collected in August and December 2013, clearly represent contamination with an atmospheric signature. In addition, samples collected in May and July 2013 are composed primarily of CO_2, yet they also contain significant amounts of N_2, Ar and O_2, indicating that air was either present in the well head or had leaked into the sample cylinder. The L-M 2-33 gas sample from October 2013 was distinct in that there was enough pressure in the well to allow the well to vent through the sample cylinder for several minutes. This sample had a composition like those measured from the Dover GPF facility and other wells— it was composed of greater than 98% CO_2. However, the $\delta^{13}C_{CO2}$ measured in the L-M 2-33 well is significantly lower than the other sites, ranging from 18.12 to 18.75‰, suggesting that either reactions in the reef or in the well casing are changing the isotopic composition, that the CO_2 is mixing with an in situ source that has a different composition, or that the injected CO_2 does not enter the L-M 2-33 monitoring well. Gas from this well typically contains H_2, suggesting that anaerobic microbial reactions with metals in the well casing may be contributing to the gas chemistry.

The gas sample from the Lawnichak 9-33 was collected following the net injection of approximately 128,000 tons of CO_2 into the Dover 33 reef and was captured at relatively high pressure (700 psi). This sample was only analyzed for general composition (isotopic analyses were not performed). The gas composition analyses indicate that the sample is primarily comprised of CO_2 at (90.5%) with balance being predominantly nitrogen (6.2%) and methane (1.3%). All other gases comprise the remaining 2% of the gas. The presence of nitrogen in the sample suggests there was some atmospheric contamination of the sample and the lack of oxygen indicates that it may have been consumed during the oxidization of the well tubulars. The lower concentration of CO_2 may also be attributed to incomplete mixing or distribution of the injected CO_2 to the western flank of the reef.

4.3.1.3 Charlton 19

Samples of the gas from the Charlton 19 reef were collected from each of the wells under baseline conditions (i.e., prior to CO_2 flooding) and then repeat samples were collected from the EMH 1-18A and EMH 1-19D wells after more than three years of CO_2 injection. The baseline samples were collected under low pressure (near atmospheric conditions), but prior to work on the wells that may have introduced atmospheric contamination. Relatively high pressures were observed during the repeat sampling events at these wells, and the sample bottles were sufficiently purged prior to sample collection.

The concentration and isotopic composition of the baseline gas samples collected from the Charlton 19 wells were substantially different than those of the Dover 33 reef or Dover 36 GPF (Table 4-6 and Table 4-7). The gas composition of the three baseline samples varied but were dominated by hydrocarbons—including methane, ethane and propane—with only trace amounts of CO_2. The gas composition of the baseline samples collected from the Charlton 19 reef was similar to the average composition for eight fields for Michigan Silurian reefs reported by Charpentier (1989), with approximately 90% short chain alkanes (C_1-C_3) and only trace amounts of N_2 and CO_2. The difference between the gas composition in the baseline samples collected from the Charlton 19 reef (dominated by alkanes) and the Dover 33 reef (dominated by CO_2) suggests that the geochemistry of the Dover 33 reef has been affected by the long-term injection of CO_2 that occurred prior to the current study.

As expected, there is a significant increase in the concentration of CO_2 in the samples collected from the EMH 1-18(A) well following the injection of CO_2. Prior to injection, the CO_2 concentrations were much lower than 0.1% and these concentrations increased to approximately 94% in the two samples collected following years of CO_2 injection. There is also a corresponding decrease in the relative concentrations

petroleum hydrocarbons between the samples collected prior to and following CO_2 injection. This decrease is caused by the increasing concentrations of CO_2 in the closed system.

The isotopic composition of the methane for the Charlton 19 samples was like those of the Dover 33 reef, with $\delta^{13}C_{CH4}$ ranging from -50.13‰ to -51.56‰ and δD of -260.9‰ to -286‰. There was insufficient CO_2 in the baseline samples collected from the Charlton 19 wells to determine isotopic composition. The gas sample collected from the EMH 1-18A following the injection of CO_2 contained enough CO_2 to obtain a $\delta^{13}C_{CO2}$ value (20.46‰).

4.3.1.4 Bagley Field

The two gas samples from the wellheads of the J-M 1-11 and J-S 3-11 wells in the Bagley Field were collected following approximately two and a half years of CO_2 injection, and are likely representative of a mixture of the injected gas and the reservoir gas present before the geochemistry effort started. The J-M 1-11 sample shows a similar general composition as samples collected from the Dover 33, Dover 36, and Charlton 19 (following CO_2 injection); however, the isotopic composition of the $\delta^{13}C_{CO2}$ in the J-M 1-11 sample (18.54‰) is more consistent with the values from the L-M 2-33 well (Dover 33). As with the L-M 2-33 well, these results suggest that either reactions in the reef or in the well casing are changing the isotopic composition, that the CO_2 is mixing with an in situ source that has a different composition, or that the injected CO_2 does not enter the well. Gas from this well also contains H_2, suggesting that anaerobic microbial reactions with metals in the well casing may be contributing to the gas chemistry.

The general and isotopic composition of the gas sample collected from the J-S 3-11 is different than the gas samples collected from other sources. The CO_2 content is relatively low (78.4%) and the $\delta^{13}C_{CO2}$ value relatively light, as well (19.49‰). These conditions point to incomplete migration of the injected CO_2 to this monitoring well or potentially microbial reactions in the well casing.

4.3.1.5 Discussion (Significance of Gas Analytical Results)

The gas analyses were primarily used to show the presence or absence of CO_2 at a sampled well. The concentration of CO_2 in the gas samples from the reefs in significantly increased by the injection of the CO_2 (as expected). These results were used to qualitatively demonstrate the “amount” of CO_2 near the sampled wells.

Also, the isotopic values of the major gases correlated with the comingled gas as the pressures increased in the well. When gas samples were collected from the L-M 5-33 and L-M 2-33 at elevated pressures (between 50 and 600 psi), the concentrations and isotopic compositions of the major constituents are similar to those measured in the “comingled” stream from the Dover 36 GPF or from the injection well, indicating that there is little evidence of isotopic exchange between the injected CO_2 and the carbonate minerals in the reef over the duration of the sampling period.

4.4 Carbonate Isotopic Analyses

Isotopes of carbon in the DIC or carbonates and of the water can be used to indicate chemical reactions and mixing taking place in the reservoir brines. Fifteen brine samples collected from the Dover 33, Charlton 19, and Bagley Field complex were analyzed for isotopes of DIC and/or water.

The isotopic composition of DIC can be used to evaluate of the extent of CO_2 dissolution into the brine and subsequent water-rock interactions (Becker et al., 2011; Mayer et al., 2015; Myrttinen et al., 2010). A total of 14 samples were collected from the three reefs for $\delta^{13}C$ analyses. As mentioned previously, the initial samples from the Dover 33 reef were not preserved by the $SrCl_2$ coprecipitation method, though all

subsequent samples were preserved to minimize the loss of CO_2 through volatilization and a resulting fractionation of the carbon isotopes. The results of the $\delta^{13}C$ of DIC in brine were compared to the $\delta^{13}C$ in the injected CO_2 and to the remainder of the samples to determine interactions between the injected CO_2 and the reservoir rocks and brine.

Table 4-8 shows the results for the $\delta^{13}C$ of DIC analyses. The analyses indicate that the $\delta^{13}C$ in the samples range from approximately -7 to 32.6‰ with elevated (heavy) values of approximately 30‰ in the Dover 33 reef (except the Fieldstone 2-33 and Lawnichak 9-33 wells) and in some of the samples from the Charlton 19 reef (approximately 20‰). Although the geochemical analysis indicated that brine samples from the Bagley Field complex (J-M 1-11 and J-S 3-11 wells) should have had sufficient alkalinity to produce enough carbonate to analyze in the preserved sample, these samples did not have detectable carbonate in the precipitate to produce a quantifiable value for δ13C.

Table 4-8. Carbon isotope values ($\delta^{13}C$) of DIC in the brine samples collected from the three Niagaran reefs.

Well ID	Date Collected	$d^{13}C$ DIC (CO_2) (‰)
L-M 1-33	10/23/12	32.61
L-M 2-33	11/7/12	31.52
L-M 2-33	8/21/13	33.3
L-M 2-33	12/16/13	26.9
L-M 5-33	11/14/12	29.42
Fieldstone 2-33	3/4/16	-5.36
Lawnichak 9-33	6/18/16	0.51
EMH 1-18	1/28/15	4.5
EMH 1-18A	6/18/18	19.72
EMH 2-18	7/7/15	19.99
EMH 1-19D	2/6/15	9.8
EMH 1-19D	6/18/18	-6.98
J-M 1-11	10/14/15	ND
J-S 3-11	10/12/15	ND

Figure 4-3 shows the $\delta^{13}C_{DIC}$ analytical results with the wells divided into those sampled prior to and following significant CO_2 interaction (injection/mixing) at the well. The wells that were sampled prior to CO_2 interaction are on the left side of the figure and those wells that interacted with CO_2 are located on the right side of the figure. In this figure, six fluid samples from L-M 1-33, L-M 2-33, L-M 5-33, EMH 1-18A, and EMH 2-18 were collected following the injection of a significant mass of CO_2 into the reefs that these wells were installed. Each of the wells that have been exposed to significant CO_2 show relatively heavy $\delta^{13}C$ of DIC (between 19 and 32‰) in the brine samples. The samples collected prior to the injection of CO_2 or represent brines that likely did not come in contact with the injected CO_2 [EMH 1-19D, EMH 1-18 (baseline), and Fieldstone 2-33] exhibit relatively light values (near 0‰) for $\delta^{13}C$ of DIC. The sample from the Lawnichak 9-33 was also collected from the Dover 33 reef, which experienced significant CO_2 injection, but the $\delta^{13}C$ of DIC in this sample was near 0‰. For reference, the injected CO_2 gas/supercritical fluid displays relatively heavy $\delta^{13}C$ values of approximately 20.5‰.

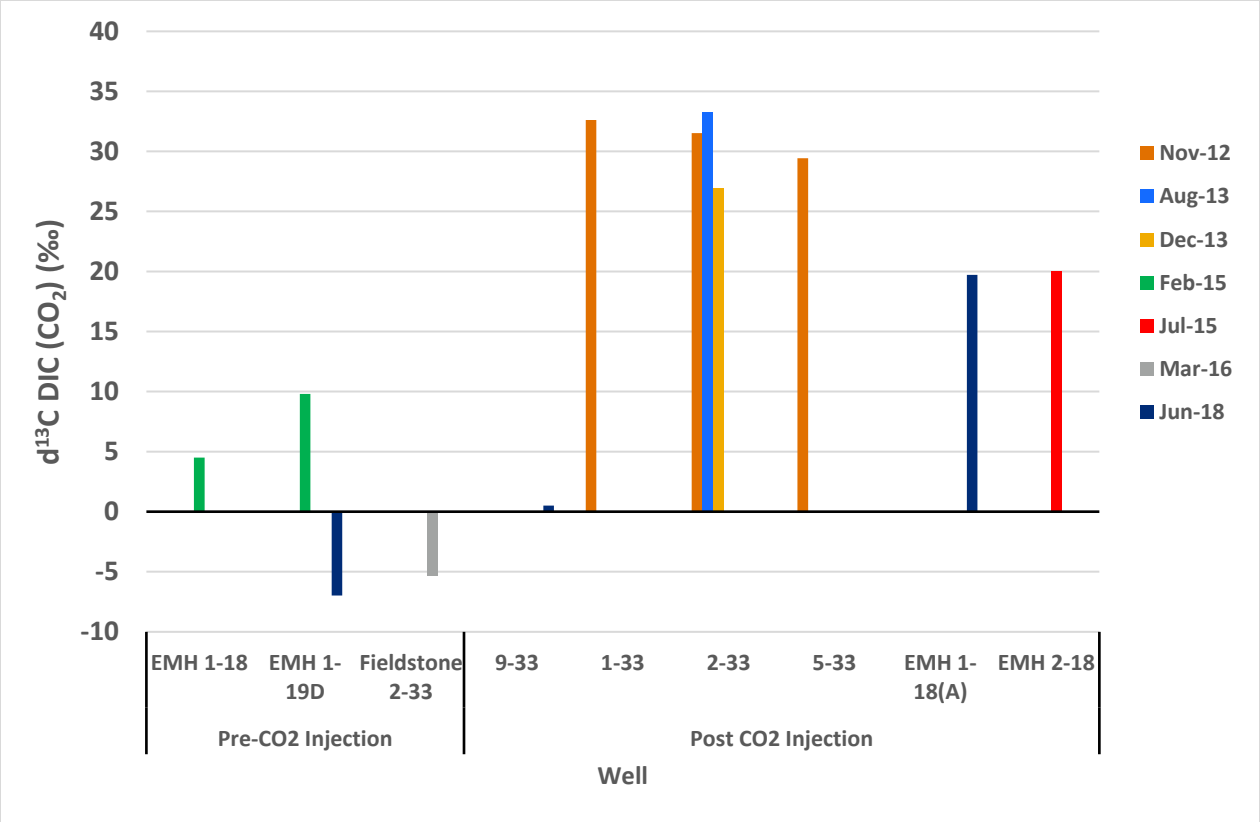

Figure 4-3. Presentation of the $\delta^{13}C$ of DIC in brine samples collected from the Dover 33, Charlton 19, and Bagley Field reefs, with wells without CO_2 interaction on the left and wells with CO_2 interaction on the right.

The increase in the $\delta^{13}C$ of DIC values between the samples collected prior to and following CO_2 injection/exposure is likely attributed to the interaction between the injected CO_2 and the brine. Prior to injection, the DIC in the brine waters is isotopically light (approximately -7 to 10‰) from interaction between the brine and the limestone/dolomite reservoir rocks. Note that marine limestones typically have $\delta^{13}C$ values near 0‰ because the reference standard (Pee Dee Belemnite) is a marine limestone. Therefore, it would be expected that both the carbonate minerals in the brines and the DIC of the fluids in contact with the brines would have $\delta^{13}C$ values near 0‰. However, the baseline samples collected from the Dover 33 reef likely degassed during collection (the brine sample from the L-M 5-33 well collected in November 2012 was notably effervescent), which could result in loss of the total dissolved CO_2 either as ^{13}C depleted CO_2 gas, or precipitation of carbonate minerals from the change in pH. Both processes, particularly the loss of CO_2 gas, could result in a change of the isotopic composition leading to an increase in the measured $\delta^{13}C_{DIC}$. However, a comparison between a $SrCO_3$ precipitated sample and DIC from a fluid sample indicate that these changes would be less than 4‰.

Following the injection of CO_2 for EOR, the brines display heavier $\delta^{13}C$ of DIC because of the interactions between the brine and the injected CO_2, which has a heavy (20.5‰) isotopic signature. The dissolution of the injected CO_2 would result in relatively heavy isotopic composition of the DIC in the brines. Figure 4-4 displays the fractionation in $\delta^{13}C$ during the dissolution of the injected Antrim CO_2 with a $\delta^{13}C$ value of 20 ‰ and the formation/disassociation of carbonic acid to bicarbonate ions (the predominant ion of DIC in the sampled brines). When CO_2 reacts with the brine water to form H_2CO_3, a fractionation process takes place where the $\delta^{13}C$ of the DIC becomes slightly lighter (lower value) (Becker et al., 2011, 2015; Clark and Fritz, 1997; Mayer et al., 2015; Myrttinen et al., 2012a,b). Another fractionation process

occurs when carbonic acid (H_2CO_3) dissociates to form bicarbonate (HCO_3^-), which drives the $\delta^{13}C$ of the DIC heavier (greater value) by approximately 8‰. Through the dissociation of bicarbonate to carbonate and the precipitation of calcite, the $\delta^{13}C$ of the DIC remains at a similar, but slightly heavier value. Therefore, the reaction/dissolution of the injected CO_2 to from bicarbonate or the precipitation of calcite would result in an increase in the value of the $\delta^{13}C$ of the DIC or solid-phase from approximately 20‰ to 30‰. This fractionation and alteration are shown in the brine samples collected before and following the interaction with the injected CO_2. The brine waters start with a $\delta^{13}C_{DIC}$ value of near 0‰, but this value increases to nearly 30‰ as the brine waters interact with the injected CO_2 that begins with a value of approximately 20‰.

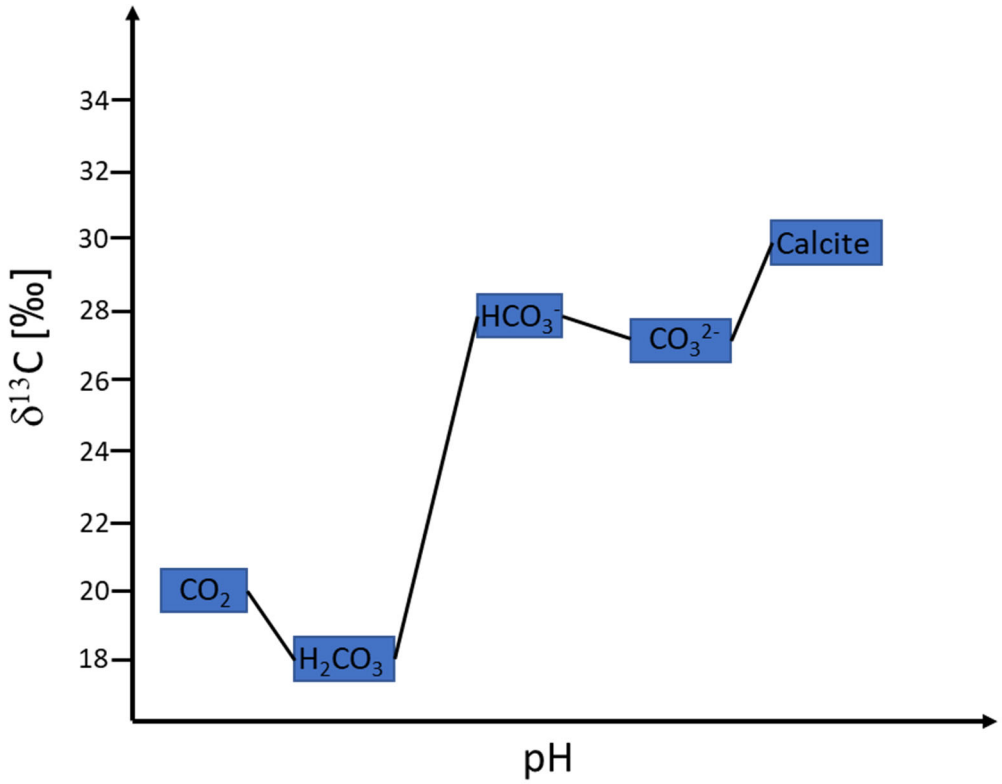

Figure 4-4. Fractionation of ^{13}C during the dissolution of CO_2 and the dissociation of carbonic acid.

This interaction is shown in both the Dover 33 and the Charlton 19 reefs. Unfortunately, repeat samples could not be collected from the Bagley Field wells for comparison. While the majority of the samples from the Dover 33 (from the L-M 1-33, L-M 2-33, and L-M 5-33 wells) were collected following the injection of CO_2, the Fieldstone 2-33 well is located in a lobe of the reef that is hydraulically isolated has never shown the presence of CO_2 at the well. Therefore, the wells that have interacted with the injected CO_2 show relatively heavy $\delta^{13}C$ in the DIC, while the Fieldstone 2-33 remains relatively light at -5.36‰. The sample from the Lawnichak 9-33 displays $\delta^{13}C_{DIC}$ values similar to the original $\delta^{13}C_{DIC}$ values in the brine prior to the injection of the Antrim CO_2, suggesting limited interaction between the injected CO_2 and the brines in this area of the reef. This limited interaction may be the result of the location of the well in the reef. This well is located along the western flank of the reef and apart from the other wells in the reef. Without EOR production of oil, water, and CO_2 from nearby wells, this area of the reef may not have experienced thorough sweeping with the injected CO_2.

A similar response to CO_2 injection is observed in the Charlton 19 reef where samples were collected prior to and following CO_2 injection and interaction. The baseline samples collected from the EMH 1-18 and EMH 1-19D wells indicate relatively light values of $\delta^{13}C$ in the DIC with an average value of 7.1‰ between the two samples. These values are somewhat heavier than the unperturbed samples from the Dover 33 wells, which may be the result of volatilization of the CO_2 and fractionation during the sampling of the Dover 33 wells. Following several months to years of the CO_2 injection into the Charlton 19 reef, the $\delta^{13}C_{DIC}$ values increase to nearly 20‰ in the samples collected from the EMH 2-18 and EMH 1-18A wells. At the Charlton 19 reef, the EMH-19D is hydraulically isolated (like the Fieldstone 2-33 well in Dover 33) and was not expected to interact with the injected CO_2. The $\delta^{13}C_{DIC}$ values from the well are indicative of this limited interaction. Between the baseline and repeat samples, the $\delta^{13}C_{DIC}$ values decrease from 9.8‰ to -6.98‰. The decrease in the $\delta^{13}C_{DIC}$ values in this well over time may be caused by fractionation or errors during sampling/preservation.

Although it is believed that the changes in the $\delta^{13}C_{DIC}$ values are the result of CO_2 injection, it is possible that the $\delta^{13}C_{DIC}$ collected from the wells reflect a non-equilibrium fractionation between $\delta^{13}C$ of CO_2 and DIC or the isotopically heavy $\delta^{13}C$ of DIC is controlled by the long-term in situ microbially mediated methanogenesis within the reef structure. Given the limited number of samples that were collected from the reefs and the possibility of sample degassing from the baseline samples from the Dover 33 reef, this non-equilibrium fractionation could be altering the isotopic composition of the DIC in the brine waters. Also, notably, the fluids from the L-M 1-33 and L-M 5-33 wells were collected near the beginning of the study (before CO_2 was injected in the current study), thus these samples could reflect prior CO_2 flooding that occurred in the decades before the injection tests or water flooding events. In addition, the $\delta^{13}C_{DIC}$ of the Dover 33 brine was significantly higher than those measured from a fluid sample obtained from the Fieldstone 2-33 well (an adjacent lobe of the reef) with $\delta^{13}C_{DIC}$ of approximately 5.5‰.

Martini et al. (1996; 2003; 2008) report similar elevated $\delta^{13}C_{DIC}$ from the Antrim Shale brine (approximately 25 to 30‰), which they attribute to microbially mediated reduction of CO_2 to produce methane. The difference between the isotopic composition of CO_2 and methane $\Delta_{CO2\text{-}CH4}$ is approximately 70‰ in the Dover 33 reef, which falls within the expected range of isotopic compositions for both biogenic and thermogenic methane production, (Clark and Fritz, 1997; Martini et al., 1996, 2003, 2008; McIntosh et al., 2004) suggesting that in situ methanogenesis could exert some control on the $\delta^{13}C_{DIC}$ in these reefs.

Reactions between the injected CO_2 gas and carbonate minerals within the reef could also impact the $\delta^{13}C_{DIC}$ and be used to predict the extent of water-rock interaction (Myrttinen et al., 2010, 2012a,b). The isotopic composition of core samples collected from the Lawnichak 9-33 well indicate that the carbonates are between 0‰ and 5‰, which is consistent with reported values of carbonate rocks from Niagaran pinnacle reefs from the Michigan Basin (Cercone and Lohmann, 1987; Coniglio et al., 2003). The authors noted significant variation in $\delta^{13}C$ between host rock and secondary calcite and dolomite cements. The range in the $\delta^{13}C$ of the carbonates in their study was approximately 0‰ to 6‰.

Dissolution of carbonate minerals by dissolved CO_2 and isotopic compositions of the CO_2 species can be described by:

$$CaCO_3(s) + H_2O + CO_2 \leftrightarrow Ca^{2+} + 2HCO_3^-$$

$$\delta^{13}C \sim 0\text{-}6‰ \qquad \delta^{13}C_{CO2} \sim 20‰ \qquad \delta^{13}C_{DIC} \sim 10\text{-}13‰$$

Equation 4-1

Therefore, reactions between injected CO_2 and the reef carbonates should produce $\delta^{13}C_{DIC}$ with values intermediate between those of carbonate minerals and the injected CO_2 gas (Becker et al., 2011; Mayer et al., 2015). Expected values of $\delta^{13}C_{DIC}$ from this reaction would be approximately 10-13‰, which is about 20‰ less than those measured in this study. This is consistent with little interaction between the injected gas and the carbonates in the reef over the course of the study.

Cercone and Lohmann (1987) conducted a study on the diagenetic alteration of a Northern Michigan Niagraran pinnacle reef structure. Their results show that the reefs have experienced a complex diagenetic history that is evident in the host rock and carbonate cements. Cercone and Lohmann (1987) concluded that the mineralogy and isotopic composition of the cement precipitates reflects the isotopic composition of regional fluids that infiltrated the reef structure, and that these fluids did not equilibrate with the host rock in the reef structure. This suggests that the in situ brines did not undergo extensive water-rock interaction with the reefs over geologic time.

4.4.1 Discussion (Significance of Carbon Isotope Results)

Dissolution of the injected CO_2 (with a $\delta^{13}C$ value of approximately 20‰) into the reef brines was expected to increase the $\delta^{13}C_{DIC}$ values from near zero values to approximately 25-30‰ because of fractionation during the dissolution process. The analytical results for the DIC demonstrate a change of this magnitude between the brines from reefs that had not been exposed to CO_2 to those that had experienced significant CO_2 injection. These data provide an indication that the injected CO_2 was mixing with and dissolving in the brine as it moved through the reef.

4.5 Core Analyses

Core samples from the Lawnichak 9-33 well (Dover 33 reef, see Figure 1-3 and Table 2-3) were collected during installation of the well in late 2016, and analyzed to test the hypothesis that mineralogical or geochemical changes occurred as a result of CO_2 injection into the reef. Core was acquired above, near, and below the current oil-water contact, estimated from resistivity log data between approximately 5,627 and 5,639 feet. Note that the current oil-water contact is a snapshot in time and migrates in response to climate change over geological timescales and from oil production/EOR activities currently taking place in the reef.

Three plugs from whole core samples (approximately 1.5 in. diameter by 4 in. long) were collected from the following depths: 5,606.1 feet (above the oil-water interface), 5,690.25 feet (near the oil-water interface), and 5,700 feet (below the oil-water interface). Additionally, three trim cuts from sidewall cores (1.5 in. diameter by approximately 0.5 in. long) were collected from depths of 5,588 feet (above the oil-water interface), 5,630 feet (at the oil-water interface), and 5,655 feet (in the transition zone) were then sent to OSU for a suite of analyses to investigate alteration in the rock chemistry or structure due to the injection of CO_2.

In addition to determining the minerals comprising the rocks, the Lawnichak 9-33 core analysis looked for evidence of mineral precipitation or dissolution reactions and tried to determine the distribution of minerals, pores, and fractures in the overall rock microtexture. To this end, powder XRD was performed to determine the mineralogy/crystallography of the bulk samples. XCT analyses were conducted on all six cores prior to sub-sampling for other analyses to get a sense of density contrast in 2 and 3 dimensions that arises from differential porosity and mineralogy in the cores. Light and electron microscopy provided 2D views of the fine details of the core samples, including the distribution of minerals lining mm- to µm-scale pores, fractures, and vugs. All core analyses were conducted at SEMCAL except for µXCT, which was performed by the National Energy Technology Laboratory (NETL).

After the main core characterization efforts, $\delta^{13}C$ analyses were performed on select subsamples of the core to determine the isotopic values of the matrix carbonates and secondary mineral precipitates (carbonates) found in the rock. Choice of sampling was dictated by regions thought to represent original rock matrix, as well as zones that represent vug and fracture linings and inclusions.

4.5.1 Comparative X-Ray Diffraction (XRD) Analysis

Portions of each of the three trim samples were disaggregated from the edges for XRD and SEM analysis. Of the three sidewall core trim samples, XRD analysis of samples from the 5,630 feet depth, which is within the estimated location of the oil-water contact, shows the most complex mineralogy. In this sample, dolomite and low magnesium calcite are the major phases, and quartz, anhydrite, and halite also are detected but as minor accessory phases. In contrast, XRD scans of subsamples from the trim sample depths 5,588 feet (well above the oil-water contact), and 5,655 feet (within the oil to brine transitional region) only detect dolomite (Figure 4-5). However, as shown in the petrographic section below, light microscopy (LM) and SEM are generally required to detect the more minor or trace mineral phases.

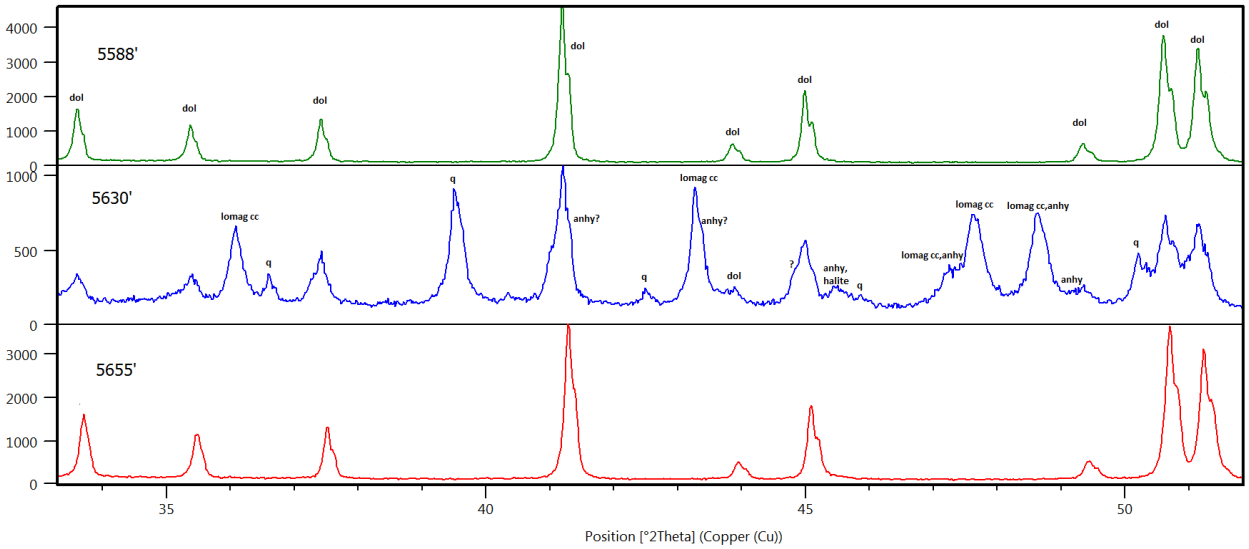

Figure 4-5. Powder X-Ray Diffraction spectra for core samples collected from depth of 5,588, 5,630, and 5,655 ft. The sample collected from a depth of 5,630 ft near the oil/water interface displays a complex mineralogy, perhaps from geochemical reactions.

One Lawnichak 9-33 core sample (depth 5,690 feet) was disaggregated for XRD analysis before thin sectioning, due to the discovery (with XCT) of a vug inclusion that displayed euhedral boundaries and obvious density differences relative to the rock matrix. The matrix of this core sample (from below the oil-water contact) consisted predominantly of dolomite with minor amounts of quartz and alkali feldspar (Figure 4-6). The precipitated, fine-grained material in the vug inclusion displayed a more complex mineralogy with the majority of the vug inclusion composed of dolomite and anhydrite, but the presence of beta cristobalite, quartz, fluorite, and albite were also detected (Figure 4-7).

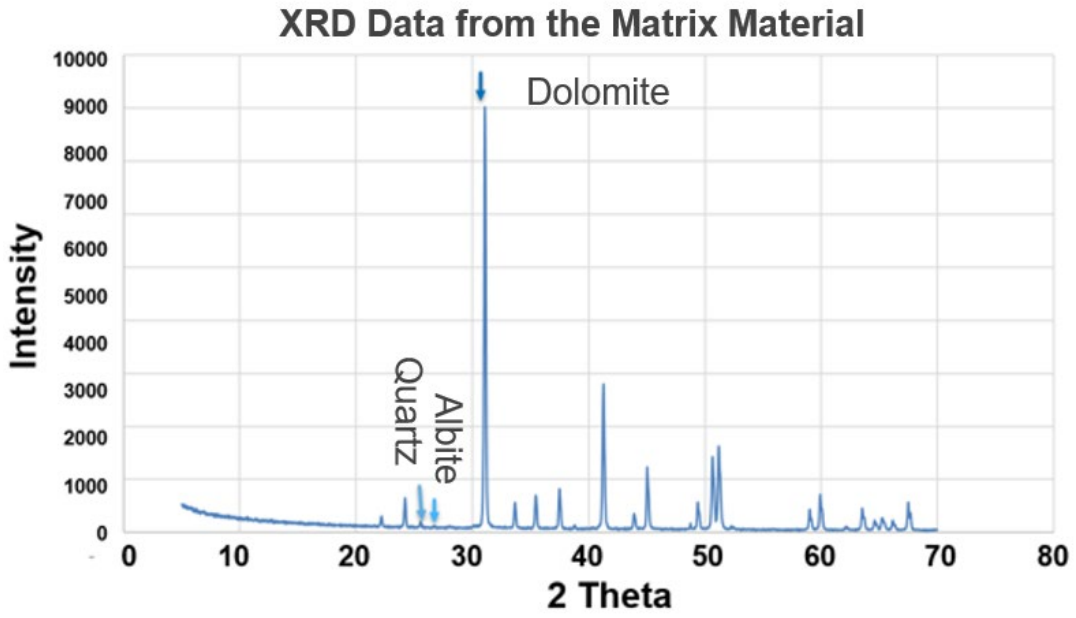

Figure 4-6. XRD analysis shows bulk mineralogy of the matrix material from the 5690.25' sample. Arrows point to key diffraction maxima that correspond to minerals identified in the core.

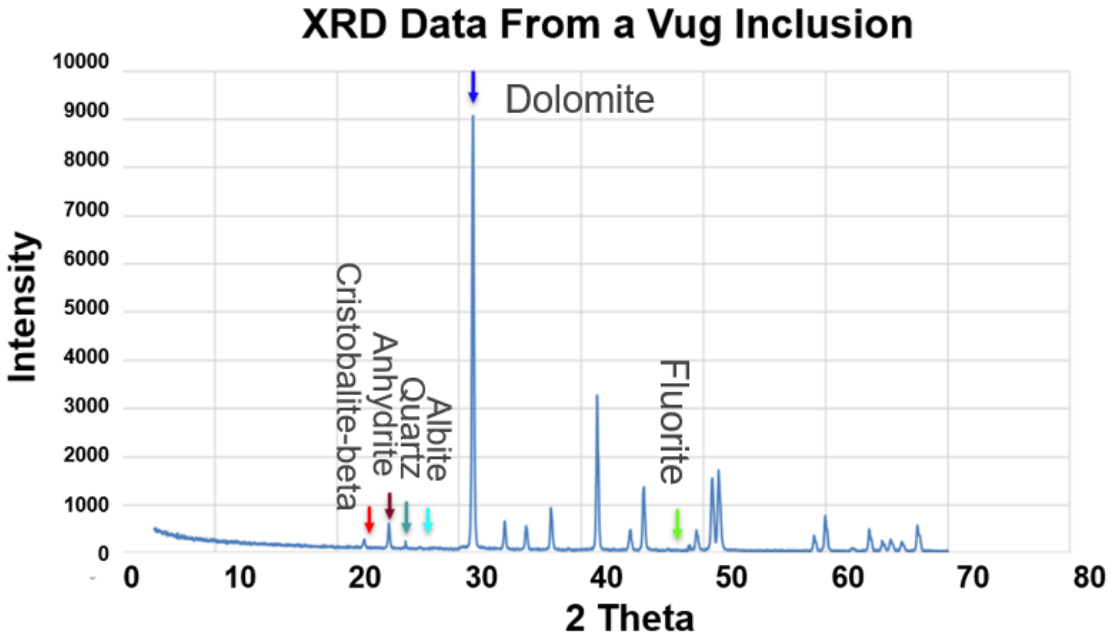

Figure 4-7. XRD analysis shows that, in addition to matrix material (dolomite, quartz, albite), the vug contains anhydrite and fluorite that may have precipitated recently.

The complex mineralogy near the oil-water contact and within the vugs suggests that this region of the reef may be more geochemically active than zones above and below the interface. At the oil-water contact, multiple phases (brine, oil, gas, and CO_2) are all in contact with one another allowing for multiple chemical and physical reactions to occur and complex mineralogies and unique precipitates in the vugs may be expected in this zone. However, neither the timing of the mineral precipitation in the vugs nor the formation of the complex mineralogy in the oil-water contact can be determined solely from the XRD data and therefore cannot be attributed to the injection of CO_2.

4.5.2 Petrographic Light Microscopy (LM) and Scanning Electron Microscopy (SEM) Analysis of Mineralogy, Fractures, and Pores

The three thin sections made from the sidewall core trim samples from the depths of 5,588 feet (above oil-water interface), 5,630 feet (within oil-water interface), and 5,655 feet (transition zone) were fully imaged with a Leica DMS 1000 digital LM and an Olympus SX50 polarizing light microscope (PLM) to record mineralogy, pores/vugs, and fractures in the 100s of µm to mm length scales. Figure 4-8 shows a digital (reflected light) micrograph of the entire thin section of the trim sample from 5,655 feet with blue dye epoxy used for the thin section embedding process defining the pores.

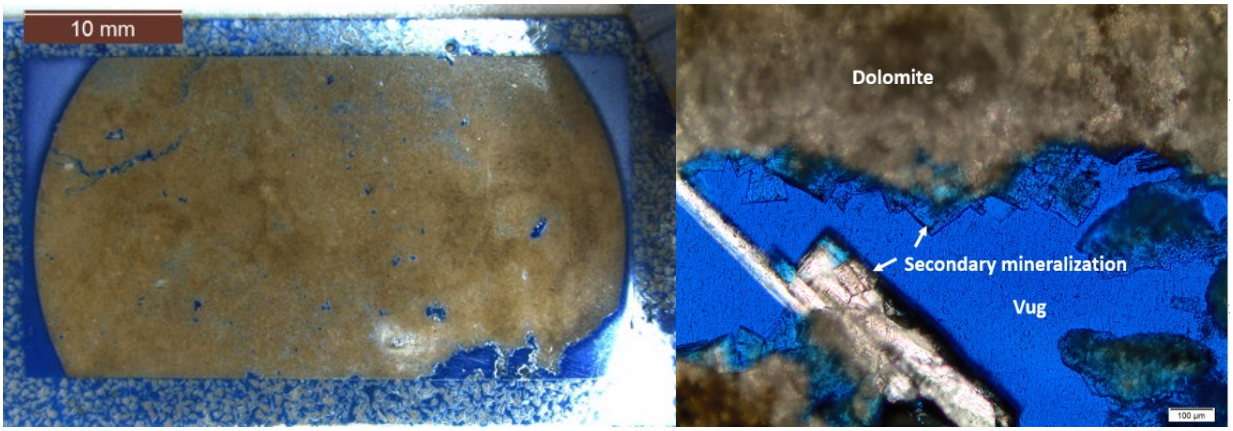

Figure 4-8. (left) Digital light micrograph of thin section prepared from sidewall core trim sample 5,655 ft, in the oil-water transition zone. Blue dye epoxy highlights the pores, (right) zoomed image of vug with secondary mineralization lining the pore space, sample 5,655 ft. Large rectangular white crystal (arrowed, lower left) is anhydrite. Transparent rhombohedral crystals (carbonates) also line the vug (arrowed, center).

Pore size and distribution in the trim samples are heterogeneous. Some areas of relatively high porosity occur near fractures, while other portions of the matrix display larger, scattered vuggy pores large enough to view with the unaided eye, as well as the digital light microscope (Figure 4-8). Most fractures are relatively small and appear to be connecting pore spaces, but a few larger fracture systems are present. A few of these fractures have open apertures, but closed fractures filled with fine sediment are more common. There also are regions where the dolomite matrix contains recrystallized fossil skeletal material, as shown below in the sample from 5,588 feet (Figure 4-9). Increased porosity is observed both within and along some grain boundaries between matrix and fossils. These recrystallized fossil grains, which appear white in Figure 4-9, are relatively void of pores, as determined by the absence of blue epoxy.

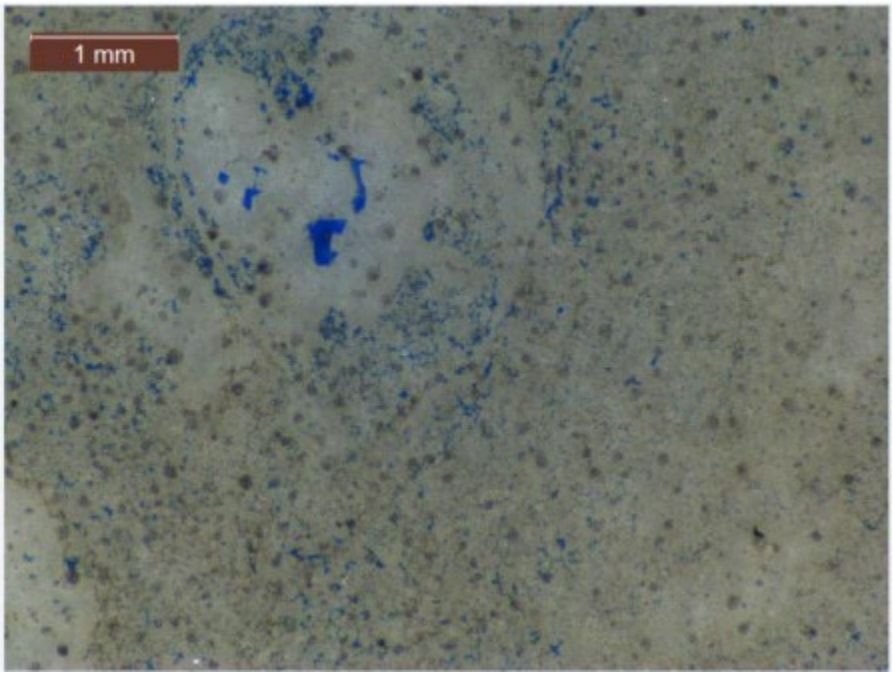

Figure 4-9. Digital light micrograph of recrystallized fossil-rich region, (white coarser-grained material) depth 5,588 ft. Blue epoxy is concentrated in areas with greater porosity, demonstrating uneven distribution of pores in the sample.

Polarized light microscopy also aided the identification of minerals based on differences in birefringence. This is shown in the image taken with cross-polarized (CP) light of a thin section produced from core collected at a depth of 5,630 feet (within the oil-water contact) (Figure 4-10). The high birefringence of dolomite that makes up the majority of the groundmass in this image is typical of all trim and core samples studied, and contrasts with the bright first order interference colors of anhydrite. A large pore (approximately 2mm wide) in this thin section contains a relatively large anhydrite grain. The grain is about 0.5mm long and precipitated from the edge of the dolomite matrix out into a vuggy pore.

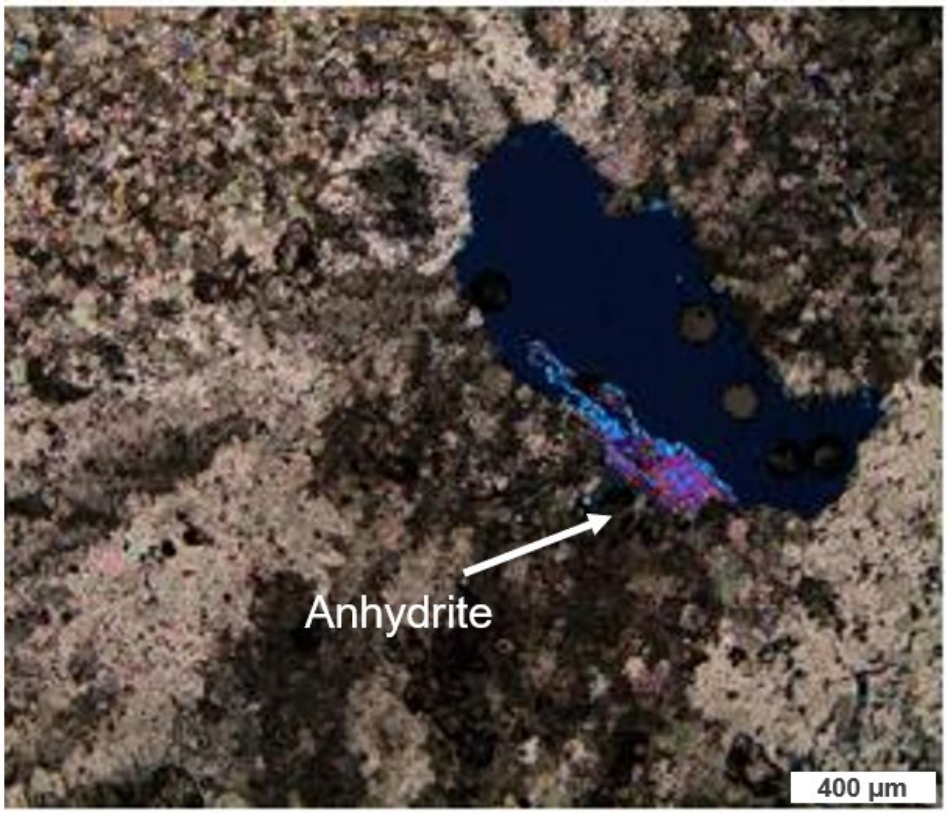

Figure 4-10. Cross-polarized light micrograph of sidewall trim sample shows dolomite matrix (high birefringence appearing milky gray) with anhydrite precipitation (first order red, blue birefringence) in a vug in the CO_2-EOR interval (5,630 ft).

SEM observations helped identify the mineralogy in the pores and fractures at the micrometer scale. Backscattered electron (BSE) imagery discerned phases based on average atomic number contrast, and energy-dispersive X-ray spectroscopy (EDXS) spot analysis yielded characteristic X-ray spectra for the elements comprising a small volume of sample (interaction volume for the X-rays is approximately 1-5 µm). The use of these detectors in the SEM allowed elemental analysis of void-filling precipitates and mineral inclusions in the dolomite matrix.

Pores with sharp euhedral boundaries and small fracture systems are abundant across the matrix. In the core sample collected from a depth of 5,655 feet, one mineral found in such pores within the dolomite matrix is a high-magnesium carbonate (Figure 4-11) that has elevated oxygen and magnesium characteristic X-ray lines, as compared to dolomite (Figure 4-12). This mineral, when observed in thin section, tended to build-up charge under the electron beam, yielding unexpectedly high brightness for a Mg-rich mineral (Figure 4-11). Other phases commonly found in pores include organic matter (OM), halides (fluorite, halite, sylvite), sulfates (gypsum-anhydrite, barite-celestite), sulfides (pyrite; arsenopyrite), and silica (quartz, cristobalite). Note that the separation of elemental polymorphs is informed by the XRD data, as EDXS cannot distinguish crystal structures. In subsamples for SEM, prepared as disaggregated fragments instead of polished thin sections, low magnesium calcite was observed on the outer surfaces of dolomite (Figure 4-13).

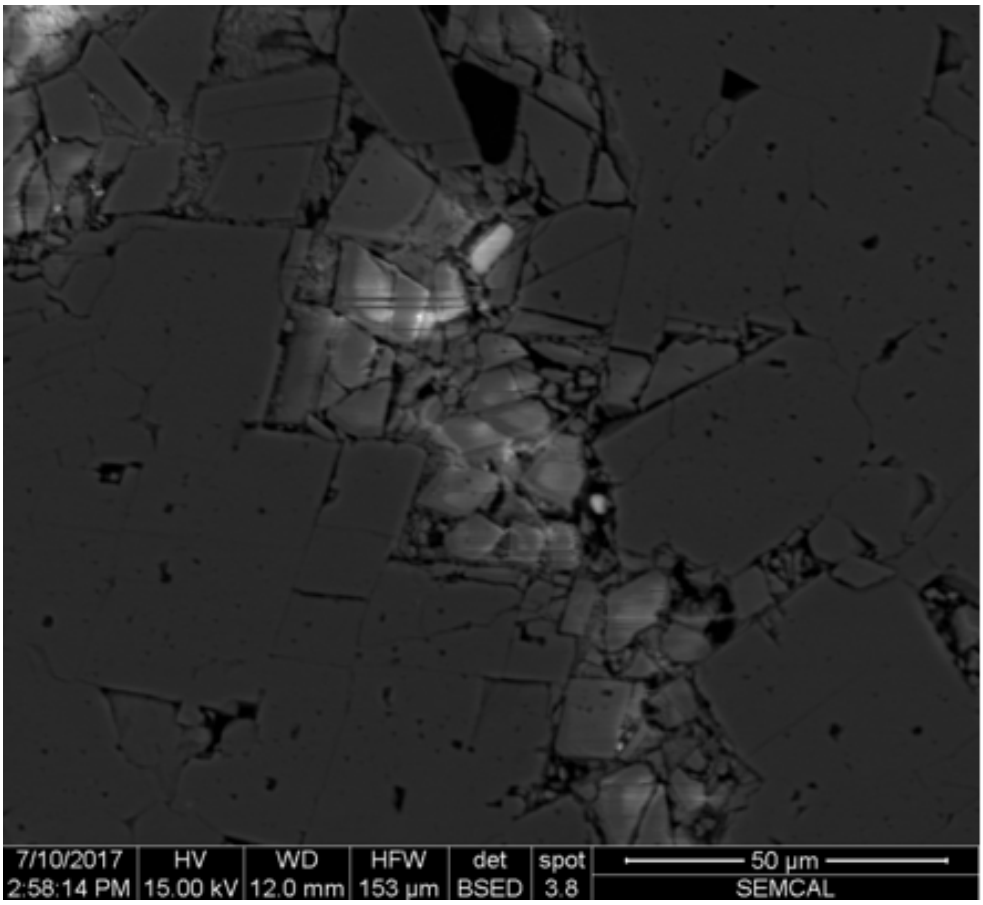

Figure 4-11. SEM BSE image of high-Mg carbonate mineral precipitate in a pore in the CO_2-EOR interval (from 5,655 ft).

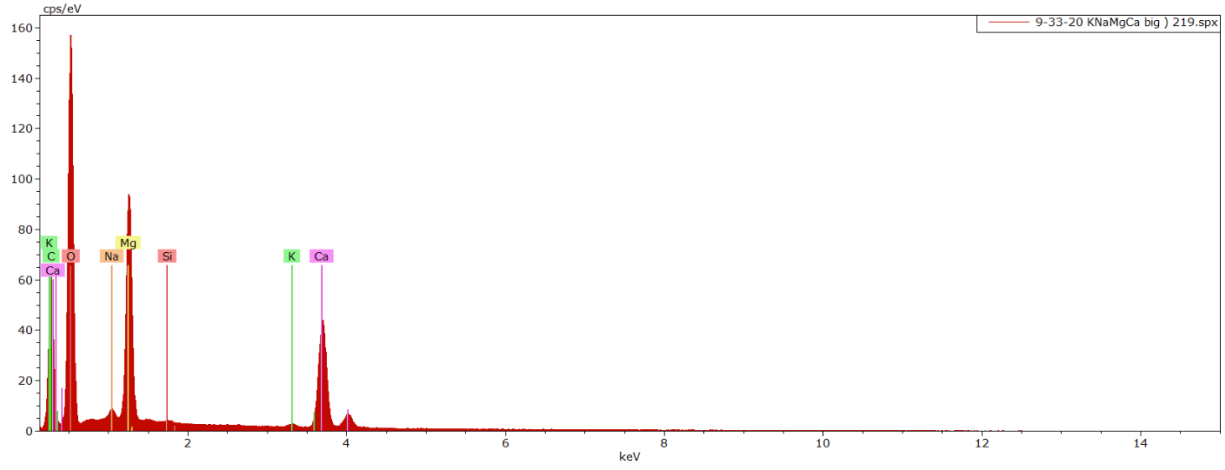

Figure 4-12. EDXS spectra of the high-Mg carbonate mineral precipitate in the sample from 5,655 ft.

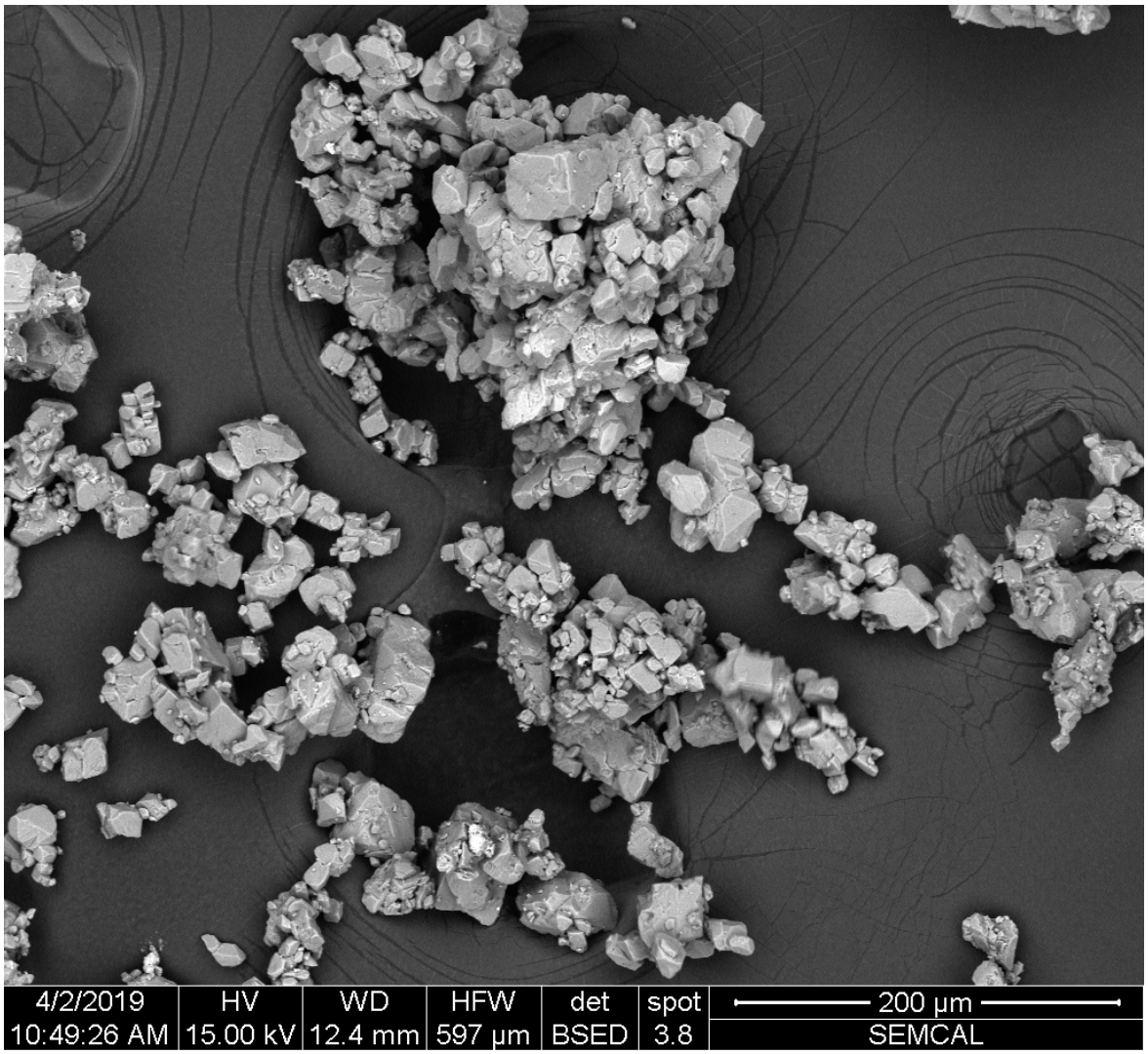

Figure 4-13. Image of low-Mg calcite detected on the aggregate sample collected from a depth of 5,690 ft.

The core sample from a depth of 5,588 feet contained examples of potassium feldspar crystals embedded in dolomite matrix (Figure 4-14). These grains existed with euhedral dolomite inclusions and were only found in this sample. Fluorite was also found in the matrix and contains inclusions of dolomite crystals (Figure 4-15). Organic material is observed in both matrix and pores. Barite-celestite grains also were identified in pore spaces of the dolomite matrix.

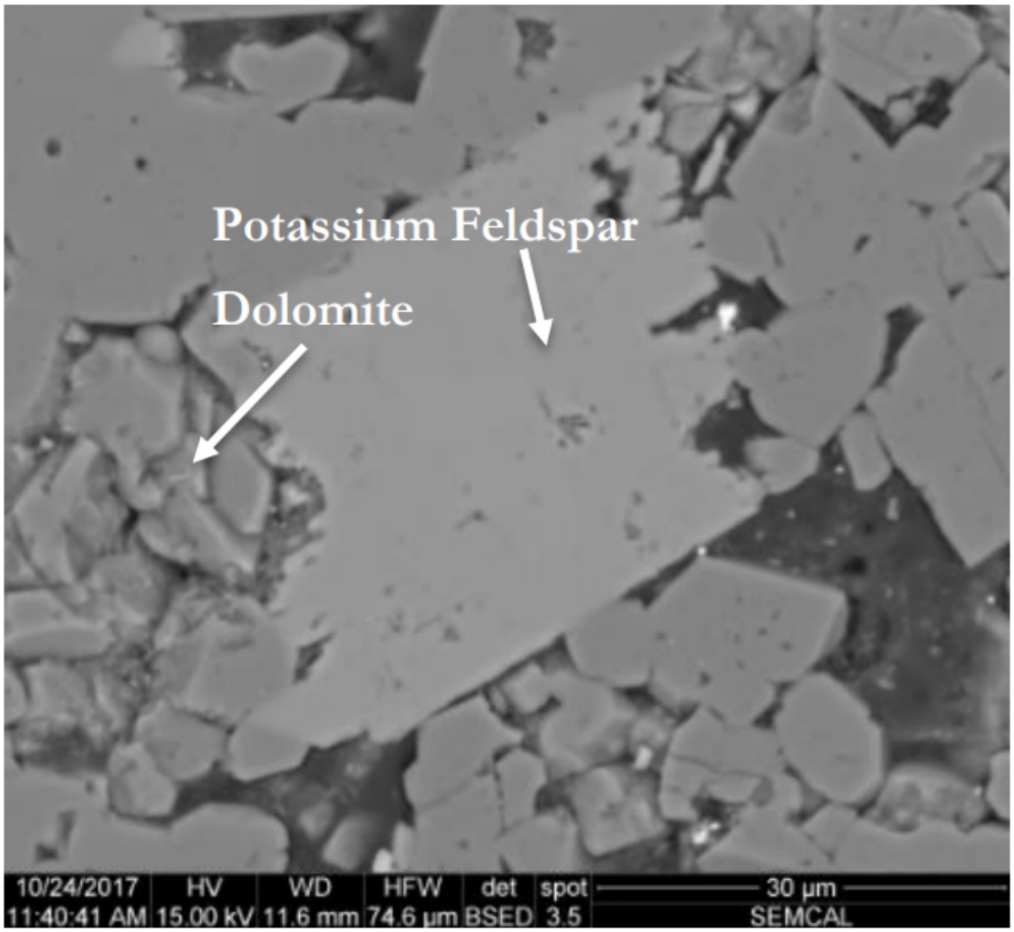

Figure 4-14. Backscattered SEM image of potassium feldspar adjacent to a vuggy pore containing dolomite. The potassium feldspar grain cleaves in a different geometry than the dolomite and displays a brighter BSE signal intensity. Some potassium feldspar grains contained euhedral dolomite inclusions.

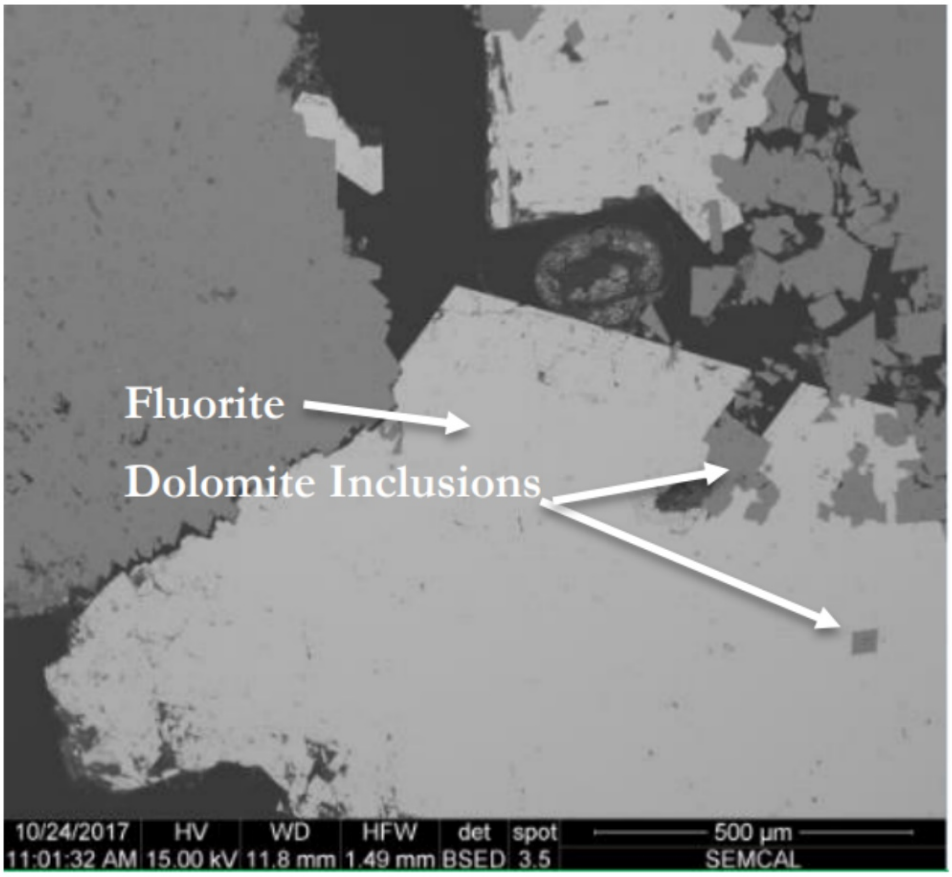

Figure 4-15. Backscattered SEM image of a fluorite infilling in a vuggy matrix region. The brighter mineral is fluorite and the darker gray mineral is dolomite. The fluorite contains inclusions of dolomite.

The pores in the sample collected from a depth of 5,630 feet contain halide minerals (Figure 4-16) and organic matter. The presence of the halide minerals is attributed to precipitation from the formation brine as the sample desiccated following collection. As detected with XRD, quartz is present as an accessory mineral along with fluorite and pyrite. Phyllosilicates were also observed with SEM, but not detected with XRD.

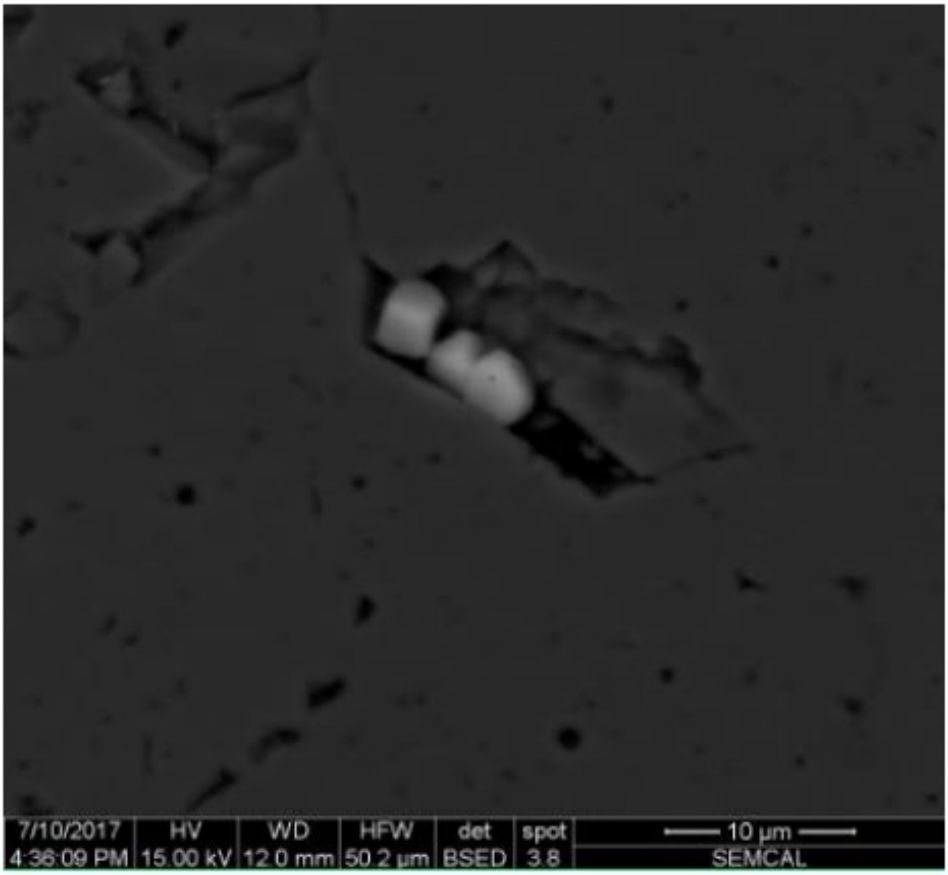

Figure 4-16. SEM imagery shows salts (sylvite) precipitated in a vug in the CO_2-EOR (5,630 ft) interval.

4.5.3 X-ray Computed Tomography (XCT)

XCT and micro-XCT scans of the core plug sample from a depth of 5,690 feet, which is below the current oil-water interface, were analyzed after 3D rendering to decipher larger-scale features that could be selected for analysis with other methods. In addition, the images were used to investigate the presence of dissolution and precipitation feature along the fractures and the inside of vugs.

Figure 4-17 shows two views of a large, relatively low density, euhedral object bounded by higher-density (and hence brighter in XCT) dolomite matrix. Adjacent 2D image slices showed natural fractures intersecting this vug. The scans led to XRD and SEM analyses of both matrix and vug inclusion material to help inform the composition of the material in the vug (discussed in Sections 4.4.1 and 4.4.2). XRD show that the core matrix is dolomite, whereas the material hand-picked from the vug consists of mostly dolomite and anhydrite, with minor halite, sylvite, and calcium chloride salt (see Figure 4-10 and Figure 4-16). The presence of these minerals within the vug and the interconnected fractures provide some evidence for fluid migration through the matrix and secondary precipitation of minerals elsewhere in the rock. The occurrence of the salts is likely attributed to post-sampling precipitation from desiccation of the sample.

Any evidence of CO_2-induced dissolution within the CO_2-EOR interval was difficult to distinguish, and there was no strong evidence of CO_2-induced dissolution in the samples that were characterized. The most compelling evidence for CO_2-induced dissolution was subtle, comprising localized areas of elevated porosity, or slight fracture widening in some cases. More commonly, mineral precipitation lining large

pores (vugs) and even fractures in the core. It is difficult to unambiguously identify the secondary mineralization from the μXCT images because gray scale variation is small. Possibilities include dolomite, microcrystalline silica, and salt, all of which have similar gray scale. Brighter regions could be calcite, gypsum, anhydrite, or fluorite.

The absence of CO_2-induced dissolution features could be attributed to four possible factors. First, there are a limited number of samples that were selected based on bias favoring more competent rock. In a variably permeable heterogeneous formation, CO_2 and brine are likely to flow through existing, high-permeability pathways. Due to poor drilling recovery from the field, sample selection was biased toward the less permeable but more competent recovered core suitable for sub-coring and tomographic analysis. Core samples that were not recovered during drilling could potentially have high-permeability pathways. Secondly, the enhanced oil recovery operations used continuous CO_2 drive, rather than water alternating gas (WAG). Continuous CO_2 drive should result in less fluid mixing where the reactive fluids quickly reach calcite and dolomite equilibrium, and consequently yield more subtle dissolution features. WAG operations repeatedly introduce out-of-equilibrium waters that promote carbonate mineral dissolution. A third factor is fluid flow rates. Slower flow rates tend to distribute CO_2 and brine and result in less pronounced dissolution features. A fourth factor concerns the miscibility of CO_2 into the oil phase. If injected CO_2 dissolves into residual oil phases, less reactive fluid will be available for reaction, leading to less widely distributed or more subtle dissolution features.

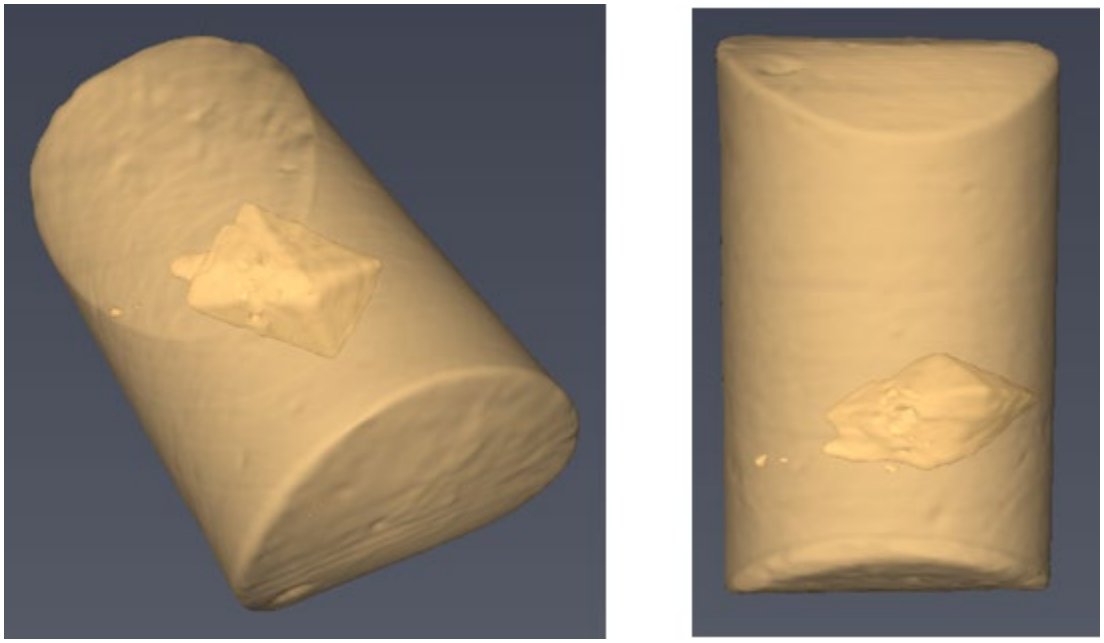

Figure 4-17. XCT scans of the core (5690.25'), a 3D image of the core and its inclusion was constructed for two different orientations. Aviso software was used to render a 3D image from XCT scans of sample 5690.25', including the partly infilled vug.

4.5.4 Carbon Isotope Analyses of the Core Matrix and Vug Precipitates

Given the prediction of mineral precipitation by the equilibrium-phase modeling, along with the direct observation of precipitates in vugs and fractures, subsamples of the core matrix and vug inclusion material were collected for $\delta^{13}C$ analyses. The use of $\delta^{13}C$ measurements would potentially permit a geochemical tracer for the mineral reactions in the vugs and fractures (i.e., pre- or post-CO_2 injection). Because of the unique isotopic signature of the injected CO_2, exchange reactions of pre-existing carbonate with this gas could yield secondary carbonates with a relatively enriched $\delta^{13}C$ isotopic

signature. A total of 13 subsamples were analyzed from three samples of the core (Table 4-9). Additional subsamples of the mineral precipitates were collected; however, the carbon content in the samples was too small to generate enough CO_2 to measure a definitive isotopic signature.

Of the subsamples analyzed, the $\delta^{13}C$ values ranged from 2.93‰ to 4.08‰, and there was no significant difference of the $\delta^{13}C$ values between the native matrix material and the mineral precipitates mined from the vugs. With similar isotopic values between the matrix and the mineral precipitates, these data suggest that the mineralization in the vugs occurred prior to the injection of the CO_2 for EOR. However, it should be noted that with the limited amount of data, these results are inconclusive. In additional, there may be cases where a small rind of post-CO_2 injection carbonates precipitate on the outside of the older mineral precipitates in the vugs. To investigate this phenomenon, attempts were made to sequentially dissolve the minerals (from outside to inside) and analyze the $\delta^{13}C$ values for each layer. A dilute solution of phosphoric acid was applied to mineral particles to minimize the dissolution of the carbonate minerals. Unfortunately, this analytical method did not yield quantifiable $\delta^{13}C$ results due to the minimal mass of carbonate dissolved with each step.

Table 4-9. Carbon isotope values for the core samples collected from depths of 5,960, 5,700, and 5,606 ft.

Core Sample	Description	Mass	$\delta^{13}C$ Value (‰)
5,690	Fine material from inclusion	22.7 mg	3.09
5,690	Matrix – coarse material	18.0 mg	2.93
5,700	Matrix – white colored material	21.8 mg	3.84
5,700	Matrix – dark colored material	31.8 mg	3.15
5,700	Matrix – dark colored material	22.1 mg	3.72
5,700	Matrix – light colored material	24.7 mg	3.97
5,700	Matrix – dark colored material	18.9 mg	3.35
5,700	Matrix – light colored material	19.5 mg	3.75
5,606	Matrix – light colored material	25.8 mg	3.32
5,606	Material from inclusion	21.7 mg	3.57
5,606	Material from inclusion	15.6 mg	3.34
5,606	Matrix – light colored material	21.5 mg	3.68
5,606	Matrix – dark colored material	25.2 mg	4.08

4.5.4.1 Discussion (Significance of Core Analytical Results)

Because the equilibrium modeling suggested that the brines were supersaturated with respect to carbonates, sulfates, and halides, and the injection of CO_2 would increase the likelihood of carbonate precipitation from the brines, core samples were examined for evidence on mineral precipitation. The XCT analyses demonstrated more evidence of precipitation than dissolution, and the light microscopy (LM) and SEM indicated the presence of carbonate, sulfate, and halide mineralization within the pore spaces and fractures. Also, the XRD analyses displayed evidence of a low-Mg carbonate that may have precipitated relatively recently. Though these analytical techniques all indicated mineral precipitation in the pores and fractures of the core, the use of carbon isotopes could not time-stamp the precipitates as occurring after or as a result of the CO_2 injection into the reef.

5.0 Conclusions

The MRCSP geochemistry study was performed at three Niagaran reefs (Dover 33, Charlton 19, and the Bagley Field) to determine the effect of CO_2 injection associated with EOR activities on the geochemical conditions in the reef reservoir. The geochemistry in reefs were monitored through the EOR process (i.e., prior to CO_2 injection through oil/CO_2 production) through the collection of brine, gas, and core samples. However, it is noted that the main reef, Dover 33, had undergone significant EOR prior to MRCSP study and therefore, had undergone geochemical changes during past EOR. In addition, gas samples of the CO_2 injection stream were collected from the Dover 36 GPF to determine the chemical (and isotopic) characteristics of the injected CO_2.

A stepwise approach was used to investigate the geochemistry in the reefs, beginning with the general geochemistry of the brines and gas from the reservoir and ending with the isotopic analysis of the matrix rock and mineral precipitates in the core samples.

5.1 Brine

1. Brine samples collected from the three reefs displayed comparable results for general geochemical properties. Overall, the brines have extremely high total dissolved solids (TDS) concentrations and are dominated by Ca, Mg, Na, and K for cations and Cl for anions, as may be expected from a brine in carbonate reef. The general geochemistry also displayed limited variation between the three reefs investigated, indicating there is not significant variation in the brine geochemistry over areal distribution of the reefs sampled. Also, the injection of CO_2 does not appear to change the general geochemistry.

2. Geochemical equilibrium modeling of the chemical parameters was performed to determine if specific mineral species were supersaturated in the brine and prone to precipitation due to CO_2 injection. The data indicate that brines are supersaturated with respect to many carbonate minerals (calcite, aragonite, dolomite, huntite, and magnesite) prior to CO_2 injection and the injection of CO_2 appears to drive the brine to greater saturation levels. It should be noted that while the Pitzer equations are used for slightly higher activity brines compared to the Debye-Huckel equations, the activity levels of the brines from the Niagaran reefs are beyond the applicable conditions of the Pitzer calculations. Therefore, the results provided by the equilibrium model have some degree of uncertainty.

3. Carbon isotope values were also measured in the brine samples to evaluate the mixing/dissolution of the injected CO_2 with the brine waters. The injected CO_2 displays a unique $\delta^{13}C$ signature (approximately 20‰), which becomes increasingly heavier due to partitioning when the injected CO_2 is dissolved in water to form carbonic acid, bicarbonate and/or carbonate ions (approximately 30‰). Brine samples collected prior to significant interaction with the injected CO_2 displayed $\delta^{13}C$ values ranging from approximately -7‰ to 10‰, but samples of the brine that had significant interaction with the injected CO_2 displayed $\delta^{13}C$ values between approximately -20‰ and 30‰. These data indicate that there was dissolution of the injected CO_2 and the brines within the reef.

5.2 Gas

Likewise, the concentration of CO_2 in the gas samples from the reefs significantly increased by the injection of the CO_2 (as expected). While the geochemical equilibrium models suggest the precipitation of carbonate minerals and secondary mineralization of carbonates are observed in the fractures and vugs of the core samples collected from the Dover 33 reef, it was not possible to correlate the timing of precipitation with the injection of the CO_2 in the core samples.

5.3 Rock Core

With the indication of dissolution of the injected CO_2 and the favorability of carbonate mineral precipitation, rock core samples were analyzed with LM, SEM, XRD, and XCT to determine if carbonate minerals are precipitating in the vugs or fractures of the rock. In addition, subsamples of the core were analyzed for $\delta^{13}C$ values to determine if the injected CO_2 had been incorporated in carbonate minerals precipitated in the pore spaces.

1. Analyses with LM and SEM indicated that there are no significant changes in porosity from above the oil-water contact to below the oil-water contact. Generally, there were more salt inclusions and fewer organic inclusions below the oil-water interface. Additionally, there is not a systematic relationship between location in the reservoir and fracture size or number of fractures. In the oil zone and in the oil-water interface, organic material is more common in fractures.

2. The LM and SEM inspections indicated the presence of secondary mineralization of carbonates and sulfates in the vugs and fractures of the core samples. Fractures in every sample also contained fragments of its matrix. The SEM analyses (using energy-dispersive detector [EDS]) also indicated the presence of high-Mg carbonates and low-Mg calcite in the vugs and on the outer surfaces of the dolomite matrix. Halide minerals also were identified in the pores of the dolomite matrix, but the presence of these minerals may be attributed to the desiccation of the samples following core collection and precipitation of these minerals from the native brines and drilling fluids. The timing of the secondary mineralization, however, could not be established from the SEM or LM analyses.

3. Portions of the core samples were analyzed with XRD to determine the mineralogy of the matrix of the core and the mineral precipitates found in the vugs. The sample collected from a depth of 5,630 feet (at the oil-water contact) displays dolomite and low-Mg calcite as the major phases of the mineralogy with minor amounts quartz, anhydrite, and halite. Core samples above and below the oil-water contact, however, only show the presence of dolomite in the bulk samples. The more complex mineralogy near the oil-water contact suggests that the combined presence of CO_2, brine, and gas may create a more geochemically active zone.

4. One core sample from a depth of 5,690 feet (from below the oil-water contact) was disaggregated for XRD analysis due to the presence of a relatively large vug inclusion identified through XCT. The matrix of this core sample consisted predominantly of dolomite with minor amounts of quartz and alkali feldspar. The precipitated, fine-grained material in the vug inclusion displayed a more complex mineralogy with the majority of the vug inclusion composed of dolomite and anhydrite; however, the presence of beta cristobalite, quartz, fluorite, and albite also were detected.

5. XCT images of the core indicated that there was no strong evidence of CO_2-induced dissolution in the samples. Any evidence of CO_2-induced dissolution was subtle, comprising localized areas of elevated porosity, or slight fracture widening in some cases. Evidence for mineral precipitation lining the large pores and even the fractures in the core was more commonly observed than dissolution. It is difficult to identify the secondary mineral from the XCT images because gray scale variation is small. Based on the gray scale in the XCT images, dolomite, calcite, gypsum, anhydrite, microcrystalline silica, and halide minerals are all possible minerals precipitated in the vugs and fractures. The XCT images provide further evidence of mineralization caused by the injection of CO_2.

6. Carbon-13 analyses were performed on the core samples to establish the timing (pre- vs. post-CO_2 injection) of carbonate precipitation indicated by the brine and core analyses. Samples of the core matrix and the mineral precipitates within the vugs were analyzed for $\delta^{13}C$ to determine whether the vug minerals are isotopically distinct from typical matrix carbonates— isotopic analyses of the

dissolved carbonate suggest that minerals formed from the injected CO_2 would be isotopically heavy (30‰) compared with the matrix carbonate minerals (3-4‰). Both the matrix material and vug precipitates displayed similar isotopic signatures of approximately 3‰ to 4‰, suggesting that post-CO_2-injection mineralization has not occurred. However, the minimal mass of carbonate precipitates in the vugs may bias the $\delta^{13}C$ values of these samples.

In summary, the geochemistry of the brines from the Niagaran reefs included in this study show extremely high concentrations of calcium, magnesium, sodium, potassium and chloride, which is consistent with geochemical conditions of other Niagaran reefs in the State of Michigan. The general chemical analyses and modeling indicate that the reef brines are supersaturated with respect to carbonate minerals (dolomite, calcite, huntite, and magnesite), and the likelihood of precipitation increases with the injection of CO_2. The $\delta^{13}C$ values of the dissolved carbonate in the brines appear to move in a positive direction (heavier) with the injection of the Antrim CO_2. The core sampled displayed evidence of carbonate, sulfate, and halide precipitation in the pores and fractures during the LS, SEM, XRD, and XCT analyses; however, the precipitates could not be directly tied to the injection of CO_2 through the isotopic analyses.

6.0 References

Battelle, 2019, Regional Assessment of the Northern Niagaran Pinnacle Reef Trend. Final Topical Report for the Department of Energy – National Energy Technology Laboratory.

Becker V., Myrttinen A., Blum P., van Geldern R., and Barth J.A.C., 2011, Predicting $\delta^{13}C_{DIC}$ dynamics in CCS: A scheme based on a review of inorganic carbon chemistry under elevated pressures and temperatures. International Journal of Greenhouse Gas Control. 5, 1250-1258.

Becker V., Myrttinen A., Nightingale M., Shevalier M., Rock L., Mayer B., and Barth J.A.C., 2015, Stable carbon and oxygen equilibrium isotope fractionation of supercritical and subcritical CO_2 with DIC and H_2O in saline reservoir fluids. International Journal of Greenhouse Gas Control, 39, 215-224.

Benson S.M. and Cole D.R. 2008, CO_2 sequestration in deep sedimentary formations. Elements 4:325-331.

Boreham C., Underschultz J., Stalker L., Kirste D., Freifeld B., Jenkins C., Ennis-King J., 2011, Monitoring of CO_2 storage in a depleted natural gas reservoir: Gas geochemistry from the CO2CRC Otway Project, Australia. Int J of Greenhouse Gas Control 5:1039-1054.

Cantucci B, Montegrossi G, Vaselli O, Tassi F, Quattrocchi F, Perkins EH, 2009, Geochemical modeling of CO_2 storage in deep reservoirs: The Weyburn Project (Canada) case study. Chem Geol 265:181-197.

Cercone K.R., and Lohmann K.C., 1987, Late burial diagenesis of Niagaran (Middle Silurian) Pinnacle Reefs in the Michgan Basin. The American Association of Petroleum Geologists Bulletin, 71, 156-166.

Charpentier R.R., 1989, A statistical analysis of the larger Silurian reefs in the northern part of the Lower Peninsula of Michigan. USGS Open-File Report 89216. Dept. of Interior, U.S. Geological Survey, 34 pp.

Clark, I.D., Fritz, P., 1997, Environmental Isotopes in Hydrogeology. CRC Press/Lewis Publishers, Boca Raton. 328 pp.

Coniglo M., Zheng Q., and Carter T.R., 2003, Dolomitization and recrystallization of middle Silurian reefs and platformal carbonates of the Guelph Formation, Michigan Basin, southwestern Ontario. Bulletin of Canadian Petroleum Geology, 51, 177-199.

DePaolo D.J., and Cole D.R., 2013, Geochemistry of geologic carbon sequestration: An overview, Reviews in Mineralogy and Geochemistry, 77, 1-14.

Emberley S., Hutcheon I., Shevalier M., Burocher K., Gunter W.D., and Perkins E.H., 2004, Geochemical monitoring of fluid-rock interaction and CO_2 storage at the Weyburn CO_2-injection enhanced oil recovery site, Saskatchewan, Canada, Energy 29, 1393–1401.

Gupta N., Cumming L., Kelley M., Paul D., Mishra S., Gerst J., Place M., Pardini R., Modroo A., and Mannes R., 2013. Monitoring and modelling of CO_2 behavior in multiple oil bearing carbonate reefs for a large scale demonstration in Lower Michigan. Energy Procedia, 37, 6800-6807.

Gupta N., Kelley M., Place M., Cumming L., Mawalkar S., Mishra S., Haagsma A., Mannes R., and Pardini R., 2013b. Lessons Learned from CO_2 Injection, Monitoring, and Modeling across a Diverse Portfolio of Depleted Closed Carbonate Reef Oil Fields – the Midwest Regional Carbon Sequestration

Partnership Experience, 13th International Conference on Greenhouse Gas Control Technologies (GHGT-13). 14-18 November 2016, Lausanne, Switzerland

Haagsma, A., Goodman, W., Larsen, G., Cotter, Z., Scharenberg, M., Keister, L., Hawkins, J., Main, J., Pasumarti, A., Valluri, M., Conner, A., and Gupta, N. (2020). Regional Assessment for the CO_2 Storage Potential in Northern Niagaran Pinnacle Reef Trend. MRCSP topical report prepared for DOE-NETL project DE-FC26-05NT42589, Battelle Memorial Institute, Columbus, OH

Hitchon B., (ed) 1996 Aquifer Disposal of Carbon Dioxide Geoscience Publishing Ltd, Sherwood Park, Alberta, Canada, p 165.

Jenkins C.R., Cook P.J., Ennis-King J., Undershultz J., Boreham C., Dance T., de Caritat P., Etheridge D.M., Freifeld B.M., Hortle A., Kirste D., Paterson L., Roman Pevzner, Schacht U., Sharma S., Linda Stalker L., and Urosevic M., 2012, Safe storage and effective monitoring of CO_2 in depleted gas fields. Proceedings of the National Academy of Sciences of the United States of America, 109, 353-354.

Johnson G., Mayer B., Nightingale M., Shevalier M., and Hutcheon I., 2011, Using oxygen isotope ratios to quantitatively assess trapping mechanisms during CO_2 injection into geological reservoirs: The Pembina case study, Chemical Geology, 283 185-193. doi:10.1016/j.chemgeo.2011.01.016

Kelley M., Abbaszadeh M., Mishra S., Mawalkar S., Place M., Gupta N., and Pardini R., 2014, Reservoir characterization from pressure monitoring during CO_2 injection into a depleted pinnacle reef – MRCSP commercial-scale CCS demonstration project. Energy Procedia, 63, 4937 – 4964.

Kendall C., and McDonald J.J., 1998, Isotope Tracers in Catchment Hydrology, Elsevier Science B.V., Amsterdam, 839 pp.

Kharaka YK, Cole DR 2011 Geochemistry of geologic sequestration of carbon dioxide. In: Frontiers in geochemistry: Contribution of Geochemistry to the Study of the Earth. Harmon RS, Parker A (eds) Blackwell Publishing Ltd, p 136-174.

Kharaka Y.K., Cole D.R., Hovorka S.D., Gunter W.D., Knauss K.G., and Freifeld, 2006, Gas-water-rock interactions in Frio Formation following CO_2 injection: Implications for the storage of greenhouse gases in sedimentary basins. Geology, 34, 577-580. doi: 10.1130/G22357.1.

Kharaka Y.K., and Hanor J.S. 2007 Deep Fluids in the Continents: I. Sedimentary basins. Surface and Ground Water, Weathering and Soils. Treatise on Geochemistry, 5, 1-48.

Kharaka Y.K., Cole D.R., Thordsen J.J., Gans K.D., and Thomas R.B., 2013, Geochemical monitoring for potential environmental impacts of geologic sequestration of CO_2. Reviews in Mineralogy & Geochemistry, 77. 399-430.

Li J., and Pang Z., 2015, Environmental isotopes in CO_2 geological sequestration, *Greenhouse Gas Sci Technol.* 5:374–388; DOI: 10.1002/ghg.

Lu J., Kharaka Y.K., Thordsen J.J., Horita J., Karamalidis A., Griffith C., Hakala J.A., Ambats G., Cole D.R., Phelps T.J., Manning M.A., Cook P.J., and Hovorka S.D., 2012, CO_2-rock-brine interactions in the Lower Tuscaloosa Formation at Cranfield CO_2 sequestration site, Mississippi, USA. Chemical Geology, 291, 269-277.

Martini A.M., Budai J.M., Walter L.M., and Schoel M., 1996, Microbial generation of economic accumulations of methane within a shallow organic rich shale. Nature, 383, 155-158.

Martini A.M., Walter L.M, Ku T.C.W, Budai J.M., McIntosh J.C., and Schoell M., 2003. Microbial production and modification of gases in sedimentary basins: A geochemical case study from a Devonian shale gas play, Michigan basin. AAPG Bulletin 87, 1355-1375.

Martini A.M., Walter L.M., and McIntosh J.C., 2008, Identification of microbial and thermogenic gas components from Upper Devonian black shale cores, Illinois and Michigan basins. AAPG Bulletin 92, 327-339.

Mayer B., Shevalier M., Nightingal M., Kwon J-S, Johnson G., Raistrick M., Hutcheon I., and Perkins E., 2013, Tracing the movement and the fate of injected CO_2 at the IEA GHG Weyburn-Midale CO_2 Monitoring and Storage project (Saskatchewan, Canada) using carbon isotope ratios. International Journal of Greenhouse Gas Control 16S (2013) S177–S184.

Mayer B., Humez P., Becker V., Dalkhaa C., Rock L., Myrttinen A., and Barth J.A.C., 2015, Assessing the usefulness of the isotopic composition of CO_2 for leakage monitoring at CO_2 storage sites: A review. International Journal of Greenhouse Gas Control 37 (2015) 46–60.

Mcintosh J.C., Walter L.M., and Martini A.M., 2004, Extensive microbial modification of formation water geochemistry, Case study from a Midcontinent sedimentary basin, United States, GSA Bulletin, 116, 743-759.

McNutt R.H., Frape S.K., and Dollar P., 1987, A strontium, oxygen, and hydrogen isotopic composition of brines, Michigan and Applachian Basins, Ontario and Michigan. Applied Geochemistry, 2, 495-505.

Myrttinen A., Becker V ., van Geldern R., Würdemann H, Morozova D., Zimmer M., Taubald H., P. Blum P., Barth JAC 2010 Carbon and oxygen isotope indications for CO_2 behaviour after injection: First results from the Ketzin site (Germany). International Journal of Greenhouse Gas Control. 4, 1000-1006.

Myrttinen A., Becker V., and Barth J.A.C. 2012a, A review of methods used for equilibrium isotope fractionation investigations between dissolved inorganic carbon and CO_2. Earth-Science Reviews 115 (2012) 192–199.

Myrttinen A., Jeandel E., Ukelis O., Becker V., van Geldern R., Blum P., and Barth J.A.C. 2012b. Stable carbon isotope techniques to quantify CO2 trapping under pre-equilibrium conditions and elevated pressures and temperatures. Chemical Geology 320-321, 456-53.

Rine M.J, Garret, J.D., and Kaczmarek, S.E. 2016. A new facies architecture model for the Silurian Niagaran pinnacle reef complexes of the Michigan basin. SEPM Special Publication no. 109, p. 1-17, doi:10.2110/sepmsp.109.02.

Tissot B.P., and Welte D.H., 1984, Petroleum Formation and Occurrence, Springer Verlag, Berlin, 699pp.

Toelle B., Pekot L., Barnes D., Grammer M., and Harrison W., 2008, EOR potential of the Michigan Silurian Reefs using CO_2, Society of Professional Engineers, SPE 113843, 8pp.

Welch S.A., Sheets J.M., Place, M.C., Saltzman M.R., Edwards C.T., Gupta, N., Cole D.R., 2019, Assessing Geochemical Reactions during CO_2 Injection into an Oil-Bearing Reef in the Northern Michigan Basin, Applied Geochemistry, 100, 380-392.

Wilson T.P., and Long D.T., 1993a Geochemistry and isotope geochemistry of Michigan Basin brines: Devonian formations. Applied Geochemistry, 8, 81-100.

Wilson T.P., and Long D.T., 1993b Geochemistry and isotope chemistry of Ca-Na-Cl brines in Silurian strata, Michigan Basin, USA. Applied Geochemistry, 8, 507-524.

BATTELLE

It can be done